Metaloxycarbene Complexes: Synthesis, Characterisation and Reactivity in Catalysis

by

Jacques Nel

THESIS

Presented in fulfillment of the requirements for the degree of

MASTER

of

SCIENCE

in the

FACULTY OF SCIENCE

at the

UNIVERSITY OF STELLENBOSCH

SUPERVISOR: Prof. H. G. Raubenheimer

MARCH 2002

I, the undersigned, hereby declare that the work contained in this thesis is my own original work and that I have not previously in its entirety or in part submitted it at any university for a degree.

Signature:

Date:

SUMMARY

This study comprises the preparation and characterisation of new dinuclear metaloxycarbene complexes from the reaction of zirconocene, titanocene or hafnocene dichloride with anionic acyl complexes of chromium, molybdenum, tungsten and iron. It also involves the study of the oligomerisation of α-olefins using these prepared dinuclear metaloxycarbene complexes.

Reaction of RLi (R = Me, Ph or *t*-Bu) with $M^1(CO)_6$ (M^1=Cr, W of Mo) or $[Fe(CO)_5]$ and $[NEt_4]Cl$ afforded the ammonium salts of the acyl complexes $[(CO)_5M^1=C(R)O]^-NEt_4^+$ which further react with $[Cp_2M^2Cl_2]$ to produce the metaloxycarbene complexes $[(CO)_5M^1=C(R)OM^2(Cl)Cp_2]$ (M = Cr, W of Mo), (R = Me, Ph or *t*-Bu) and (M^2 = Zr, Ti of Hf) and $[(CO)_4Fe=C(R)OM^2(Cl)Cp_2]$.

The first crystal structure of a hafnoxycarbene complex of tungsten, $[(CO)_5W=C(Ph)OHf(Cl)Cp_2]$, **13**, in which monodentate coordination of the metaloxycarbene ligand occurs, was determined. The molecular structure showed a W-$C_{carbene}$ bond length of 2.179(6)Å, a typical short $C_{carbene}$-O distance 1.290(6)Å and an almost linear $C_{carbene}$-O-Hf angle 171.4(3)°.

The first titanoxycarbene complex of iron, $[(CO)_4Fe=C(Me)OTi(Cl)Cp_2]$, **14**, was successfully prepared *via* the Fischer route from reaction of $Fe(CO)_5$ and MeLi. The signal of the carbene complex showed a low field chemical shift for the $C_{carbene}$ atom, in the ^{13}C NMR spectra, at δ 295.2. The acyl complex, $[(CO)_4Fe=C(Me)O]^-NEt_4$, was fluctional and showed only one carbonyl signal in the ^{13}C NMR spectrum at δ 223.1.

The metaloxycarbene complexes, $[(CO)_5Cr=C(Me)OZr(Cl)Cp_2]$, **8**, and $[(CO)_5W=C(Me)OZr(Cl)Cp_2]$, **12**, showed extraordinary high catalytic activity in the oligomerisation of long chain α-olefins. The total % conversion of 1-hexene to the oligomerisation products (dimer, trimer and tetramer) by means of the catalyst precursors, $[(CO)_5Cr = C(Me)OZr(Cl)Cp_2]$, **8**, and $[(CO)_5W=C(Me)OZr(Cl)Cp_2]$, **12**, was 38.07% and 43.44% respectively at oligomerisation temperatures below 15°C. Higher temperatures led to a decrease in the total % conversion, due to catalyst precursor degradation at high temperatures (above 60°C). Low oligomersation temperatures favoured the production of trimers.

Additional cyclopentadienyl signals were observed in the ^1H en ^{13}C NMR spectra of $[(CO)_5Cr=C(Me)OZr(Cl)Cp_2]$, **8**, $[(CO)_5W=C(Me)OZr(Cl)Cp_2]$, **12**, and $[(CO)_5W=C(Ph)OHf(Cl)Cp_2]$, **13**, and can be attributed to the presence of configurational isomers resulting from restricted rotation about the $C_{carbene}$-O bond and/or by means of O-inversion. An additional peak for the methyl group of $[(CO)_5Cr=C(Me)OZr(Cl)Cp_2]$, **8**, observed in the ^1H NMR is again due to such isomer formation .

Finally, efforts to prepare $[(CO)_5Cr=C(Me)OZr(H)Cp_2]$ by treatment of $(CO)_6Cr$ with MeLi and NEt_4Cl followed by reaction with $Cp_2Zr(H)Cl$ furnished only red crystals of

the (halo)*deca*carbonyldimetalate anion $[\{(CO)_5Cr\}_2Cl]^-$, with NEt_4^+ as counterion (complex **67**). The molecular structure revealed a Cr-Cl-Cr bond angle of 130.28(6)° and long Cr-C_{co} bond distance (1.89Å, av.).

OPSOMMING

Die bereiding en karakterisering van nuwe dikernige metaaloksikarbeen komplekse berei vanuit sirkonoseen-, titanoseen- of hafnoseendichloried en anioniese asielkomplekse van chroom, molibdeen, wolfram of yster, asook α-olefien oligomerisasie vorm die hooftema van hierdie tesis.

Die reaksie van RLi (R = Me, Ph of *t*-Bu) met $M^1(CO)_6$ (M^1 = Cr, W of Mo) of $Fe(CO)_5$ en $[NEt_4]Cl$ lewer die asielkomplekse, $[(CO)_5M^1{=}C(R)O]^-NEt_4^+$ of $[(CO)_4Fe{=}C(R)O]^-NEt_4^+$, wat verder met $[Cp_2M^2Cl_2]$ reageer om die metaaloksikarbeenkomplekse $[(CO)_5M^1{=}C(R)OM^2(Cl)Cp_2]$, (M = Cr, W of Mo), (R = Me, Ph of *t*-Bu) en (M^2 = Zr, Ti of Hf) of $[(CO)_4Fe{=}C(R)OM^2(Cl)Cp_2]$ te vorm.

Die eerste kristalstruktuur van 'n hafnoksikarbeen kompleks van wolfram, $[(CO)_5W{=}C(Ph)OHf(Cl)Cp_2]$, **13**, waarin die metaaloksikarbeen ligand monodentaat gebind is bepaal. Die molekulêre struktuur toon 'n $W\text{-}C_{karbeen}$ bindingslengte van 2.179(6)Å, 'n kenmerkende kort $C_{karbeen}$-O bindingslengte 1.290(6)Å en 'n byna lineêre $C_{karbeen}$-O-Hf-hoek 171.4(3)°.

Die eerste titanoksikarbeen kompleks van yster, $[(CO)_4Fe{=}C(Me)OTi(Cl)Cp_2]$, **14**, is suksesvol volgens die Fischer-roete vanuit die ammoniumsout van die asielkompleks, $[(CO)_4Fe{=}C(Me)O]^-NEt_4$, **5** berei. Die sein vir die $C_{karbeen}$ van die kompleks verskyn in die ^{13}C KMR spectrum by 'n laer veld δ 295.2. Die asielkompleks, $[(CO)_4Fe{=}C(Me)O]^-NEt_4^+$, is fluksioneel en toon slegs een karbonielsein in die ^{13}C KMR spektrum by δ 223.1.

Die metaaloksikarbeen komplekse, $[(CO)_5Cr{=}C(Me)OZr(Cl)Cp_2]$, **8**, en $[(CO)_5W{=}C(Me)OZr(Cl)Cp_2]$, **12**, toon buitengewone hoë katalitiese aktiwiteit vir die oligomerisasie van langer ketting α-olefiene. Die totale % omsetting van 1-hekseen na die oligomerisasieprodukte (dimeer, trimeer en tetrameer) d.m.v. die voorloper katalisatore, $[(CO)_5Cr{=}C(Me)OZr(Cl)Cp_2]$, **8**, en $[(CO)_5W{=}C(Me)OZr(Cl)Cp_2]$, **12**, is 38.07% en 43.44% onderskeidelik by lae oligomerisasie temperature (laer as 15°C). Hoër temperature lei tot 'n afname in die omsetting, weens die ontbinding van die voorloperkatalisatore by temperature bokant 60°C. Oligomerisasie by lae temperature d.m.v. die metaaloksikarbeenkomplekse bevoordeel die vorming van trimere.

Addisionele seine vir die siklopentadiëniel ringe is waargeneem in die ^1H- en ^{13}C- KMR spektra van $[(CO)_5Cr{=}C(Me)OZr(Cl)Cp_2]$, **8**, $[(CO)_5W{=}C(Me)OZr(Cl)Cp_2]$, **13**, en $[(CO)_5W{=}C(Ph)OHf(Cl)Cp_2]$, wat toegeskryf kan word aan konfigurasie-isomere wat ontstaan weens beperkte rotasie om die $C_{karbeen}$-O binding en/of d.m.v. O-inversie. 'n Addisionele metielsein is ook waargeneem in die ^1H-KMR-spektrum van $[(CO)_5Cr{=}C(Me)OZr(Cl)Cp_2]$, **8**.

Ten slotte is pogings aangewend om $[(CO)_5Cr{=}C(Me)OZr(H)Cp_2]$ vanuit die ammoniumsout van die asielkompleks, $[(CO)_5Cr{=}C(Me)O]^-NEt_4^+$ en $[Cp_2Zr(H)Cl]$ te

berei. Slegs rooi kristalle van die (halo)*deca*karbonieldimetalaat-anioon $[\{(CO)_5Cr\}_2Cl]^-$ met teenioon NEt_4^+ (**67**) is geisoleer. Die molekulêre struktuur toon 'n Cr-Cl-Cr bindingshoek van 130.28(6)° en 'n lang Cr-C_{co}-bindingsafstand (1.89Å, gemiddeld).

IN LOVING MEMORY OF

MY FATHER AND BROTHER

CONTENTS

CHAPTER 3

OLIGOMERISATION OF α-OLEFINS USING METALOXYCARBENE COMPLEXES

ACKNOWLEDGEMENTS

I would like to express my gratitude to all whom supported and encouraged me during this thesis. In particular would I like to thank the following people and institutions:

- Prof. H.G. Raubenheimer for outstanding leadership, guidance and wisdom.
- The FRD and SASOL/Stellenbosch 2000 for financial assistance.
- A special thanks to Dr. Stephanie Cronje for availability, patience, advice and practical guidance.
- Elisna Maree and the late Mr. Hendrik Spies for NMR spectra, and Dr. Stephanie Cronje for her help in interpreting them.
- Mr. Ian Voster of RAU and Dr. Louis Fourie of PU for mass spectra.
- Dr. John Bacsa of UCT for collection of X-ray crystallographic data. Dr. Catharine Esterhuysen and Matthias Esterhuysen for solving the crystal structures and the collection of reference data.
- Dr. Udo Wahner for his help regarding the catalytic test performed.
- Mr. Eric Ward for the prompt delivery of glassware and his wonderful sense of humor.
- Elsa Malherbe, Tommy and Naazier for ensuring the smooth running of laboratory.
- Maggel Deetlefs, Matthias Esterhuysen, Greta Heyndenrych, Gerrit Julius, Arno Neveling, Leon van Kralingen, Dr. An Jin and Dr. Oleg Stenzel for patience and advice.
- Special thanks to my friends and family for your love, support, encouragement and patience, especially while I was writing up. The Lord my God to Whom I owe everything.

ABBREVIATIONS

ν	Wavelenght (cm^{-1})
t-Bu	tert-Butyl
Cp	Cyclopentadienyl
Cp*	1,2,3,4,5-pentamethylcyclopentadienyl
Cy	Cyclohexyl
d	Doublet
DMSO	Dimethyl Sulfoxide
Et	Ethyl
Fc	Ferrocenium ion
HDPE	High density polyethylene
Ind	Indenyl
L	Ligand
LDPE	Low density polyethylene
Me	Methyl
MAO	Methylaluminoxane
md	Medium
m	Multiplet (NMR)
M.p.	Melting point
Ph	Phenyl
P	Polymer
Ph	Phenyl
PP	Polypropylene
Pr	Propyl
q	Quartet
rac	racemic
R	Alkyl
r_p	Propagation rate
r_t	Tranfer rate

RT	Room temperature
s	Singlet
sh	Shoulder
st	Strong
t	Triplet (NMR)
t	ton
thf	Tetrahydrofuran
tt	Triplet of triplets
w	Weak

CHAPTER 1

INTRODUCTION AND AIMS

1.1 INTRODUCTION

Carbenes have played an important role in organic chemistry ever since their postulation and synthesis. The term " carbene ", defined by Doering, Winstein, and Woodward in 1951, refers to a divalent carbon species, where the carbene carbon is linked to two adjacent groups with covalent bonds and the two remaining carbon electrons are localised on the carbon atom.[1] The two nonbonding electrons may have antiparallel spins (singlet ground state) or parallel spins (triplet ground state).[2]

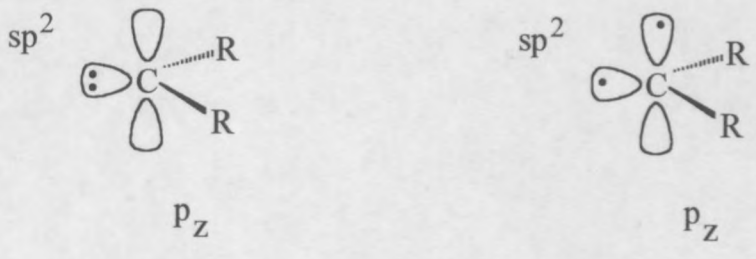

Figure 1.1: Singlet- and triplet ground states of carbene carbon

1.2 HISTORY OF CARBENES

The first attempts to prepare free carbenes were made by Dumas and Regnault when they tried to prepare methylene by dehydrating methanol using phosphorus pentoxide or concentrated sulfuric acid.[3] Later, Butlerov obtained ethylene from the reaction of methyl iodide with copper and suggested that it was formed by the dimerisation of methylene.[3] In 1862 Geuther proposed that the basic hydrolysis of chloroform involves the intermediate formation of dichloromethylene, which has now been well established.[3,4]

The discovery of isonitriles and fumic acid revived carbene chemistry, with Staudinger at the forefront, studying the decomposition of diazo compounds and ketenes.[5] The real

breakthrough came in 1964, with the preparation of the first stable carbene complex, $[(CO)_5W{=}C(OMe)Ph]$ (**1a**), by Fischer and Maasböl (Scheme 1.1).[6,7] This preparation involves alkylation of a hydroxycarbene complex with diazomethane and elimination of N_2. The resulting carbene complex is electrophilic.

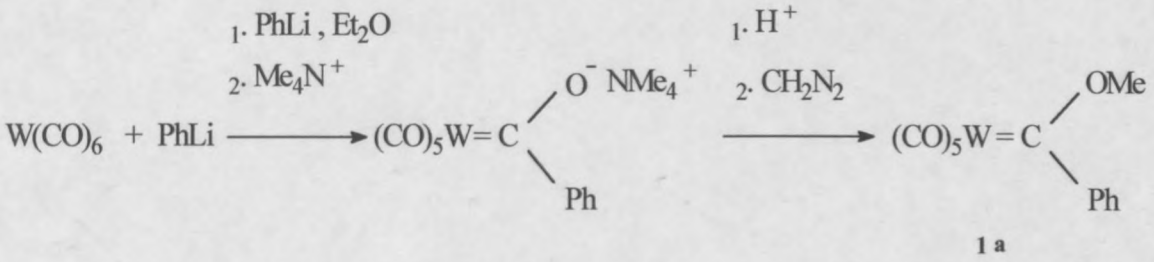

1 a

Scheme 1.1: The first stable carbene complex

Ten years after Fischer's discovery, Schrock in the USA isolated a group of nucleophilic carbene complexes.[8] The isolation of a carbene complex containing the parent methylenegroup was not achieved until 1975. In 1991 Arduengo demonstrated the high stability of cyclic diaminocarbenes by reporting the synthesis and structure determination of 1,3-diadamantylimidazol-2-ylidene, unquestionably the first isolable, stable carbene.[9,10]

1.3 STRUCTURAL CONSIDERATIONS AND REACTIVITY

Carbene complexes are usually represented as a carbon atom bonded to a metal with a double bond. Its general structure is $L_nM{=}C(X)(Y)$, with X and Y being alkyl, aryl, H, halogens or heteroatom (O, N, S)-containing groups. In so-called Fischer-type carbene complexes, one or two highly electronegative atoms such as O, N, S, or a halogen are directly attached to the carbene carbon, while the Schrock–type carbene complexes have only H, alkyl-, or aryl groups directly bonded to the carbene carbon. The latter are more difficult to prepare. The Schrock-type carbene complexes do not form part of this thesis and will only be mentioned in passing.

Experiments and calculations on rotation energies of metal-carbene bonds have shown alkoxycarbene complexes to have a number of resonance forms (Scheme 1.2).[11] The relative contribution of the individual resonance forms A, B, C and D depends on the relative π-donor properties of the metal and the substituents X and Y at the carbene carbon. Resonance structure C (or D) is most prominent for alkoxy- and aminocarbene complexes, because of the p_π -p_π -interaction between the carbene carbon atom and the heteroatom.

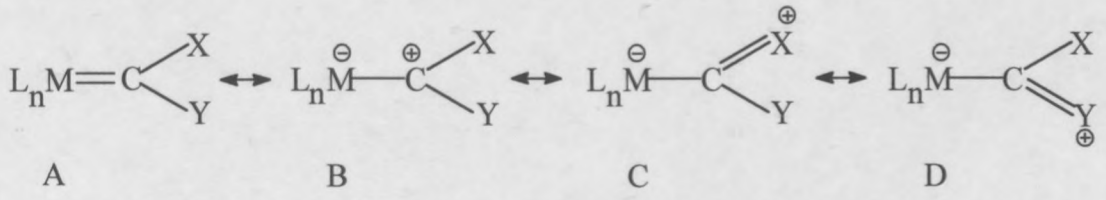

Scheme 1.2: Resonance structures of Fischer-type alkoxycarbene complexes

The carbene carbon in the complex is sp^2 hybridised and formally possesses an empty p-orbital leading to its electrophilic character [Figure 1.2, (ii)]. Part compensation for this strong electron deficiency is provided by a p_π-p_π bond between one of the free electron pairs on the heteroatom and the unused p-orbital of the carbene carbon or between filled d-orbitals on the metal and this orbital (back bonding).

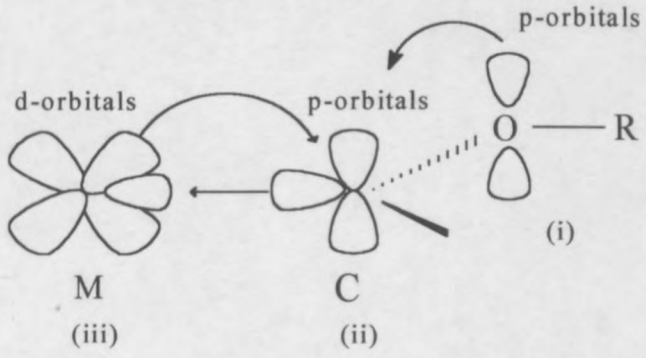

Figure 1.2: π-Bonding in Fischer Carbene Complexes.

All the interactions afford a three atom π-system leading to the Fischer carbene complexes being more thermodynamically stable than their Schrock analogues, because of a lowering in the energy of the bonding molecular orbital (Figure 1.3).[12]

The bond order of the metal-$C_{carbene}$ is distinctly less than that of metal-$C_{carbonyl}$ bonds in the same complex, but it is higher than that of a single bond. This is due to the above-mentioned back donation.

The reactivity of non-heteroatom-stabilised carbene complexes is mainly frontier-orbital-controlled and the energies of the HUMO and LUMO of carbene complexes are determined by the amount of orbital overlap and by the energy-difference between the empty carbene 2p orbital and a d orbital (of suitable symmetry) of the group L_nM (and then, of course, the heteroatoms come into play as well).

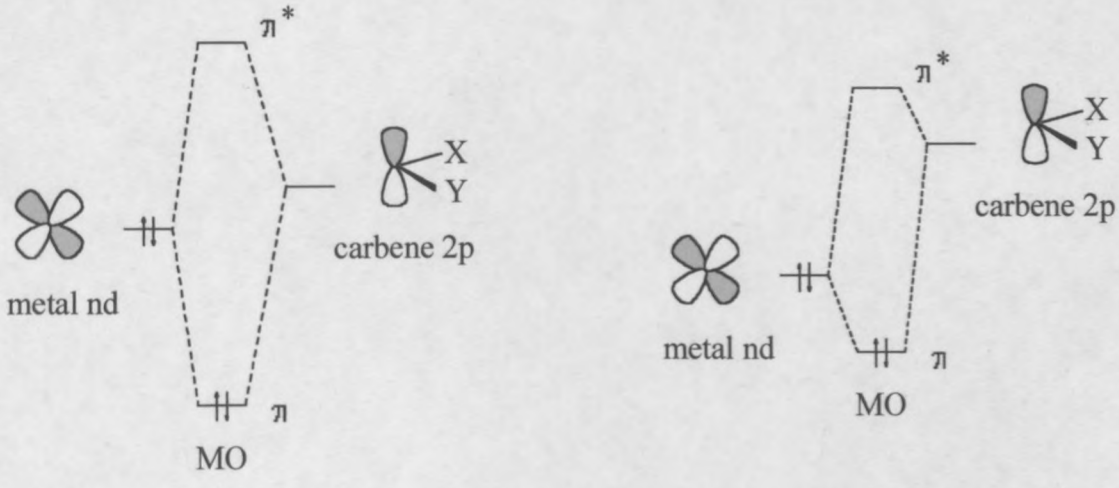

small energy difference between metal nd and carbene 2p orbitals

large energy difference between metal nd and carbene 2p orbitals

a) **nucleophilic carbene complex**

b) electrophilic carbene complex

Figure 1.3: Orbital interaction in nucleophilic and electrophilic carbene complexes

Complexes with weak π interaction between the metal and the carbene fragment will have an energetically low-lying π* orbital. In addition to this, electron-transfer from the metal M to $C_{carbene}$ will be less efficient, thus leading to a more positively charged carbene fragment (Figure 1.3b). Hence, carbene complexes with a large energy gap and poor orbital overlap between the metal d orbital and the carbene 2p orbital will be prone to react with nucleophiles (Fischer-type carbene complexes).[13]

Complexes with strong π interaction between the metal and the carbene fragment will have energy-rich π * orbitals, and will, therefore, not be good substrates for nucleophilic additions. In complexes with large d (M)-2p(C) overlap, electrons will be transferred to a greater extent from the metal to the electron-deficient (and more electronegative) $C_{carbene}$. Thereby the partial negative charge and electron density at $C_{carbene}$ will increase and facilitate electrophilic attack at this atom (Figure 1.3a) (Schrock carbene complexes).

1.4 SYNTHETIC METHODS OF FISCHER CARBENE COMPLEXES

A wide range of transition metal complexes, have been prepared by various methods, since 1964. These complexes play an important role as reaction intermediates in organic synthesis and in catalytic processes. Various review articles have been published describing these preparation methods.[14-18] Only methods related to this study will be discussed in this section, other interesting methods will be mentioned in Chapter 2.

1.4.1 Alkylation of acyl lithium complexes

This two-step conversion of metal carbonyls to metal carbene complexes (**3a**) was developed by E.O.Fischer.[12] Metal carbonyls can react with organolithium compounds to yield nucleophilic acyl complexes (**2a**). O-alkylation of these complexes lead to the formation of alkoxycarbene complexes.

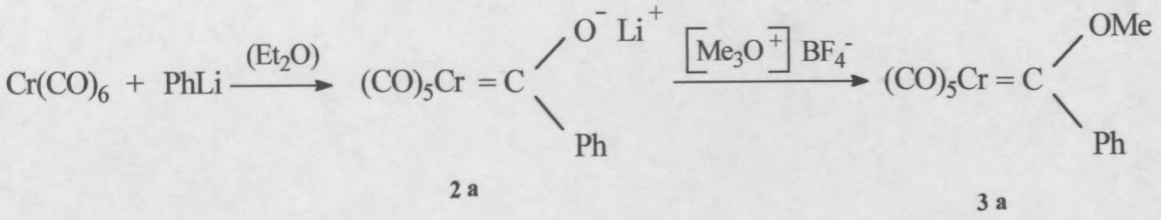

2 a 3 a

Scheme 1.3: Fischer carbene complexes from metal carbonyls

1.4.2 Protonation and alkylation of the acyl carbene complex

The acyllithium complex (**2a**) can be converted to its ammonium salt (**4a**) by reaction with tetra alkylammonium halides. Protonation and subsequent alkylation also results in a carbene complex (**3a**), as mentioned before.[19]

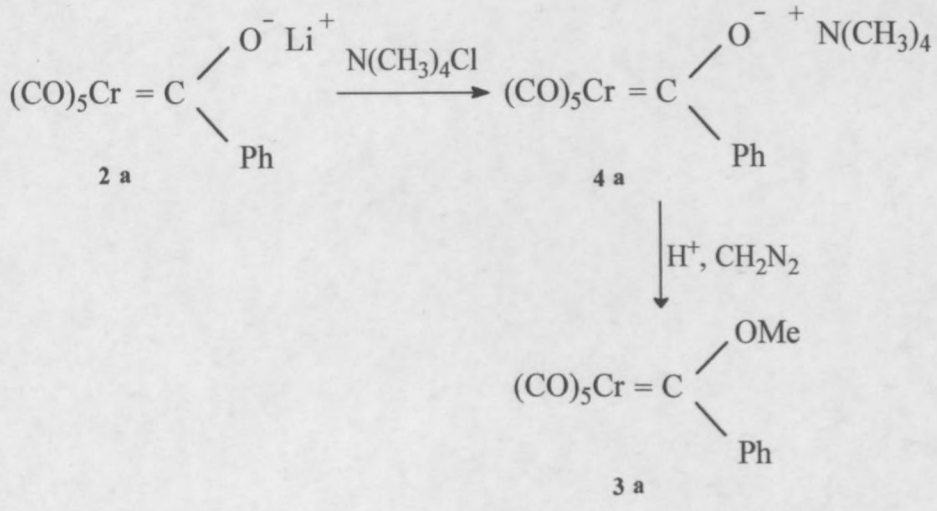

2 a 4 a 3 a

Scheme 1.4: Fisher carbene complexes *via* the ammonium salt of the acyl complex

This investigation focuses on derivatives of Fischer-type carbene complexes and the original preparation method is primarily of interest. The methods used to synthesise these complexes are discussed in detail in Chapter 2.

1.5 AIMS AND OBJECTIVES

Fischer, Grubbs, Erker and others have prepared complexes wherein the X or Y group is a group 4 metallocene moiety, for example as in $[(CO)_5Cr=C(CH_3)OTiCp_2Cl]$.[20]

Recently it was established in our laboratory that such compounds devised from zirconium and in the presence of MAO $\{[(CO)_5W=C(Me)OZrCp_2Cl]\}$, catalises the polymerisation of 1-pentene.[21-23]

It is also presently accepted that the real catalyst in such reactions is the hydride cation Cp_2MH^+.[24,25] Metallocenes, $Cp_2M(halide)_2$, as a precursors for α-olefin polymerisation have been studied in detail, but $Cp_2M(halide)OR$, which is related to a metaloxycarbene complex, does not fulfill this role effectively (M=Zr,Hf).[21]

A number of questions remained after the first study and some of them became the goals of the present investigation:

1. How to prepare the metaloxycarbene complexes in good yield?
2. Which one of the possible resonance structures of the metaloxycarbene is the best representation of the structure of the compounds based on single crystal X-ray investigations?
3. What could be the mechanism of the polymerisation reaction be?
4. Can a metallocene hydride derivative of a carbene complex be prepared, and would it be an active catalysts in the absence of MAO?

Although the synthesis of iron aminocarbene and alkoxycarbene complexes are well documented, no known iron metaloxycarbene complexes exist.[26-30] An aim in this project is to synthesise, characterise and study the properties of iron titanoxy and zirconoxycarbene complexes $[(CO)_4Fe=C(Me)OM^1Cp_2Cl]$.($M^1$=Ti, Zr).

The crystallographic data of the new complexes $[(CO)_5W=C(Ph)OTiCp_2Cl]$, **11**, and $[(CO)_5W=C(Ph)OHfCp_2Cl]$, **13**, are also reported.

REFERENCES

1. W. Kirmse in *Carbene Chemistry*, Academic Press, New York, 1964, 1-3.
2. H. Werner, E.O. Fisher, *J. Organomet. Chem.*, 1971, **28**, 367.
3. Kirmse in *Carbene Chemistry*, Academic Press, New York, 1964, 5-6.
4. C.P. Casey., *J. Am. Chem. Soc.*, 1979, **101**, 7282.
5. J. Hine in *Divalent Carbon,* The Ronald Press Company, New York, 1964.
6. E.O. Fischer and A. Maasböl, *Angew. Chem., Int. Ed. Engl.*, 1964, **3**, 580.
7. J.F. Lehmann, S.G. Urquhart, L.E. Ennis, A.P. Hitchcock, K. Hatano, S. Gupta and M. Denk, *Organometallics*, 1999, **18**, 1862.
8. R.R.Schrock, *J. Am. Chem. Soc.*, 1974, **96**, 6796.
9. A.J. Arduengo III, R.L. Harlow and M. Kline, *J. Am. Chem. Soc.*, 1991, **113**, 361.
10. A.J. Arduengo III, J.R. Goerlich, and W.J. Marshall, *J. Am. Chem. Soc.*, 1995, **117**, 11027.
11. H. Nakasuji, J. Ushio, S. Han and T.Yonezawa, *J. Am. Chem. Soc.*, 1983, **105**, 426.
12. E.O. Fischer and A. Maasböl, *Chem. Ber.*, 1967, **100**, 2445.
13. Ch. Elschenbroich and A. Salzer, in *Organometallics,* VCH Publishers, 1989, 227-228.
14. W.A.Herrmann and C. Köcher, *Angew. Chem., Int. Ed. Engl.*, 1997, **36**, 2162-2187.
15. J. Barluenga and F.J. Fañanás, *Tetrahedron*, 2000, **56**, 4597-4628.
16. K.H. Dötz, H. Fischer, P. Hoffmann, F.R. Kriessl, U. Schubert and K.Weiss, in *Transition Metal Carbene Complexes*, Verlag Chemie, Weinheim, 1983, 2-68.
17. H. Fischer, in *The Chemistry of the Metal Carbon Bond*, Ed. S Patai, Wiley Interscience, New York, 1982, **1**, 181.
18. F.J. Brown, *Prog. Inorg. Chem.*, 1980, **27**, 1.
19. E.O. Fischer and A Maasböl, *Chem. Ber.*, 1967, **100**, 2445.
20. E.O. Fischer, H. Fischer, *Chem. Ber.*, 1974, **107**, 657.
21. A. Neveling, *M.Sc.-thesis*, University of Stellenbosch, 1999.
22. L. van Niekerk, *M.Sc.-thesis*, University of Stellenbosch, 2000.
23. G. Heydenrych, *M.Sc.-thesis*, University of Stellenbosch, 2001.

24. H.G. Raubenheimer and E.O. Fischer, *J. Organomet. Chem.*, 1975, **91**, C23.

25. N.J. Long in *Metallocenes*, Blackwell Science, London, 1998, 230-231.

26. M. Bochmann in *Organometallics Part 1: Complexes with transition metal-carbon σ-bonds*, Oxford University Press, Oxford, 1996, 70.

27. V. Crocq, J.C. Daran, Y. Keannin, B. Eber and G. Huttner, *Organometallics*, 1991, **10**, 448.

28. M. Havranek, M. Husak and D. Dvorak, *Organometallics*, 1995, **14**, 5024.

29. F.E. Haln and M. Tamm, *J. Chem. Soc., Chem. Comm.*, 1993, 842.

30. W. Petz, F. Weller and F. Schmock, *Z. Anorg. Allg. Chem.*, 1998, **624**, 1123.

31. B. Neumuller, H. Riffel and E. Fluck, *Z. Anorg. Allg. Chem.*, 1996, **588**, 47.

32. W. Petz, F. Weller and E.V. Avtomonov, *J. Organomet. Chem.*, 2000, **598**, 403.

CHAPTER 2

PREPARATION AND CHARACTERISATION OF METALOXYCARBENE COMPLEXES

2.1 INTRODUCTION

One group of metaloxycarbene complexes is represented by the general formula:

$[L^1_nM^1{=}C(R)OM^2L^2_n]$

with $L^1_nM^1$ a metal in low oxidation state containing one or more carbonyl ligands. In this thesis $L^1_nM^1$ will be [$(CO)_5M$ (M=Cr, Mo, W) or $(CO)_4M$ (M=Fe)]. Whereas $M^2L^2_n$ will contain dicyclopentadienyl complex units of Zr, Ti and Hf.[1-3]

In the past these complexes proved difficult to synthesise, as the group 4 transition metals are oxophilic. Column separation proved impossible for zirconium complexes.

2.2 HISTORICAL OVERVIEW AND METHODS OF PREPARATION

Numerous publications and review articles on carbene chemistry have been published since its humble beginnings.[4-7] This is not the place for another extensive review and only some results that are particularly interesting or related to the current work, are reported here.

The first metaloxycarbene complex was synthesised by Fischer and Fontana in 1964 from $[(CO)_5Cr{=}C(O)CH_3\}]Li$ and Cp_2TiCl_2 in methylenechloride, at room temperature.[8] The reaction yielded both the mono- (**5a**) and disubstituted titaniumoxycarbene complexes (**6a**) as products (Scheme 2.1).

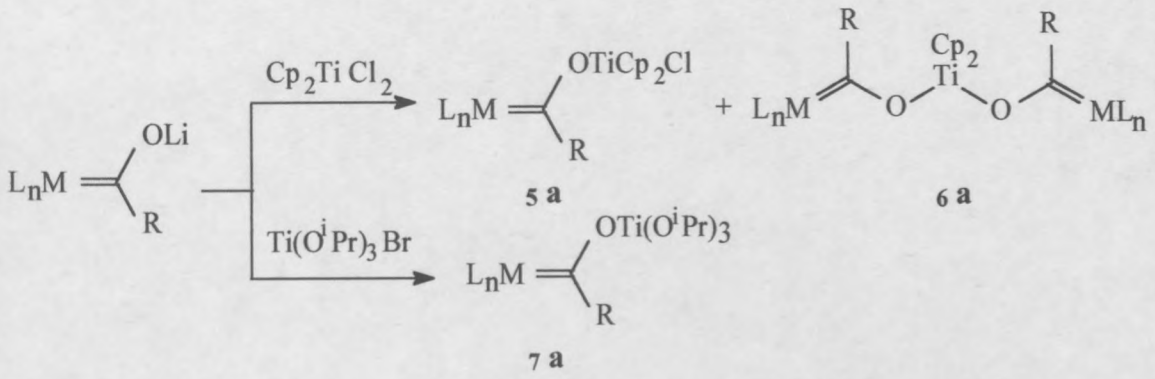

L_nM=$(CO)_5Cr$, $(CO)_5Mo$, $(CO)_5W$, $Cp^1(CO)_2Mn$, (Cp^1 =MeC_5H_4)

R=NMe_2, Me, Bu, C(Me)=CH_2, Ph, 4-MeC_6H_4

Scheme 2.1: Mono- and disubstituted titaniumoxycarbene complexes (**5a** and **6a**) prepared by Fischer and Fontana

A few years later Raubenheimer and Fischer did similar reactions with $[(CO)_5Cr=C(R)O]Li$, (R=Ph or NMe_2), and $[Cp_2TiCl_2]$ to obtain the metaloxycarbene complexes $[(CO)_5Cr=C(R)OTi(Cl)Cp_2]$, (R=Ph or NMe_2).[9] Organic solutions at –30°C and at room temperature of these complexes showed the solutions of the complex containing the phenyl substituent to be less stable than the corresponding solutions of the complex containing the anionic group. This is probably due to the strong double bond character of the $C_{carbene}$-N bond, which helps to stabilise the electron poor carbene carbon atom.

Alder and co-workers later confirmed this assumption. They showed the barrier of rotation around the $C_{carbene}$-N bond, for the aminooxycarbene complex, to be 88 kJ/mol. Thus the nitrogen atom provides most of the stabilisation of the carbene.[10]

Petz used a second synthesis route to prepare metaloxycarbene complexes (Scheme 2.2).[11] He inserted a group 6 metalcarbonyl (M=Cr, Mo, W) into an early transition metal ligand bond eg. $[Ti(NMe_2)_4]$. The insertion route can be controlled by the Fischer route (Scheme 2.3) that involves the nucleophilic attack on the electrophilic carbon metaloxycarbene complex, followed by the reaction with an electrophile (oxophilic group 4 metal unit).[12]

$L_nM = (CO)_5Mo, (CO)_5W, (CO)_4Fe, (CO)_3Ni$

Scheme 2.2: Petz's carbonyl insertion

The success of this method depends on the reactivity equilibrium of the acylmetalate, it needs to be stabilised in order for **8a** to form, but if it is too stable (strong localisation of the negative charge on the L_nM group), it will resist the O-alkylation in the next step. Alkylation of the metal forms an acylcomplex, while C alkylation forms a ketone.[13-15]

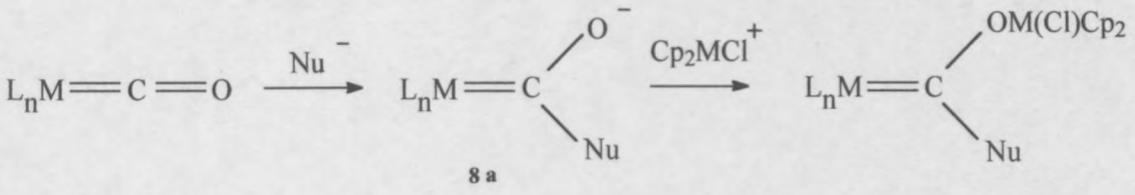

Scheme 2.3: Metaloxycarbene complex synthesised *via* the Fischer route

The carbonyl insertion method overcomes the limitations of the Fischer route by changing the sequence in the above-mentioned synthesis. The electrophilic group 4 metal (M^2) is first bonded to the metal carbonyl, followed by nucleophilic ligand transfer from the group 4 metal to the group 6 (M^1) metal carbonyl carbon atom.

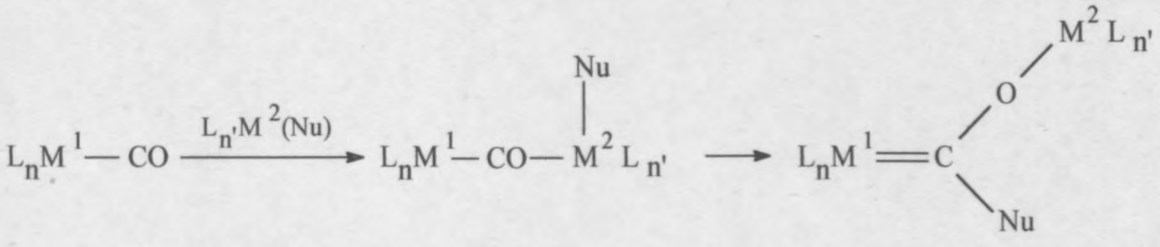

Scheme 2.4: Carbonyl insertion method

A wide range of metaloxycarbene complexes have been prepared, Grubbs used the Fischer method to synthesise $[(CO)_5Cr{=}C(Me)OM(Cl)L_2]$, (M = Ti, Zr; L = Cp, Cp*), while Finn developed titanoxycarbene complexes with the general formula $[(CO)_5Cr{=}C(R)OTi(O\text{-}i\text{-}Pr)_3]$ (Scheme 2.1, complex **7**).[16,17] Beck synthesised

rhenoxycarbene complexes, $[L(CO)_4M{=}C(Me)ORe(CO)_5]$ (M = Cr, Mo, W; L = CO, PPh_3; R = Me, Ph, Fc), from $[Re(CO)_5]^+$ and the related carbene complexes.[18]

Bercaw and coworkers focused their research on the insertion reactions of free CO into Zr-H- and Zr-R-bonds, resulting in an interesting product, $[Cp^*_2ZrH]_2(\mu\text{-O-CH=CHO})$ was obtained from the reaction of $[Cp^*_2Zr(CO)_2]$ with $[Cp^*_2ZrH_2]$ under H_2 (1atm).[19,20] They also synthesised zirconoxycarbene complexes using $[Cp^*_2ZrH_2]$ as a hydride source for coordinated metal carbonyls.

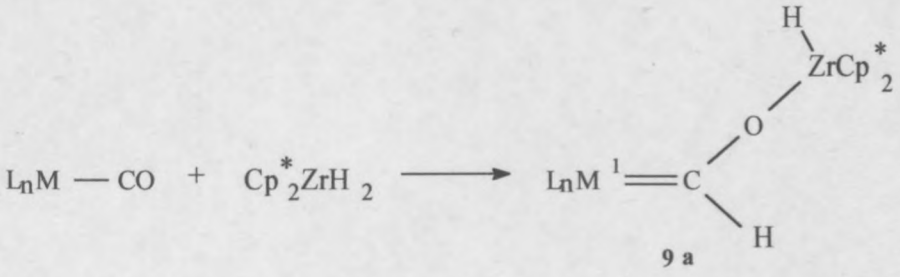

9 a

Scheme 2.5: Insertion reaction involving $[Cp^*_2ZrH_2]$

Erker and co-workers synthesised metaloxycarbene complexes using a method that avoids nucleophilic addition to metal carbonyls.[21] They found that metal carbonyls could be converted to carbenes by reacting the metal carbonyls with reactive η^2-olefin carbene complexes of group 4 metallocenes. Erker and co-workers have formed the titanoxycarbene complex **10a** from reaction of (η^2-benzyne)titanocene with diphenytitanocene in situ at 90°C.[21]

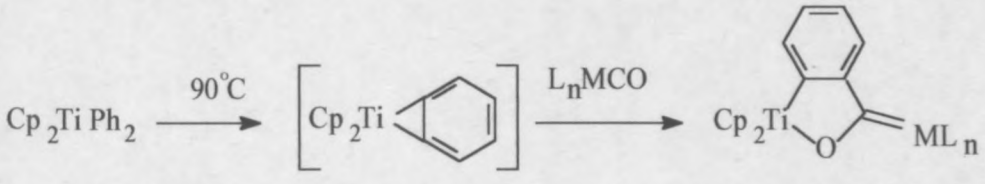

10 a

$L_nM = (CO)_5Mo, (CO)_5W$

Scheme 2.6: Fischer carbene complexes prepared without nucleophilic addition to metal carbonyls

Erker also used (butadiene)bis(cyclopentadienyl)zirconium to produce metallacyclic (η3-allyl)-metaloxycarbenes **11a** (Scheme 2.7), where M^1 = Zr; M^2L_n = $Cr(CO)_5$, $W(CO)_5$, Co(CpCl)CO, Co(Cp)Co, Rh(Cp)CO, $V(CO)_3Cp^7$ M^1 = Hf, M^2L_n = $Nb(CO)_3Cp$.[22-27]

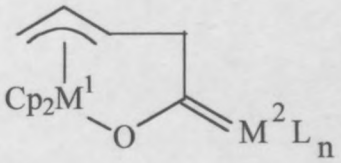

11 a

Scheme 2.7: Metallacyclic (η^3-allyl)-metaloxycarbenes complexes synthesised from (butadiene)bis(cyclopentadienyl)zirconium.

The reaction of (η^4-isoprene)zirconocene with [$W(CO)_6$] produced similar (π-allyl) zirconoxycarbene complexes.[28] Beckhaus and Thiele prepared similar metaloxycarbene complexes from [Cp*M($CH=CH_2$)$_2$] (M=Ti or Zr) and [$M^1(CO)_6$] (M^1=Cr, W or Mo).[29] Heterobimetallic complexes **14a** and **15a** were synthesised from the reaction of the metoxycarbene complexes **13a** and the vinylidenetitanocene **12**. This was the first example of an intermolecular coupling of inversely polarised carbene ligands.[30]

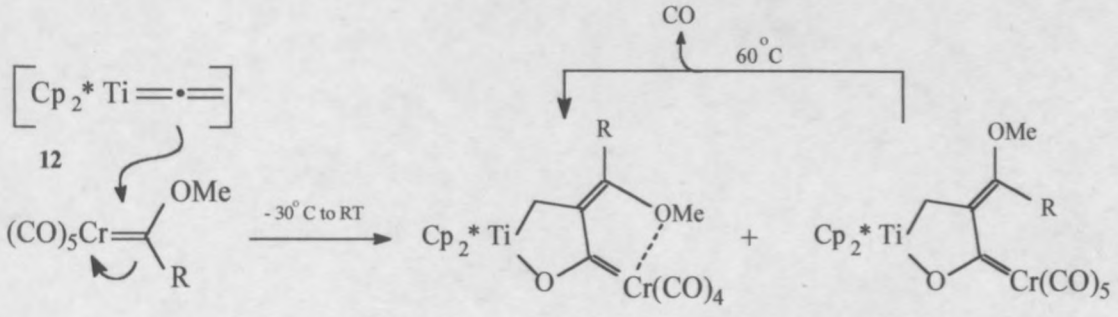

13 a **14 a** **15 a**

Scheme 2.8: Carbene complexes from vinylidenemetallocenes

After the discovery of Fischer-type metal-carbene complexes, independently Wanzlick and Öfele reported the existence of N-heterocyclic carbene complexes (**16** and **17**) (Figure 2.1).[31-33]

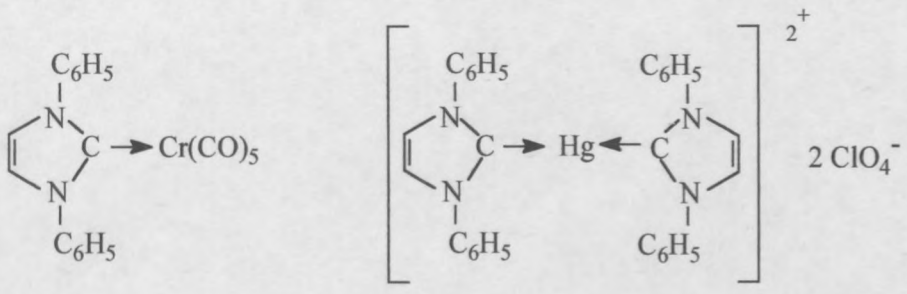

16 **17**

Figure 2.1: Heterocyclic carbene complexes

These complexes were obtained from imidazolium salts and metal-containing precursors able to deprotonate the organic substrate. In the first case a carbonylmetalate was used, while the mercury complex resulted from the metal acetate. In 1991 Arduengo opened the access to free isolable N-heterocyclic carbenes (**18**) and proved that these heterocyclic carbenes are in principle thermodynamically stable.[34]

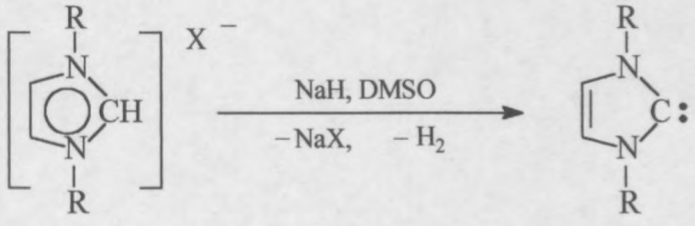

18

Scheme 2.9: Free isolable N-heterocyclic carbenes

His work started a revival. Others that followed in his wake were Herrmann, Denk, Tomioka, Kuhn and Cavell synthesising a range of heterocyclic and metaloxycarbene complexes consisting of various main group elements and lanthanides (Ge, Se, Te, Mg, Zn, Sc and Sm).[35-44]

Various methods are employed to synthesise metaloxycarbene complexes. Fischer's method is the most widely used synthesis route to prepare metaloxycarbene complexes. The activation of neutral acyl complexes, addition of electrophiles to carbyne complexes, and products fromed from isonitriles, or from alkynes, also afford carbene complexes.[45-49]

2.3 OTHER RECENT DEVELOPMENTS

Novel preparative routes and products have resulted from the ongoing research in the field of carbene chemistry, including cyclopropanation, the Dötz reaction, intramolecular C-H activation and photoluminescence.[50-57]

Recently Landman and Lotz reported the synthesis of carbene complexes with conjugated thiophene units (Scheme 2.10).[58] These polythiophenes **19** have been identified as molecules with potential electro-optical properties and some of the most stable molecular switching devices discovered to date include thiophene derivatives with conjugated thiophene units.

Thiophenes also feature as building units in spacer ligands of binuclear complexes focusing on molecular wires and in polynuclear conducting polymers.

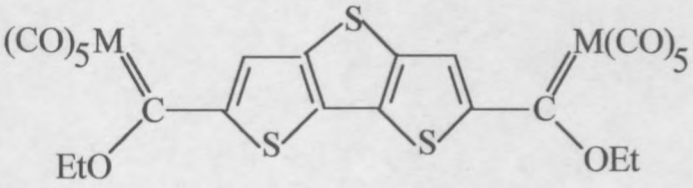

19

M = Cr , W

Scheme 2.10: Polythiophene carbene complexes

2.4 STRUCTURAL CONSIDERATIONS

Metaloxycarbene complexes like carbene complexes have more than one resonance form. In fact there are five contributing resonance structures with varying importance. The resonance structures A, E and B (Scheme 2.11) are similar to the resonance structures A, B and C (Scheme 1.2, Chapter 1) for the Fischer-type alkoxycarbene complexes. The resonance structures C and D (Scheme 2.11) are probably important due to the ability of the metal fragment [M^1] to accommodate the charge (negative or positive) compared to the alkyl group in alkoxycarbene complexes.

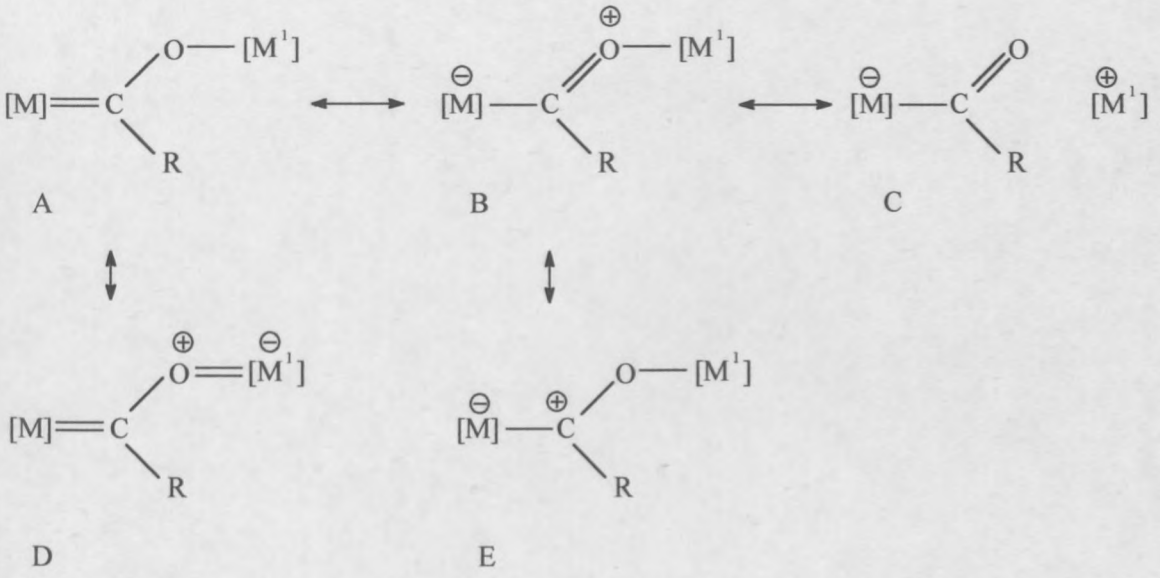

Scheme 2.11: Resonance structures: metaloxycarbene complexes

The contribution of the covalent acyl structure B and the anionic structure C are more important in metaloxycarbene complexes. Structure E is important in both the alkoxy- and metal alkoxycarbene complexes, while the contribution of structure A is probably marginal.

2.5 RESULTS AND DISCUSSION

2.5.1 Preparation of $[(CO)_5Cr{=}C(Me)O][NEt_4]$ **1**, $[(CO)_5Mo{=}C(Me)O][NEt_4]$ **2**, $[(CO)_5W{=}C(Me)O][NEt_4]$ **3**, $[(CO)_5W{=}C(Ph)O][NEt_4]$ **4**, $[(CO)_4Fe{=}C(Me)O][NEt_4]$ **5**, $[(CO)_5Cr{=}C(Me)OTi(Cl)Cp_2]$ **6**, $[(CO)_5Cr{=}C(t\text{-}Bu)OTi(Cl)Cp_2]$ **7**, $[(CO)_5Cr{=}C(Me)OZr(Cl)Cp_2]$ **8**, $[(CO)_5Mo{=}C(Me)OTi(Cl)Cp_2]$ **9**, $[(CO)_5W{=}C(Ph)OTi(Cl)Cp_2]$ **10**, $[(CO)_5W{=}C(Me)OTi(Cl)Cp_2]$ **11**, $[(CO)_5W{=}C(Me)OZr(Cl)Cp_2]$ **12**, $[(CO)_5W{=}C(Ph)OHf(Cl)Cp_2]$ **13**, $[(CO)_4Fe{=}C(Me)OTi(Cl)Cp_2]$ **14**

Oxycarbene complexes **1-5** were prepared according to the Fischer method. Reaction of these ammonium salts with $[Cp_2ZrCl_2]$ (for **8** and **12**) or $[Cp_2TiCl_2]$ (for **6**, **7**, and **10**) or $[Cp_2HfCl_2]$ (for **13**) in CH_2Cl_2 at –40°C produced metaloxycarbene complexes **6-8**, **10**, **13** and **14** (Scheme 2.1) after filtration and crystallisation from toluene. Complexes **9**, **12** and **14** were prepared in toluene using a similar method.

The first step in this synthesis involved the attack of an alkyllithium reagent on the electrophilic carbon of the metalcarbonyl unit. The reaction of methyl-, phenyl- and *t*-butyllithium (synthesis **1-5**) with $Cr(CO)_6$, $W(CO)_6$, $Mo(CO)_6$ and $Fe(CO)_5$ respectively, was conducted in diethylether or toluene. The final removal of unreacted metal carbonyl starting material by column chromatography was not feasible as the zirconoxycarbenes decompose on the Si-column. Filtering the aqueous solution of the lithium carbene salt and then crystallising the carbene salt thus removed the metal carbonyl. Higher yields of the metaloxycarbene complexes were obtained by first converting the lithium carbene salt to a tetraethylamonium carbene salt (Route A). Extraction of the aqueous filtrate with CH_2Cl_2 and removal of the solvent under vacuum resulted in a light yellow **1**, orange **2**, yellow **3**, **4** and purple **5** ammonium salt respectively.

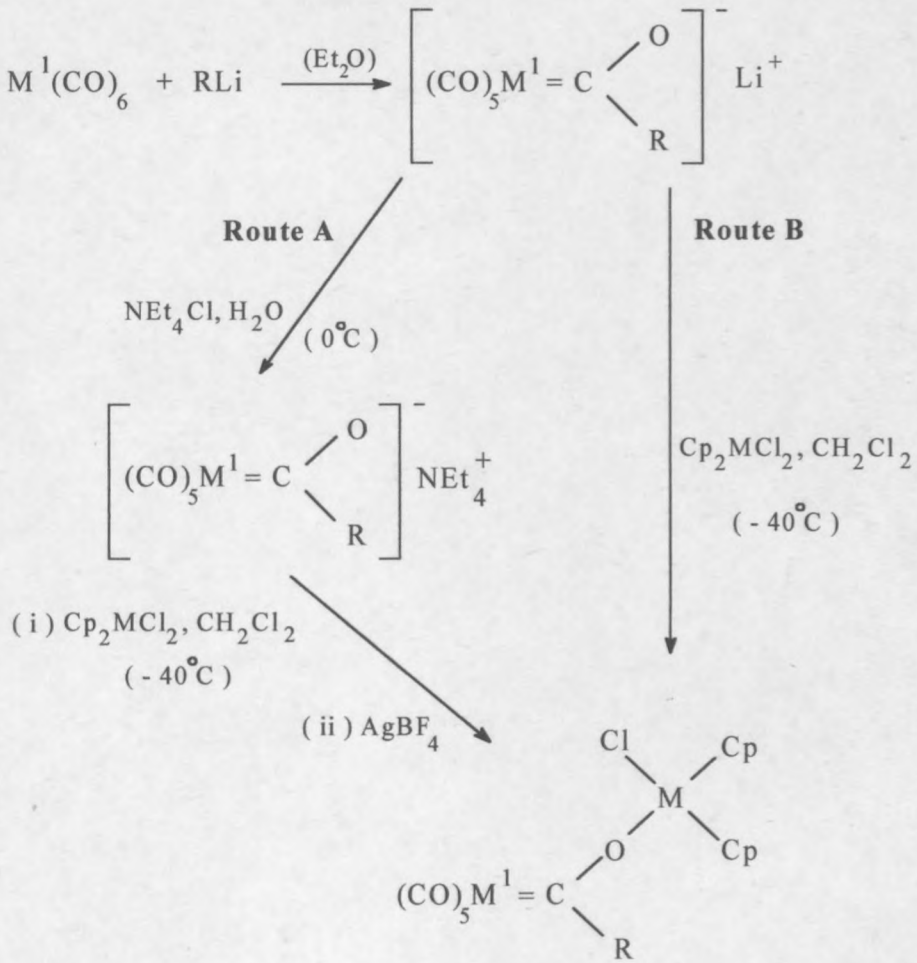

Scheme 2.12: Preparation of metaloxycarbene complexes from metalcarbonyls *via* the Fischer route

Addition of $AgBF_4$ to a mixture of compound **1** and $[Cp_2ZrCl_2]$ in dichloromethane encouraged removal of the chloride form the zirconocene center, and formation of the Zr-O bond. AgCl and Et_4NBF_4 precipitated and was removed *via* filtration. Filtration, concentration and subsequent layering afforded dark yellow crystals of compound **8** at -6°C. Similarly complexes **6, 7, 9-14** were prepared from the reaction of the respective ammonium salts and the metallocenes.

Crystals and microcrystalline powders of complexes **1-4** were stable in air for short periods of time, while the ammonium salt **5** decomposed even at slight exposure to air or moisture. Complexes **6-14** were stable in the absence of oxygen or water in solid form, but decomposed slowly in solution.

The alkoxycarbene complexes **1-5** and the metaloxycarbene complexes **6-14** were thermally unstable and decomposed in solution at elevated temperatures. The ammonium salts **1-5** were soluble in water and CH_2Cl_2, and complexes **6-14** dissolved in aromatic and polar organic solvents.

The reaction of ammonium salts with $[Cp_2ZrCl_2]$ (performed at -40°C) was also carried out in toluene. Diethyl ether may inhibit the reaction, due to solvent association to the zirconocene (the Zr(IV) center is oxophilic). During the synthesis of titanoxycarbene complexes, Fischer and Raubenheimer found that the disubstituted product was evident for reactions carried out at room temperature, while reactions performed at –30°C mainly afforded the monosubstituted product.[9]

2.5.2 Spectroscopic characterisation of the new compounds

2.5.2.1 NMR Spectroscopy

The NMR results will be presented as follows: the first part contains the results obtained for the ammonium salt of the acyl complexes **1-5**, while the second part contains the results for the metaloxycarbene complexes **6-14**. The NMR results for aryl and alkyl substituents on the carbene carbon, comparable results, trends and literature references are discussed alongside the NMR data table of each compound.

The ^{1}H and ^{13}C NMR results for complexes **1-5** are summarized in Tables 2.1, 2.2 and 2.3 respectively. Tables 2.4, 2.5, 2.6, 2.7 and 2.8 contain the NMR results obtained for complexes **6-14** respectively.

The NMR spectra for complexes **1** and **2** are very similar, with the carbonyls (*cis* and *trans*) of complex **1** resonating downfield from those obtained for complex **2**.

The chemical shift of a carbon is affected by the electronegativity of the atoms it is bonded to. Electronegative atoms attract electrons by pulling it away from the neighboring carbon atoms, causing the carbons to be deshielded and to resonate at lower field strength.

The chromium atom is slightly more electronegative (1.6 Allred-Rochow) than the molybdenum atom (1.3); this explains the differences observed in the chemical shifts of these complexes. Electron back donation from the transition metal atom to the carbonyl ligands is less in compound **1** due to the higher electronegativity of the chromium metal atom.

Table 2.1: ^{1}H and ^{13}C NMR data for complexes **1** and **2**

		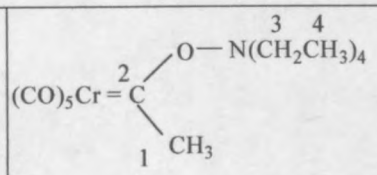	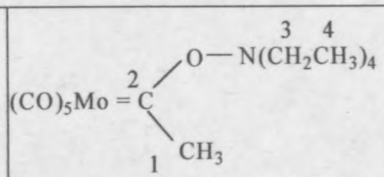
Complex		**1**	**2**
Solvent		Acetone-d_6	Acetone-d_6
^{1}H NMR:	H^1	2.42 (3H, s)	2.31 (3H, s)
	H^3	3.67 (2H, q, J=7.3)	3.67 (2H, q, J=7.3)
	H^4	1.55 (3H, tt, J=7.3, J=1.9)	1.54 (3H, tt, J=7.3, J=1.9)
^{13}C NMR:	C^1	53.5	55.7
	C^2	286.1	285.8
	C^3	53.0	53.5
	C^4	8.0	8.0
cis -	CO	226.1	214.5
trans -	CO	230.3	220.9

The carbonyls (*cis* and *trans*) resonate at higher field strengths from complex **1** to **2** and to **3**. This movement to lower frequency on descending down a triad is typical and is observed for the starting materials $Cr(CO)_6$ (212.5ppm), $Mo(CO)_6$ (202 ppm) and $W(CO)_6$ (192.5 ppm).[61]

The CO σ donor/π acceptor ratio becomes less for the carbonyl ligands from complex **1-3**, orbital overlap between the p-orbitals (carbonyl ligand) and the d-orbitals (metal atom) increases down the group from Cr to Mo and to W and leads to an increase in the π acceptor capability of the carbonyl ligands (valence bond approached).

Table 2.2: ^1H and ^{13}C NMR data for complexes **3** and **4**

Complex		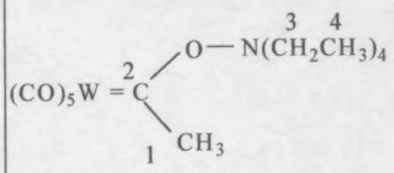 **3**	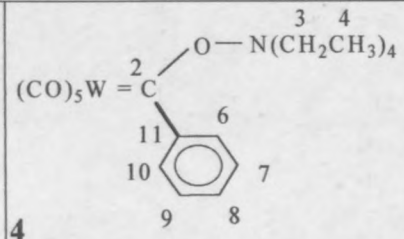 **4**
Solvent		Acetone-d_6	Acetone-d_6
^1H NMR:	H^1	2.26 (3H, s)	7.68 (5H, m)
	H^3	3.53 (2H, q, J=7.3)	3.64 (2H, q, J=7.3)
	H^4	1.41 (3H, tt, J=7.3, J=1.9)	1.52 (3H, tt, J=7.3, J=1.9)
^{13}C NMR:	C^1	58.0	-
	C^{11}	-	158.7
	$C^{6, 10}$	-	129.3
	$C^{7, 9}$	-	127.3
	C^8	-	128.7
	C^2	274.0	285.5
	C^3	53.5	53.5
	C^4	8.0	8.0
cis -	CO	206.4	205.4
trans -	CO	210.5	209.5

The chemical shifts of protons and carbon atoms are directly related to their electronic environment. In complexes **3** and **4** the effect of substituents (on the carbene atoms) becomes evident (Table 2.2).

The methyl group is inductively electron donating (compound **3**), while the phenyl group is an electron attracting substituent (compound **4**). The increase in electron density (due to the electron donating methyl group) stabilises the electron poor $C_{carbene}$ atom and it resonates at higher field strength.

Only one carbonyl chemical shift with high intensity is observed for the ammonium salt of the acyl complex **5**. At first glance one might conclude that complex **5** has a symmetric square pyramidal structure (Figure 2.2, b) in solution resulting in these carbonyl ligands being chemically equivalent.

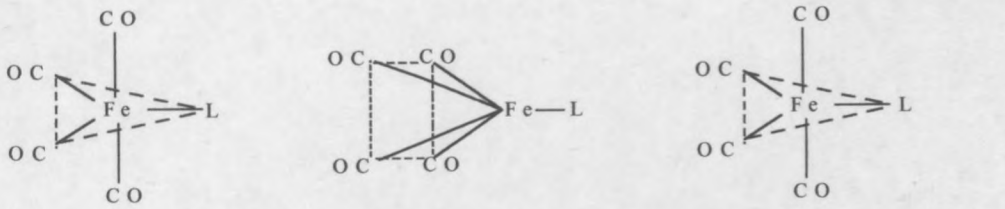

Figure 2.2: CO ligand interchange form trigonal bipyramidal to square pyramidal and back to trigonal bipyramidal (Berry's pseudorotation)

Table 2.3: ^{1}H and ^{13}C NMR data for complexes **5**

Complex		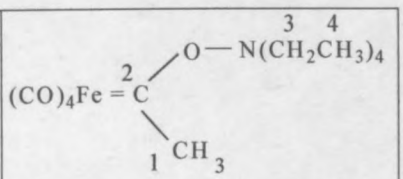 **5**
Solvent		Acetone-d_6
^{1}H NMR:	H^1	2.62 (3H, s)
	H^3	3.63 (2H, q, J=7.28)
	H^4	1.52 (3H, tt, J=7.28, J=1.87)
^{13}C NMR:	C^1	52.3
	C^2	262.9
	C^3	53.6
	C^4	8.1
	CO	223.1

Closer inspection of $(CO)_4Fe$-L type molecules shows that the one carbonyl chemical shift observed in the ^{13}C NMR spectrum is due to the fluxionality of complex **5**. It is well known that scrambling of axial and equatorial CO ligands occur rapidly in $Fe(CO)_5$, even at –170°C. Equatorial-axial exchange of CO groups occur, probably through Berry's pseudorotation from trigonal bipyramidal geometry to trigonal bipyramidal geometry *via* a square pyramidal geometry (Figure 2.2).[59]

The carbene carbon for the ammonium salt of the acyl complex **5** (262.9 ppm, Table 2.1) resonates at a higher field strength compared to the $C_{carbene}$ of complex **1** (286.1 ppm, Table 2.3). The carbene carbon atom is more shielded for complex **5** due to an increase in electron density available to help stabilise the electron poor carbene carbon atom. Four carbonyl ligands compete for electron backdonation for complex **5** compared to five for complex **1**, and the electron density available to the carbene carbon atom increases with former. The next section contains the results and subsequent discussion of the NMR results obtained for the metaloxycarbene complexes **6-14.**

Table 2.4: ^{1}H and ^{13}C NMR data for complexes **6** and **7**

Complex		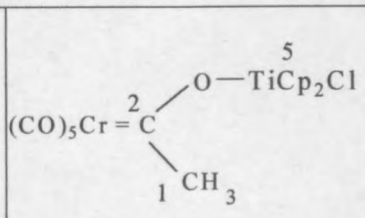 **6**	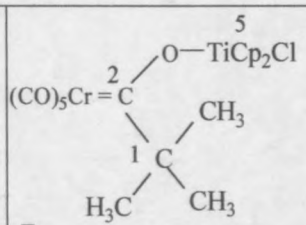 **7**
Solvent		Acetone-d_6	Acetone-d_6
^{1}H NMR:	H^1	2.83 (3H, s)	2.77 (3H, s)
	Cp	6.74 (10H, s)	6.66 (10H, s)
^{13}C NMR:	C^1	52.0	72.3
		-	26.6
		-	15.8
		-	13.7
	C^2	355.7	366.0
	C^5	120.5	121.0
cis -	CO	219.7	220.0
trans -	CO	226.8	225.9

The $C_{carbene}$ atom of complex **7** resonates at a lower field shift compared to complex **6** (Table 2.4). Van Niekerk prepared a complex similar to complexes **6** and **7**, but with n-butyl as substituent on the carbene carbon atom.[60] An NMR spectrum recorded in acetone-d_6 revealed a carbene signal at 361.6 ppm. Deshielding of the $C_{carbene}$ is probably due to decrease in the inductive electron donating ability of the alkyl as a result of branching or an increase in chain length.

The chromium(0) metal atom is slightly more electronegative than the tungsten(0) transition metal atom, the electron density on the carbene carbon atom decreases and it comes into resonance at a lower field (deshielded).[11]

Table 2.5: ^{1}H and ^{13}C NMR data for complexes **8** and **12**

Complex	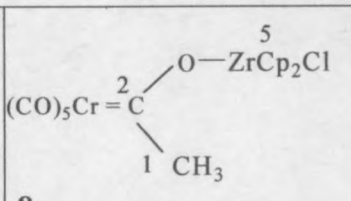 **8**	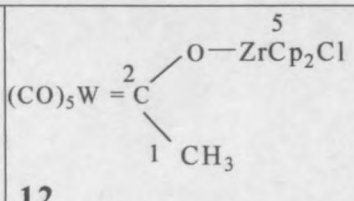 **12**
Solvent	Toluene-d_8	Toluene-d_8
^{1}H NMR: H^1	2.54 (3H, s), 2.44 (3H, s)	2.46 (3H, s)
Cp	5.88 (5H, s), 6.01 (5H,s)	5.93 (5H, s), 6.04 (5H, s),
^{13}C NMR: C^1	53.1	55.8
C^2	369.4	342.5
C^5	116.6, 116.2, 115.	116.1, 115.8, 114.5
cis - CO	219.7	191.6
trans - CO	225.8	199.8

Results obtained for complexes **8** and **12** show the effect the group 6 metal atoms have on the chemical shift observed, and the role electronegativity and the metal ligand σ-donor π-acceptor interactions have on the chemical shift observed. Electron back donation from the transition metal atom to the carbonyl ligands is less in compound **8**, compared to complex **12**, due to the higher electronegativity of the chromium metal atom.

The carbonyls (*cis* and *trans*) resonate at higher field strengths from complex **8** to **12**, increased orbital overlap between the p_π-orbitals (carbonyl ligand) and the d_π-orbitals

carbonyl ligands. Thus the carbonyl ligands of complex **12** are more shielded than the carbonyl ligands of complex **8**, and resonate at a higher field shift.

The ^{1}H and ^{13}C NMR spectra show more than one cyclopentadienyl signal for metaloxycarbene complexes **8** and **12** (Table 2.5). This is possibly due to configurational isomers (Figure 2.3).[61] Restricted rotation around the $C_{carbene}$-O bond changes 1a into 1c and 1b into 1d, while rotation around the Zr-O bond changes 1a into 1d and 1b into 1c. The two sets of isomers 1a/1b and 1c/1d exist due to inversion at the oxygen atom (Figure 2.3).[61,62] The differences in the intensities of the signal observed can be attributed to the stability of each configuration, with the less sterically hindered configuration favored.

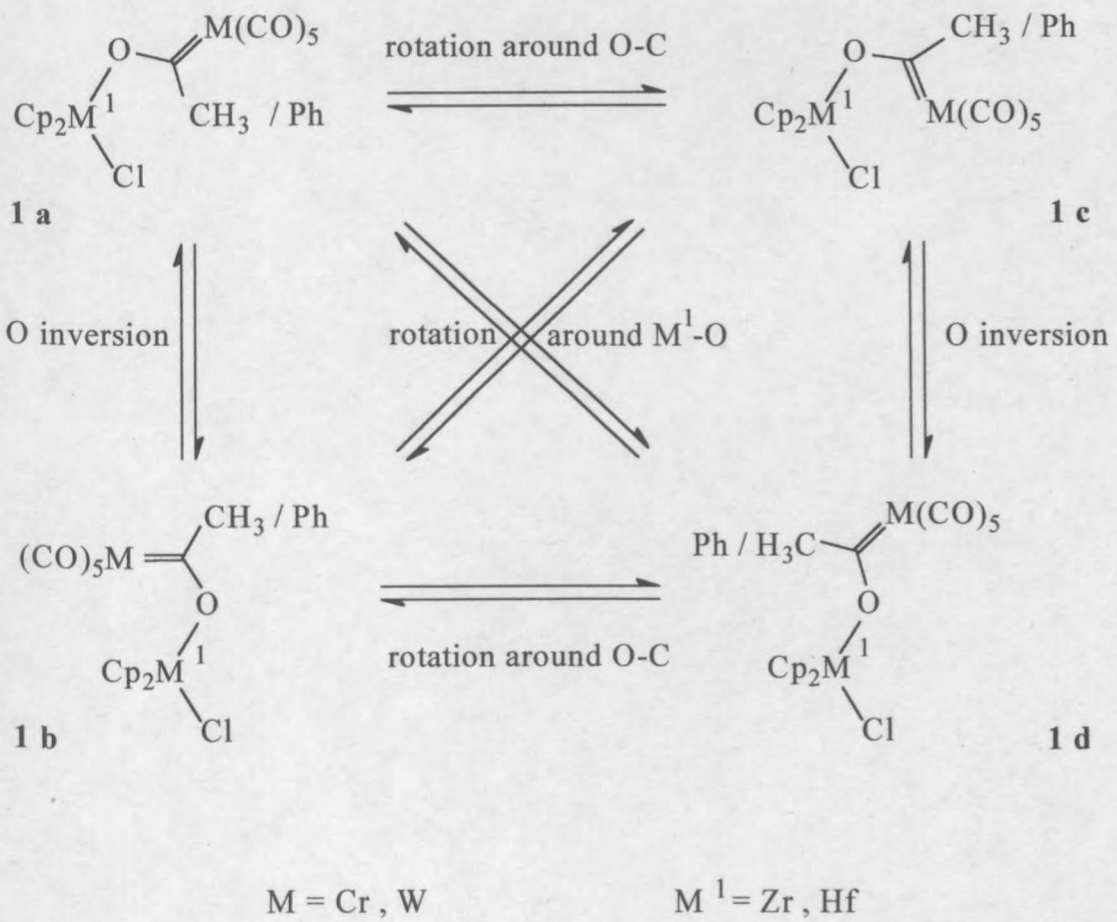

Figure 2.3: Different confonfigurational isomers for complexes **8, 12** and **13**

Similarly the ^{1}H NMR spectrum of complex **8** shows an additional methyl peak (with low intensity) at a chemical shift of 2.44 ppm, but only one methyl peak is observed for

complex **12**. The low intensity or absence of methyl peaks of the configurational isomers is probably a reflection of the relative importance of these configurational isomers. The short acquisition time of the ^{1}H NMR run, due to instability of complexes in solution, also lowers the intensity of the peaks observed.

The low intensity and absence of additional methyl peaks in the ^{1}H and ^{13}C NMR spectra can also be attributed to spin-rotational relaxation.[63,64] The methyl groups undergo transitions between one rotational state and another. The rate of relaxation induced is related to the spin-rotation correlation time (the average time between rotational transitions) and becomes significant for fast rotational speeds.

The carbon atom of sterically hindered methyl groups relaxes largely by dipole-dipole relaxation, while sterically unhindered methyl groups receive a large contribution from spin-rotation relaxation. The intensity of the signal observed for unhindered methyl groups is much lower than that observed for the hindered methyl groups, due to the contribution through spin-rotational relaxation.[63,64]

The results for complexes **9** and **10** are tabulated in Table 2.6.

Table 2.6: ^{1}H and ^{13}C NMR data for complexes **9** and **10**

Complex		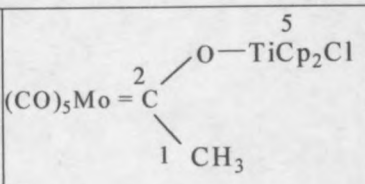 **9**	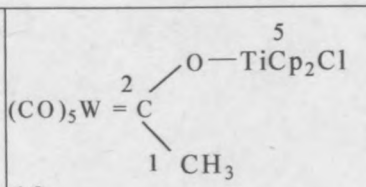 **10**
Solvent		Acetone-d_6	Toluene-d_8
^{1}H NMR:	H^1	2.74 (3H, s)	2.67 (3H, s)
	Cp	6.66 (10H, s)	5.99 (10H, s)
^{13}C NMR:	C^1	53.3	56.1
	C^2	349.4	322.5
	C^3	120.3	122.5
cis -	CO	208.6	195.5
trans -	CO	216.9	203.9

The carbonyls (*cis* and *trans*) resonate at higher field strength from complex **6** to **9** and to **10** (similar to the results observed for complexes **8** and **12**, Table 2.5). As was discussed earlier orbital overlap increases down the group and leads to an increase in the π acceptor capability of the carbonyl ligands, hence the chemical shift observed at higher field strength.

The carbene carbon atom resonates at higher field strength from complex **6** to **9** and to **10**. As was discussed earlier for complexes **8** and **12,** increased electronegativity of the transition metal and increased M-CO orbital overlap decrease the electrondensity available to help stabilise the electron poor carbene carbon atom.

Table 2.7: ^{1}H and ^{13}C NMR data for complexes **11** and **13**

Complex		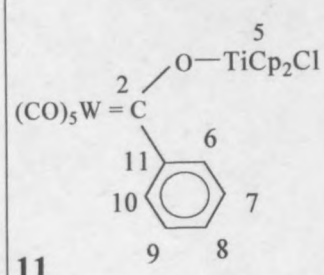 **11**		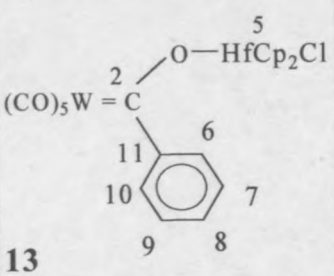 **13**
Solvent		Acetone-d_6	Toluene-d_8	Dichloromethane-d_2
^{1}H NMR:	H^{6-11}	7.24 (5H, m)	7.13 (5H, m)	7.45 (5H, m)
	Cp	6.04 (10H, s)	5.91 (10H, s)	6.50 (5H, s), 6.49(5H, s) 6.40 (5H, s), 6.37(5H, s)
^{13}C NMR:	C^{11}	155.3	156.2	156.4
	$C^{6, 10}$	133.2	138.8	132.9
	$C^{7, 9}$	127.3	130.4	127.4
	C^{8}	129.7	133.1	128.6
	C^{2}	326.2	328.9	333.1
	C^{5}	120.5	119.7	116.3, 115.4, 114.7, 113.5
cis -	CO	201.1	201.2	199.
trans -	CO	206.7	205.7	205.6

The ^{1}H and ^{13}C NMR spectra for complex **11** show only one cyclopentadienyl signal, 6.04 ppm and 120.5 ppm in acetone-d_6 and 5.91 ppm and 119.7 ppm in toluene-d_8 respectively. The ^{1}H NMR spectrum shows a multiplet at 7.05 to 7.40 ppm, which was assigned to the protons of the phenyl ring. The peaks observed correspond to the expected chemical shift values for aromatic rings.

Both the ^{1}H and ^{13}C NMR spectra show more than one cyclopentadienyl chemical shift for complex **13** (Table 2.7). As discussed earlier for complexes **8** and **12**, this is probably due to different configuration isomers (Figure 2.3). The phenyl group showed a signal at 7.45 ppm (average of multiplet). Although additional peaks were not identified, it cannot be ruled out as they might overlap, due to the complexity of the multiplet observed.

The phenyl group is bulky (in rotation) and we would expect the phenyl group to be hindered as is depicted for the relative configuration isomers in Figure 2.1. Thus fast rotation around the $C_{carbene}$-phenyl bond would be limited and the subsequent contribution of spin-rotational relaxation negligible.

Table 2.8 shows the results for the iron metaloxycarbene complex **14**. The carbene carbon atom of the anionic acyl carbene complex **5,** resonates at a lower field strength (262.9 ppm, Table 2.3) than the $C_{carbene}$ of the titanoxycarbene complex **14** (295.2 ppm, Table 2.8). This is probably due to the loss of negative charge in complex **14**, which in the anionic acyl complex is partly-delocalised.

Table 2.8: ^{1}H and ^{13}C NMR data for complexes **14**

Complex		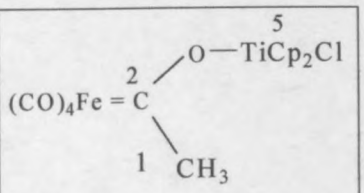 **14**
Solvent		Acetone-d_6
^{1}H NMR:	H^1	2.81 (3H, s)
	Cp	6.57 (10H, s)
^{13}C NMR:	C^1	47.8
	C^2	295.2
	C^5	117.8
Equatorial -	CO	212.2
Axial -	CO	211.1

20 **21**

Scheme 2.13: Resonance structures for the anionic acyl complex **5**

It was reported earlier that only one signal is observed for the anionic acyl complex **5**, due to fluxionality of complex **5**. Complex **14** shows two signals for the carbonyl groups in the ^{13}C NMR spectrum. The axial and equatorial carbonyl ligands are chemically non-equivalent. The metaloxycarbene ligand ($OTiCp_2Cl$) prefers an axial position (due to its σ-donor π-acceptor properties), which also does not allow scrambling between axial and equatorial CO ligands (because $OTiCp_2Cl$ disfavours occupation of an equatorial site).[63]

2.5.2.2 Mass Spectrometry

Mass spectra of complexes **6-14** were recorded using electron impact (EI) and fast atom bombardment (FAB) mass spectrometry techniques. EI transfers a large amount of energy, of high-energy electrons, to the sample molecules fragmenting them. FAB uses atoms, accelerated over a potential difference, to bombard the sample molecules, this is a softer technique compared to EI.

The results obtained for complexes **6-14** will be presented as follows: A short discussion will follow the FAB and EI fragmentation patterns of each complex and a general discussion and trends observed will follow at the end of this section.

2.5,2.2.1 Mass spectrometry of $[(CO)_5Cr{=}C(Me)OTi(Cl)Cp_2]$, **6**

The molecular ion of complex **6** is obtained with both techniques (FAB and EI). The fragmentation pattern, as illustrated in Scheme 2.11 consists of three main fragmentation routes. Route 1 involves the fragmentation of the group 4 metallocene ligand followed by the loss of four carbonyl ligands. Route 2 and 3 can be grouped together; they exhibit exactly the opposite sequence. Initially three and five carbonyl ligands, respectively, are fragmented followed by fragmentation of the cyclopentadienyl ligand. The [(CO)Cr-

$C(CH_3)]^+$ fragment observed can result following two different pathways. Although they are presented in Scheme 2.14 as pathway 1 and 2, conclusive proof of the mechanism involved can only be ascertained after further mechanistic studies have been conducted. For the purpose of this discussion both possibilities will be presented in the FAB fragmentation diagram for complex **6**.

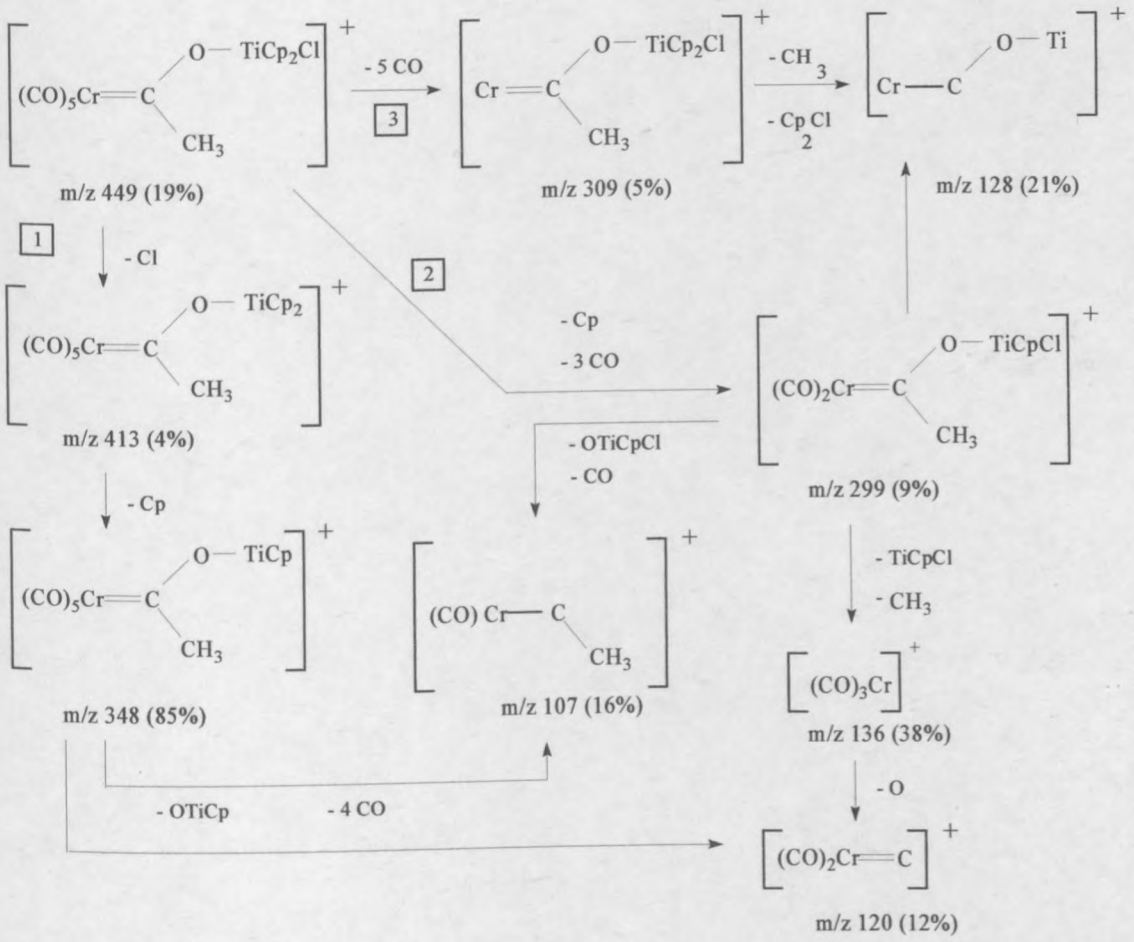

Scheme 2.14: FAB fragmentation diagram of $[(CO)_5Cr{=}C(Me)OTi(Cl)Cp_2]$ **6**

The resulting fragmentation pattern of complex **7** derived from EI mass spectrum data, represented in Scheme 2.15, is much more complex. The stepwise loss of carbonyl ligands results in a range of $[(CO)_xCr{=}C(Me)OTi(Cl)Cp_2]$ fragments (x=0-5), followed by fragmentation of the metallocene ligand to produce smaller fragments like $[(CO)_2Cr{=}OTi]^+$, $[Cr\text{-}C(CH_3)]^+$ and $[Cr\text{-}C\text{-}O]^+$. The fragments $[Cr\text{-}C(CH_3)O]^+$ and $[Cr\text{-}C(CH_3)]^+$ presented in Scheme 2.15 are possible following pathways 3 or 5.

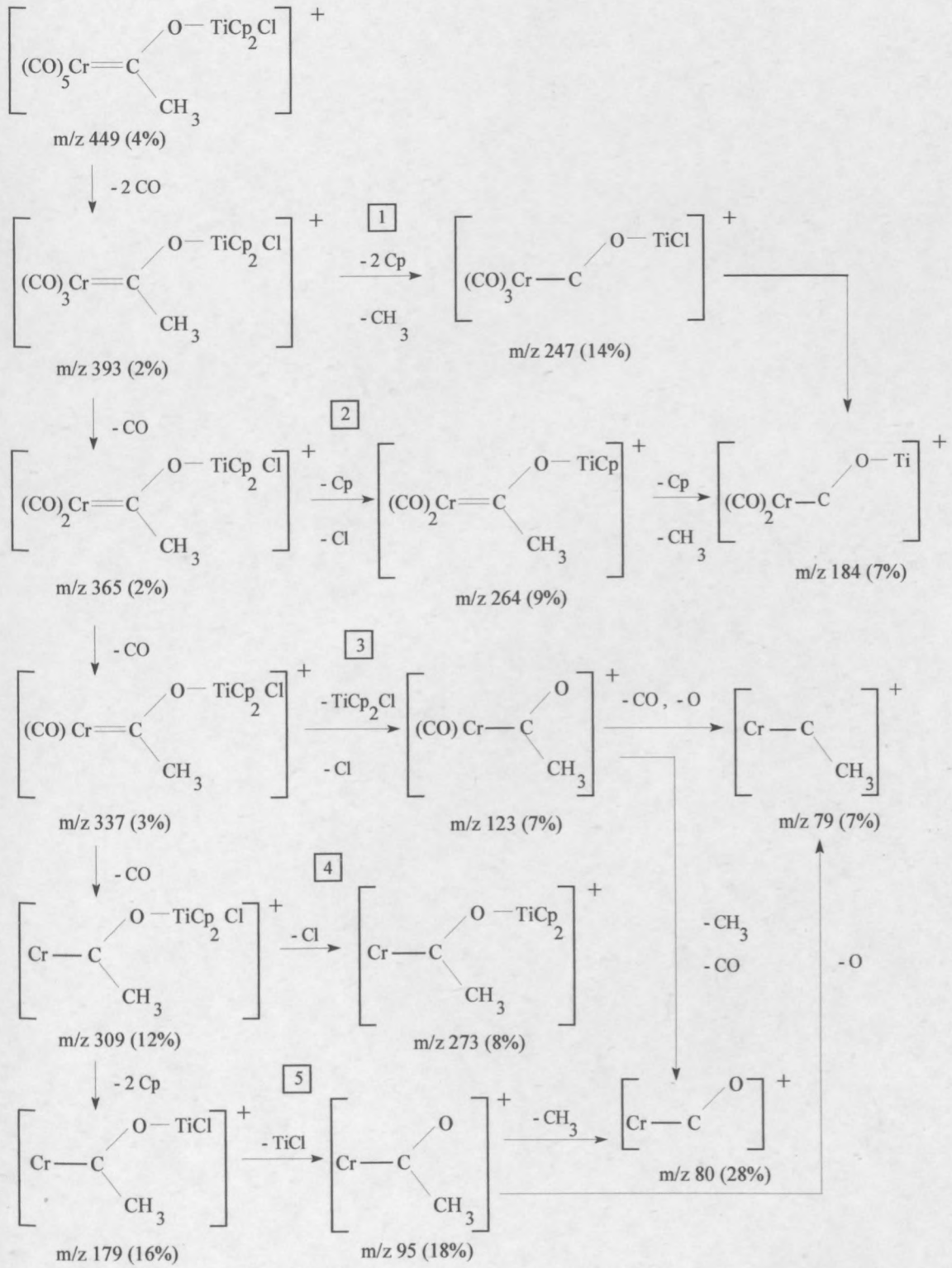

Scheme 2.15: EI fragmentation diagram of $[(CO)_5Cr{=}C(Me)OTi(Cl)Cp_2]$ **6**

2.5.2.2.1.2 Mass spectrometry of $[(CO)_5Cr{=}C(t\text{-Bu})OTi(Cl)Cp_2]$, **7**

The molecular ion is present in both the FAB and EI mass spectra of complex **7**. Scheme 2.16 shows the same branching pattern as the EI fragmentation pattern of $[(CO)_5Cr{=}C(Me)OTi(Cl)Cp_2]$ complex **6** (Scheme 2.15). Again stepwise loss of carbonyl ligands occurs resulting in a range of $[(CO)_xCr{=}C(t\text{-Bu})OTiCp_2Cl]^+$ fragments (x=0-5). Further fragmentation of these ions occurs forming smaller fractions (Scheme 2.16).

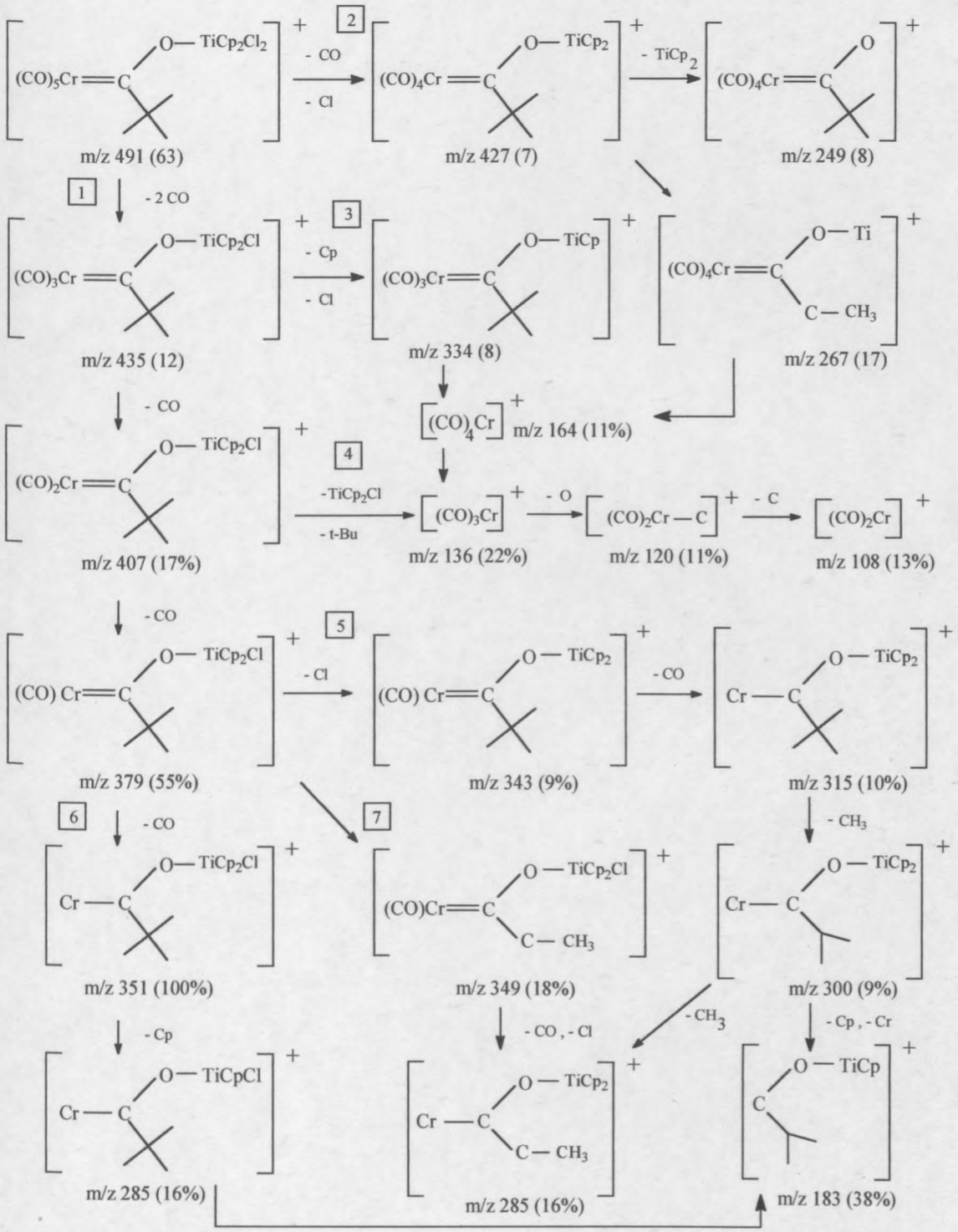

Scheme 2.16: FAB fragmentation diagram of $[(CO)_5Cr{=}C(t\text{-Bu})OTi(Cl)Cp_2]$ 7

The $[(CO)_3Cr]^+$ ion forms *via* steps 3 and 4, while the $[Cr\text{-}C(CCH_3)OTiCp_2]^+$ ion results from either steps 5 or 7. The $[TiCp_2Cl]^+$,- and $[TiCp_2]^+$-ions are very prominent in the FAB mass spectrum with intensities of 54% and 56% respectively.

The EI mass spectrum of complex **7** (Scheme 2.17) shows three main routes. Route 1 involves the loss of two carbonyl ligands, the methyl substituent on the carbene carbon and two cyclopentadienyl rings followed by fragmentation of the metallocene ligand.

Route 2 is characterised by metallocene ligand fragmentation (after initial CO loss) followed by stepwise loss of the carbonyl ligands, resulting in a range of $[Cr(CO)_x]$ fragments (x=0-5). Step 3 is concerned with the loss of five carbonyl ligands followed by the loss of the chromium metal atom and the fragmentation of the titanocene ligand (step 4).

The $[Cp]^+$ ion that is present forms the $[C_3H_3]^+$ radical after the loss of an acetylene fragment. The $[C_3H_3]^+$ ion is occasionally present in the spectra of dichlorometallocene compounds.[43] See Scheme 2.27 for the formation of the $[C_3H_3]^+$ ion.

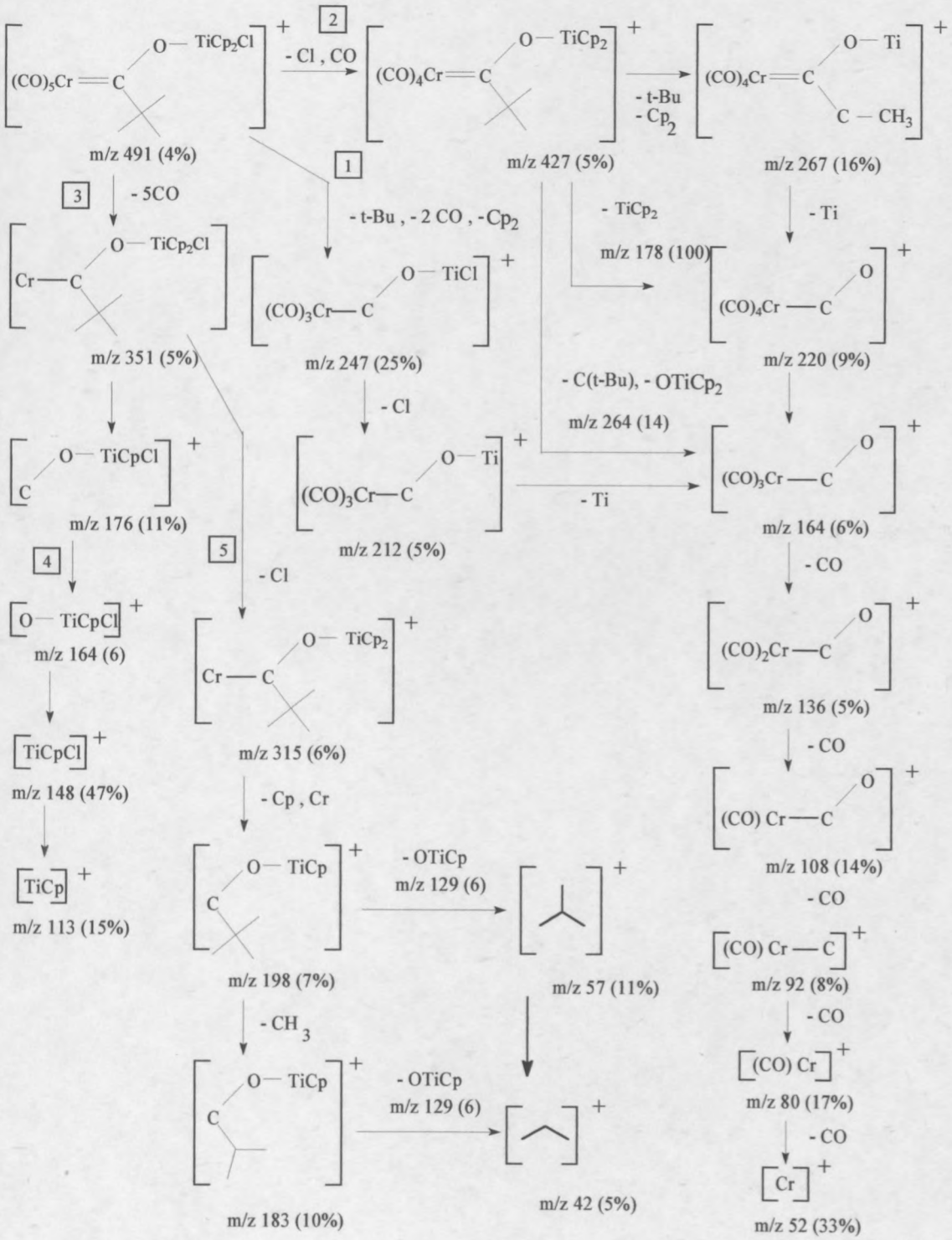

Scheme 2.17: EI fragmentation diagram of $[(CO)_5Cr{=}C(t\text{-Bu})OTi(Cl)Cp_2]$ **7**

2.5.2.2.1.3 Mass spectrometry of $[(CO)_5Cr{=}C(Me)OZr(Cl)Cp_2]$, **8**

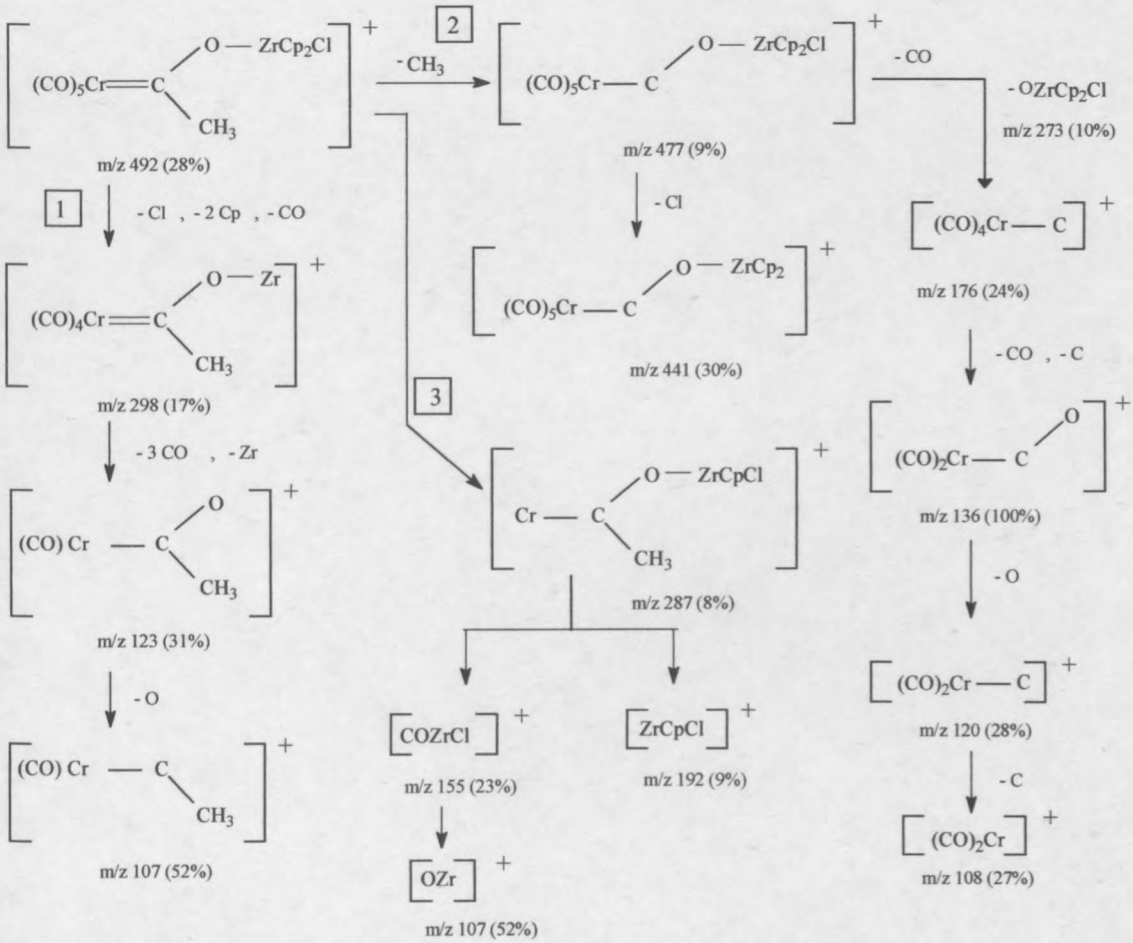

Scheme 2.18: FAB fragmentation diagram of $[(CO)_5Cr{=}C(Me)OZr(Cl)Cp_2]$ **8**

Complex **8** undergoes fragmentation of the metallocene ligand and loss of a carbonyl ligand simultaneously to form the $[(CO)Cr\text{-}C(CH_3)]^+$ ion (Scheme 2.18, route 1). During route 2 loss of the methyl group occurs followed by loss of the $[OZrCp_2Cl]^+$ ion and a carbonyl ligand to form the $[(CO)_4Cr\text{-}C]^+$ ion. This ion is fragmented with stepwise loss of a carbonyl ligand to form the $[(CO)_2Cr]^+$ ion.

Route 3 is concerned with initial carbonyl loss and fragmentation of the metallocene ligand, followed by the loss of three carbonyl ligands and the zirconium atom. The molecular ion is observed in the FAB mass spectrum for complex **8**.

In the EI spectrum a range of $[Cr(CO)_x]^+(x=5)$ and $[(CO)_yCr=C(OZrCp_z)]^+(y=2, 3$ and $z=1, 0)$ fragments result from fragmentation of the metallocene ligand and carbonyl loss (Scheme 2.19).

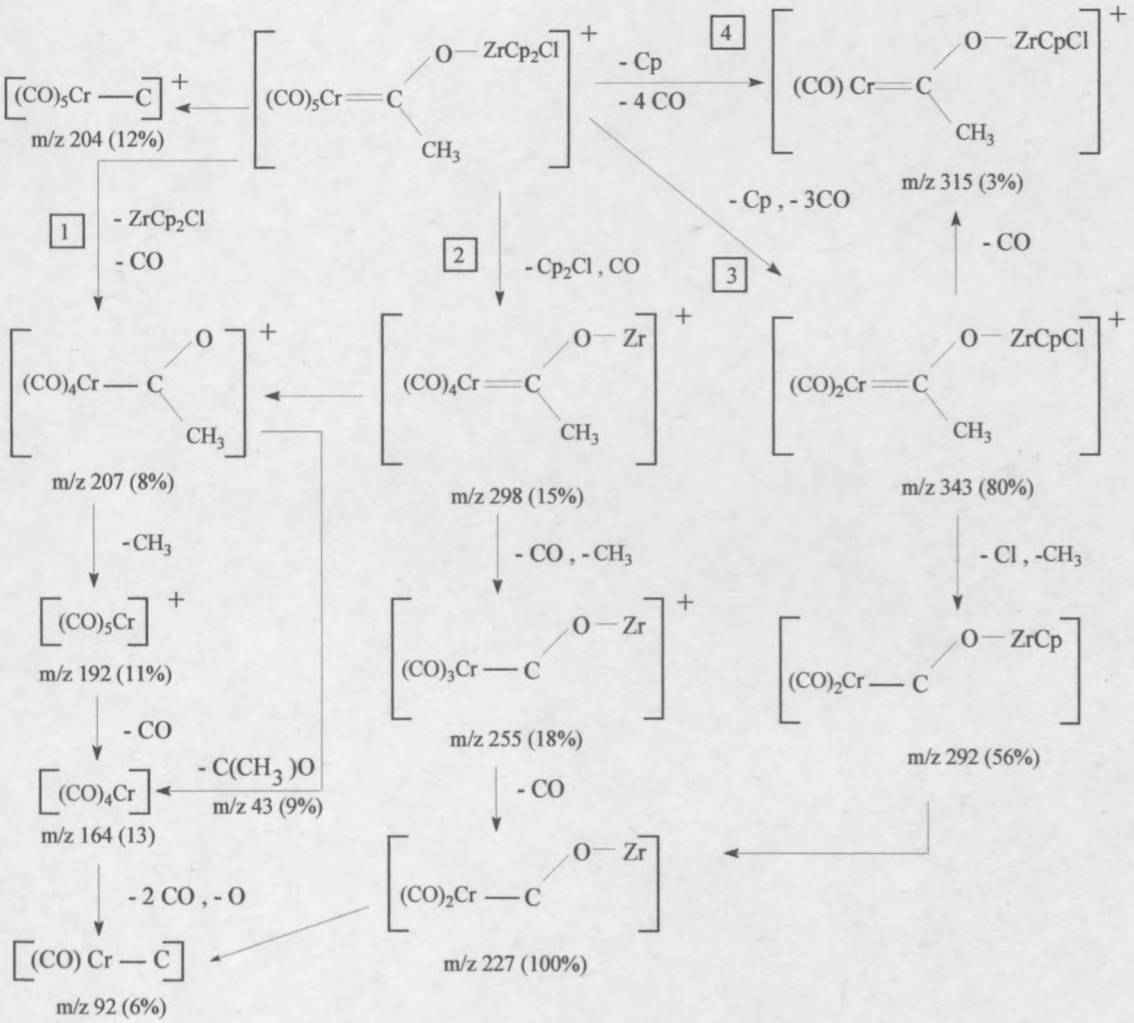

Scheme 2.19: EI fragmentation diagram of $[(CO)_5Cr=C(Me)OZr(Cl)Cp_2]$ **8**

Four main fragmentation routes are identified. Route 1 involves the loss of the bis(cyclopentadienyl)zirconocene-chloride fragment and a carbonyl ligand. After the loss of a methyl group the $[(CO)_5Cr]^+$ ion is formed and further carbonyl loss resulted in the formation of the $[(CO)Cr\text{-}C]^+$ ion. Route 2 formed the $[(CO)_4Cr=C(CH_3)OZr]^+$ ion, which underwent further fragmentation to form $[(CO)_4Cr\text{-}C(CH_3)O]^+$ and $[(CO)_xCr\text{-}COZr]^+$ as ions (x=2, 3).

Routes 3 and 4 are characterised by the initial loss of a cyclopentadienyl ring and the loss of three and four carbonyl ligands, respectively. The $[(CO)_4Cr{=}C(CH_3)O]^+$ ion can form through routes 1 and 2, and $[(CO)Cr{=}C(CH_3)OZrCpCl]^+$ can form via routes 3 or 4.

2.5.2.2.1.4 Mass spectrometry of $[(CO)_5Mo{=}C(Me)OTi(Cl)Cp_2]$, **9**

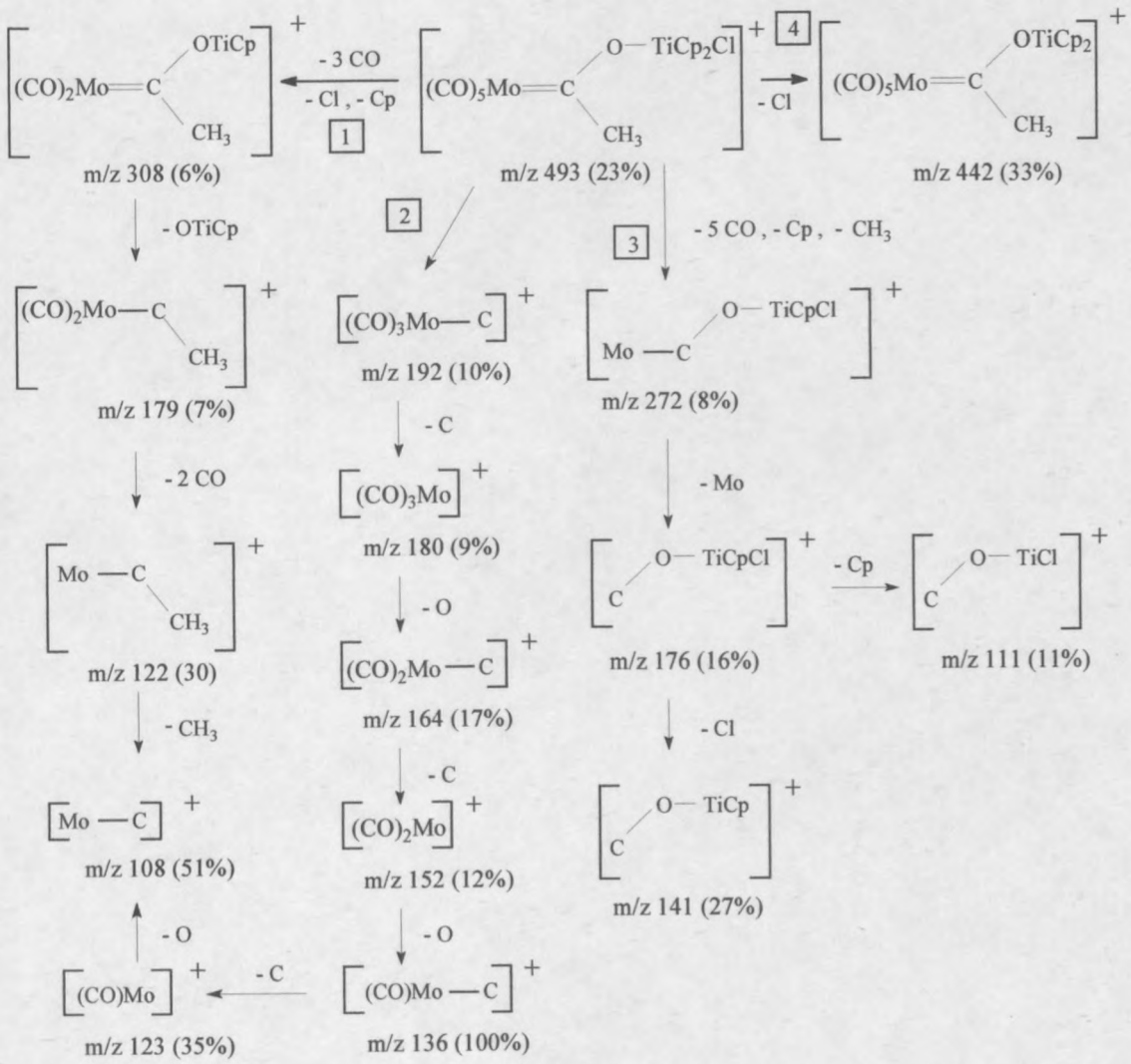

Scheme 2.20: FAB fragmentation diagram of $[(CO)_5Mo{=}C(Me)OTi(Cl)Cp_2]$ **9**

Four fragmentation routes are identified (Scheme 2.20). Route 1 involves the initial loss of three carbonyl ligands followed by the fragmentation of the metallocene ligand and loss of two additional carbonyl groups. In the last step the $[Mo\text{-}C]^+$ ion is formed with the loss of the methyl substituent on the carbene carbon atom. The $[(CO)_3Mo\text{-}C]^+$ ion forms at the start of fragmentation pathway 2 and is followed by alternative loss of a

carbon atom and a oxygen atom to yield a range of $[(CO)xMo\text{-}C]^+$ and $[(CO)xMo]^+$ ions (x=0-3).

Five carbonyl groups and the methyl substituent are lost at the start of route 3. The resulting $[Mo\text{-}C(OTiCp_2Cl)]^+$ ion undergoes loss of the Mo and Cl atoms and/or cyclopentadienyl rings to form $[C(OTiCp)]^+$ and $[C(OTiCl)]^+$ as ions. The loss of a single chloride atom represents route 4. The $[Mo\text{-}C]^+$ ion forms according to route 1 or 2, both possibilities are presented in Scheme 2.20.

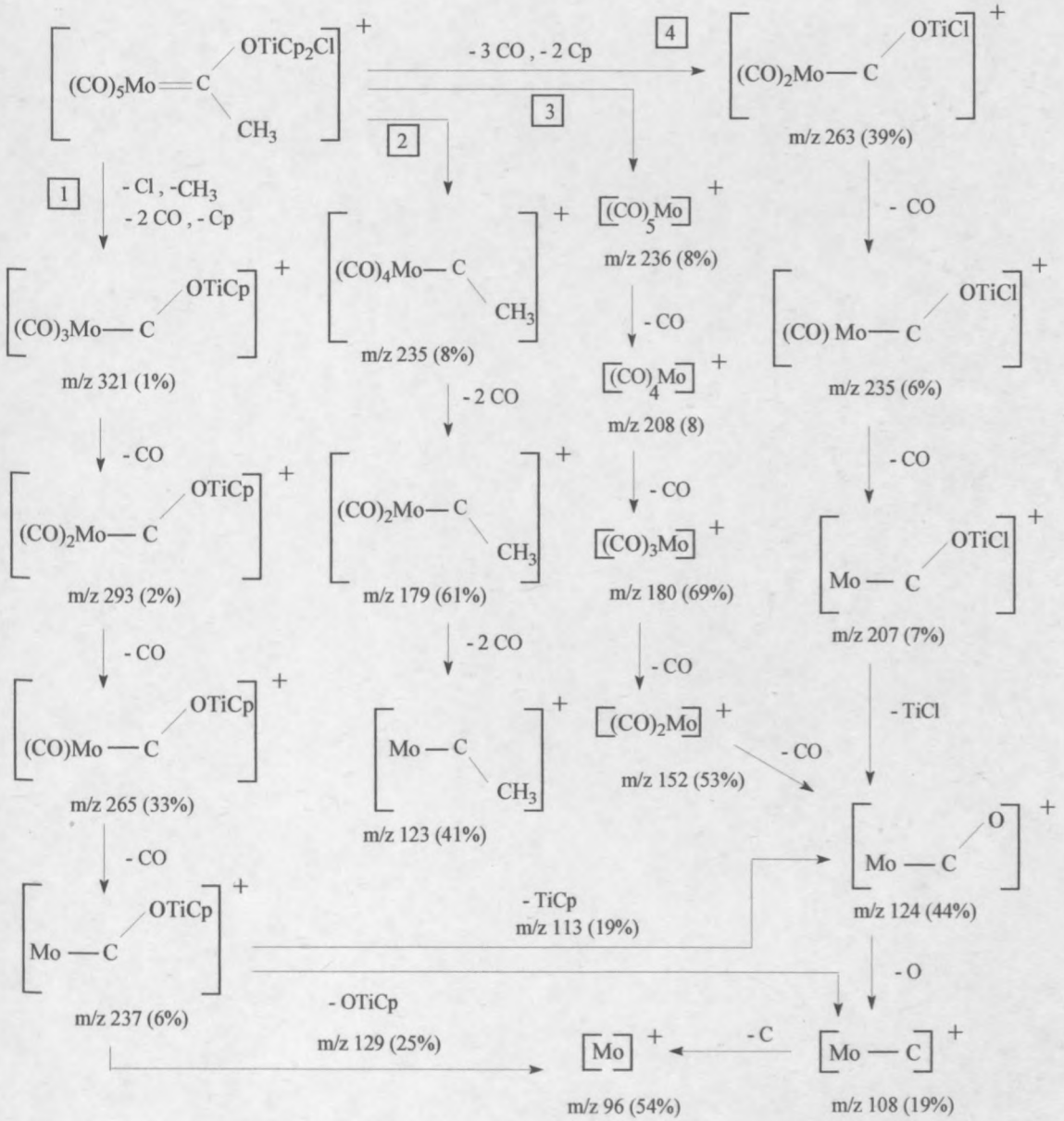

Scheme 2.21: EI fragmentation diagram of $[(CO)_5Mo{=}C(Me)OTi(Cl)Cp_2]$ **9**

The molecular ion present in the FAB spectrum is not observed in the EI spectrum of complex **9**. Four main pathways are identified. The start of the EI fragmentation pattern is characterised by the loss of two and three carbonyl ligands and the partial fragmentation of the metallocene ligand (routes 1 and 4 respectively).

The formed $[(CO)_3Mo\text{-}C(OTiCp)]^+$ and $[(CO)_2Mo\text{-}C(OTiCl)]^+$ ions undergo further fragmentation through stepwise carbonyl ligand loss forming a range of $[(CO)_xMo\text{-}C(OTiNu)]^+$ ions (x=3 or 2 as is relevant and Nu=Cp or Cl). The loss of a TiCp or a TiCl fragment leads to formation of the $[Mo\text{-}CO]^+$ ion (Scheme 2.21).

Route 2 is characterised by the loss of the $TiCp_2Cl$ fragment and one carbonyl ligand, followed by stepwise carbonyl loss. The $[(CO)_5Mo]^+$ ion that forms (route 3) undergoes stepwise carbonyl loss resulting in a range of $[(CO)_xMo]^+$ ions (x=0-5).

2.5.2.2.1.5 Mass spectrometry of $[(CO)_5W{=}C(Me)OTi(Cl)Cp_2]$, **10**

The molecular ion is present in both the FAB and EI spectra of complex **10**. Three different routes are identified. Route 1 shows the loss of the $[OTiCp_2Cl]$ fraction, the methyl group on the carbene carbon atom and a carbonyl ligand, forming the $[(CO)_4W\text{-}C]^+$ ion.

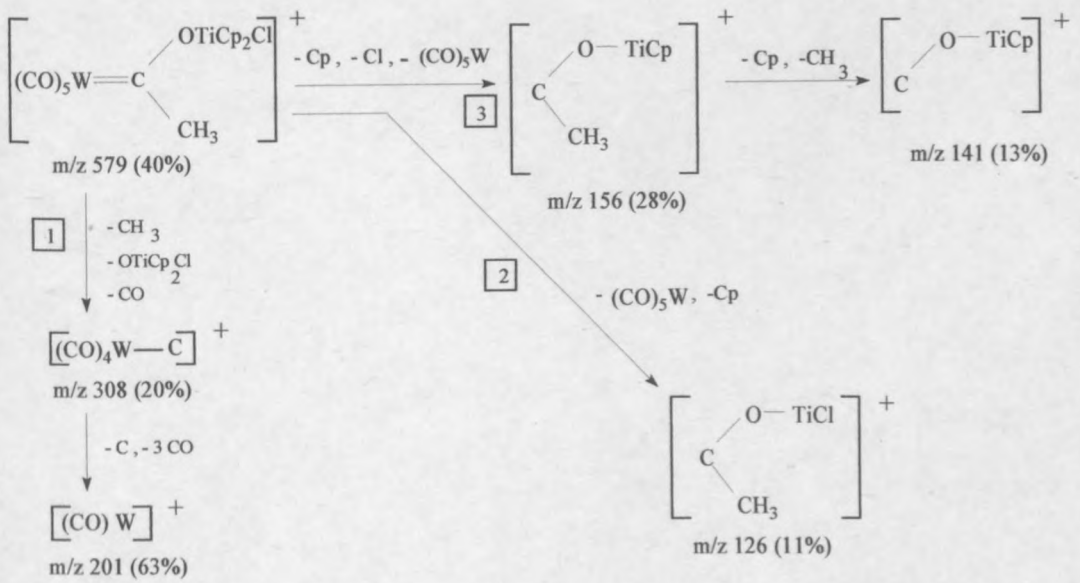

Scheme 2.22: FAB fragmentation diagram of $[(CO)_5W{=}C(Me)OTi(Cl)Cp_2]$ **10**

Route 2 and 3 favours the loss of $[W(CO)_5]$ and the fragmentation of the metallocene ligand. Route 2 leads to formation of the $[C(CH_3)OTiCl]^+$ ion, while $[C(CH_3)OTiCp]^+$ and $[COTiCp]^+$ are formed as ions according to route 3 (Scheme 2.22).

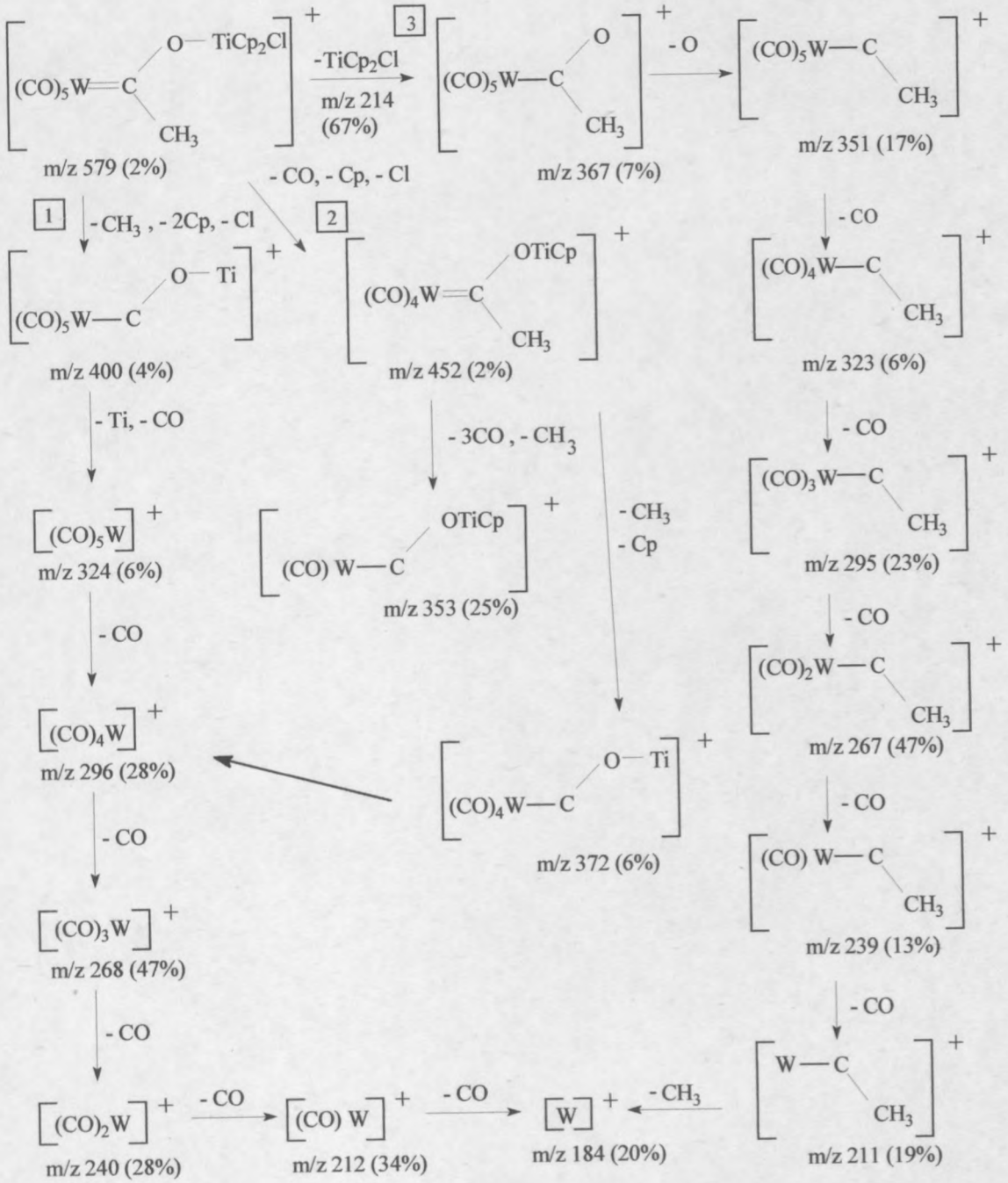

Scheme 2.23: EI fragmentation diagram of $[(CO)_5W{=}C(Me)OTi(Cl)Cp_2]$ **10**

The complex EI fragmentation pattern reveals three fragmentation pathways for complex **10** as depicted in Scheme 2.23. Routes 1 and 3 are similar; in both stepwise carbonyl loss occurs, but starting from two different fragment ions, and forming two different sets of ions.

The loss of the metallocene ligand and the methyl substituent leads to formation of the $[W(CO)_5]^+$ ion (route 1). Further fragmentation forms a set of $[W(CO)_x]^+$ ions (x=0-5). The $[C(CH_3)OTiCp_2Cl]^+$ ion that forms undergoes further fragmentation according to Scheme 2.24.

The loss of $TiCp_2Cl$ at the start of route 3, is followed by subsequent carbonyl loss leading to the formation of a range of $[(CO)_xW{=}C(CH_3)]^+$ ions. The $[W]^+$ ion forms *via* route 1 or 3. Step 2 involves the initial loss of a carbonyl, a cyclopentadienyl and a chloride ligand.

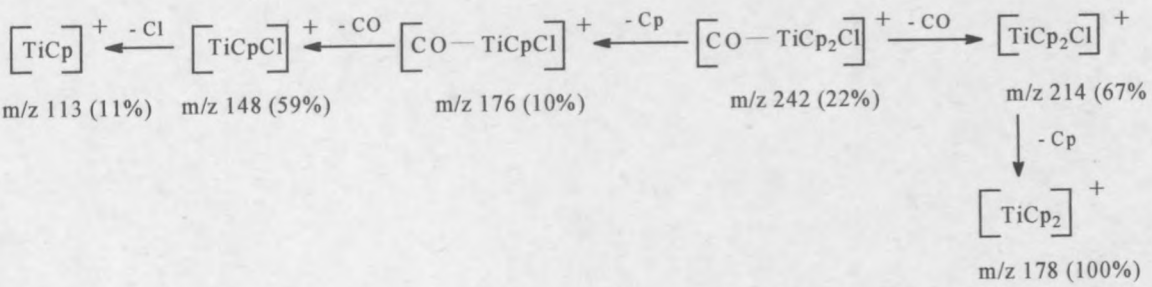

Scheme 2.24: Fragmentation diagram of the $[C(CH_3)OTiCp_2Cl]^+$ ion

2.5.2.2.1.6 Mass spectrometry of $[(CO)_5W{=}C(Ph)OTi(Cl)Cp_2]$, **11**

The FAB mass spectrum of complex **11** (Scheme 2.25) shows two main routes. Route 1 involves the loss of two carbonyl ligands, followed by the loss of $W(CO)_3$ producing the $[C(Ph)OTiCp_2Cl]^+$ ion. Step 2 is characterised by the loss of the metallocene fragment forming the $[(CO)_5W{=}C(Ph)O]^+$ ion.

The stepwise loss of carbonyl ligands (step 3), results in a range of $[(CO)_xW{=}C(Ph)O]^+$ ions (x=0, 3-5). The molecular ion is present in the FAB mass spectrum (Scheme 2.25), m/z 643 (52%), but is absent in the EI mass spectrum (Scheme 2.26).

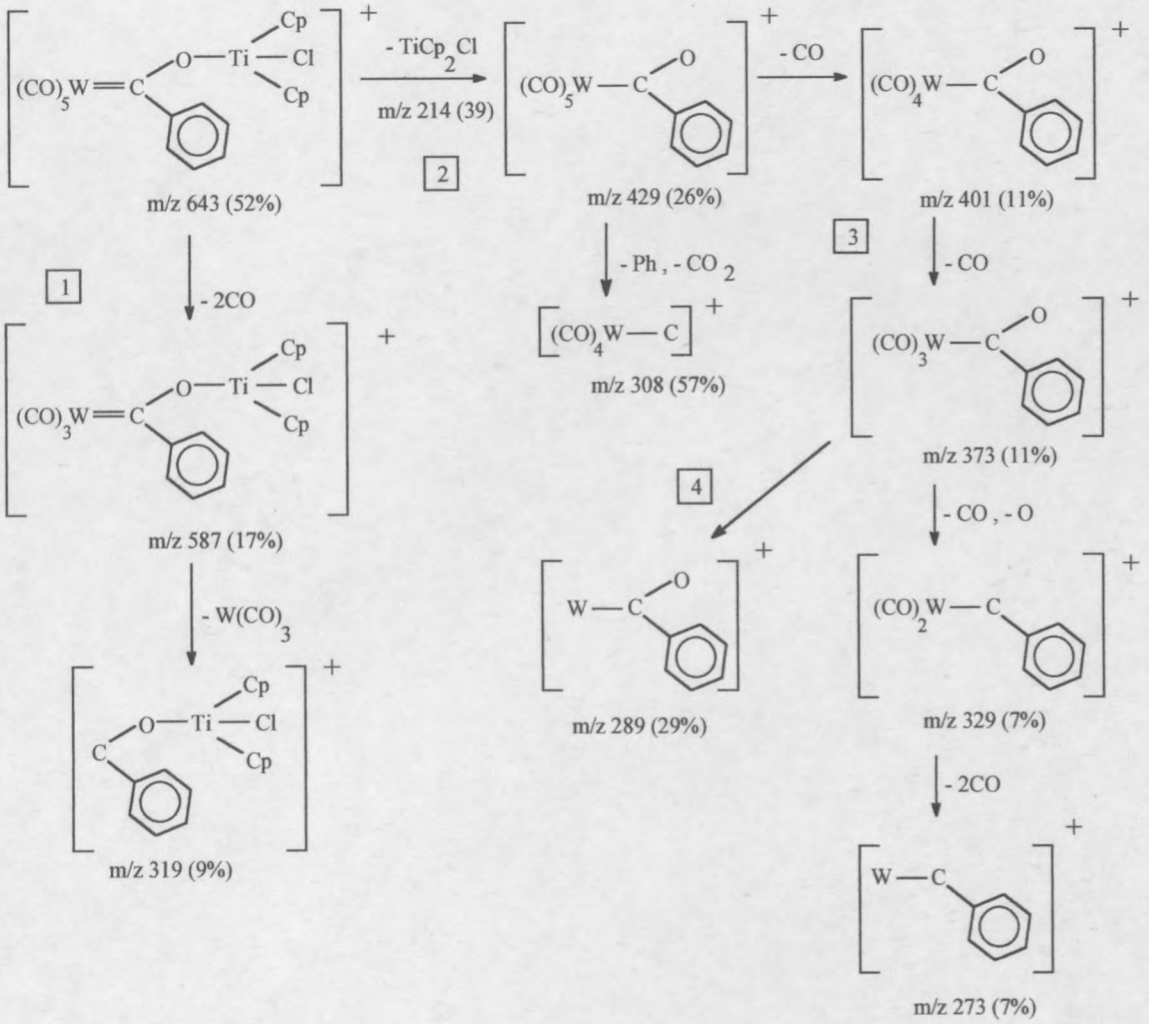

Scheme 2.25: FAB fragmentation diagram of $[(CO)_5W{=}C(Ph)OTi(Cl)Cp_2]$ **11**

Scheme 2.26 represents the three main fragmentation routes identified for complex **11** (EI mass spectrum). Step 1 involves the loss of the cyclopentadienyl and chloride ligands, followed by the loss of three carbonyl ligands. Further fragmentation of the metallocene ligand results in formation of the $[(CO)_2W{=}C(Ph)OTi]^+$ ion. The loss of the titanium atom forms the $[(CO)_2W{=}C(Ph)O]^+$ ion, which also forms according to the proposed fragmentation pattern, step 2.

Step 2 starts of with the loss of two cyclopentadienyl ligands and a chloride ligand. The loss of the titanium metal atom and subsequent stepwise carbonyl loss forms a range of $[(CO)_xW{=}C(Ph)O]^+$ ions (x=2,4 and 5). The loss of the phenyl substituent forms the $[(CO)_3W]^+$ ion.

The $[Cp]^+$ ion present after fragmentation, forms the $[C_3H_3]^+$ radical after loss of an acetylene fragment (Scheme 2.27). The $[C_3H_3]^+$ ion is usually present in the spectra of aromatic compounds, and occasionally in the spectra of dichlorometallocene compounds.[60]

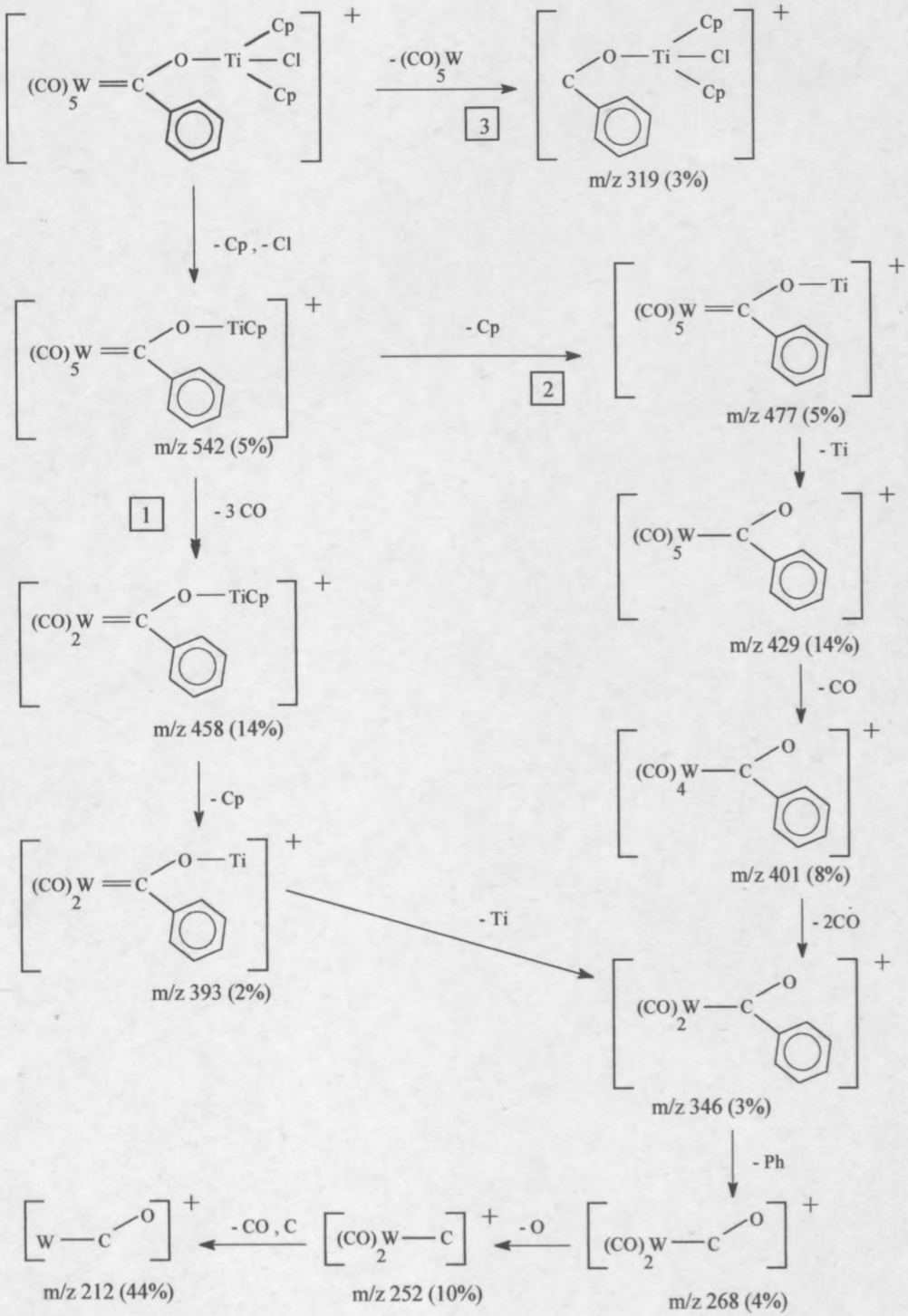

Scheme 2.26: EI fragmentation diagram of $[(CO)_5W{=}C(Ph)OTi(Cl)Cp_2]$ **11**

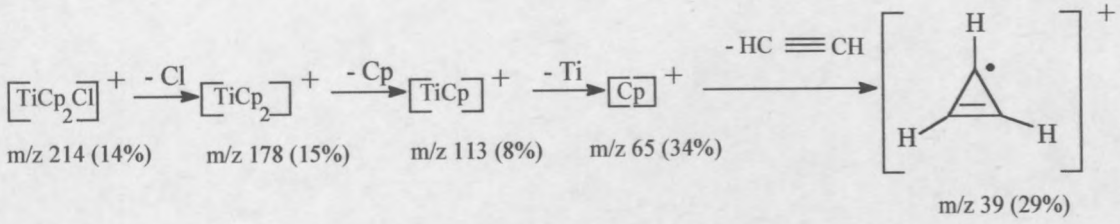

Scheme 2.27: The $[C_3H_3]^+$ radical

The $[Cp]^+$ ion present after fragmentation, forms the $[C_3H_3]^+$ radical after the loss of an acetylene fragment. The $[C_3H_3]^+$ ion is usually present in the spectra of aromatic compounds,[42] and occasionally in the spectra of dichlorometallocene compounds.[43]

2.5.2.2.1.7 Mass spectrometry of $[(CO)_5W{=}C(Me)OZr(Cl)Cp_2]$, **12**

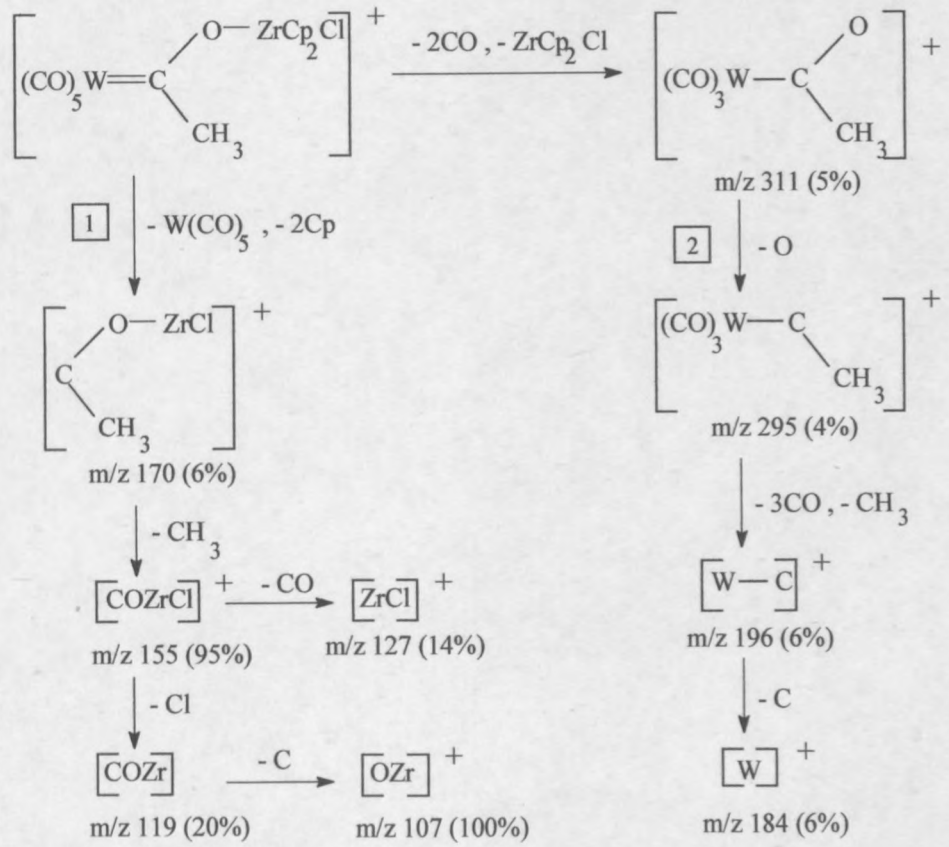

Scheme 2.28: FAB fragmentation diagram of $[(CO)_5W{=}C(Me)OZr(Cl)Cp_2]$ **12**

A simple FAB mass spectrum was obtained for complex **12** (Scheme 2.28). The loss of the $W(CO)_5$ fragment and two cyclopentadienyl ligands yields the $[C(Me)OZrCl]^+$ ion, which fragments to form the $[COZrCl]^+$ ion [m/z 155 (95%)] and the $[OZr]^+$ ion [m/z 107 (100%)] (route1). Route 2 involves the loss of the zirconocene ligand and two carbonyl ligands to form the $[(CO)_3W\text{-}C(CH_3)O]^+$ ion [m/z 311(5%)] (Scheme 2.28).

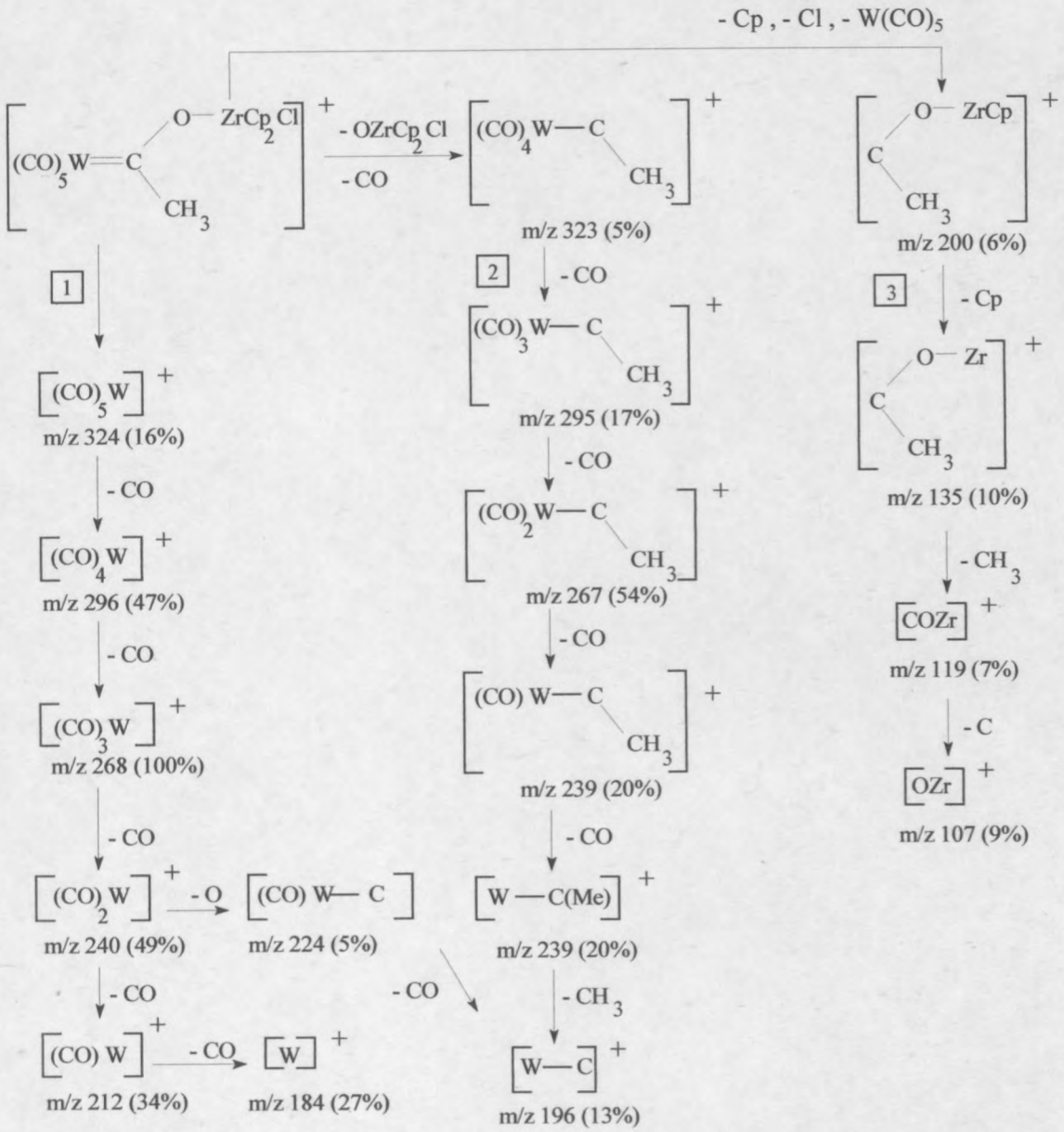

Scheme 2.29: EI fragmentation diagram of $[(CO)_5W{=}C(Me)OZr(Cl)Cp_2]$ **12**

The EI mass spectrum of complex **12**, revealed three main fragmentation routes (Scheme 2.29). According to route 1 $[W(CO)_5]^+$ ion forms, which undergoes stepwise carbonyl loss, leading to formation of a range of $[(CO)_xW]^+$ ions (x=0-5).

A range of $[(CO)_xW\text{-}C(Me)]^+$ ions, (x=0-4), forms along route 2. The formed $[C(Me)OZrCp]^+$ion fragments to produce a range of zirconocene ions (route 3, Scheme 2.29). Similar ions are also formed in the FAB mass spectrum of complex **12** (Scheme 2.28). The $[W\text{-}C]^+$ ion forms according to routes 1 and 2, both possibilities are shown.

2.5.2.2.1.8 Mass spectrometry of $[(CO)_5W{=}C(Ph)OHf(Cl)Cp_2]$, **13**

The FAB mass spectrum of complex **13** (Scheme 2.30) shows two main fragmentation routes. Route 1 involves the stepwise loss of carbonyl ligands (from the molecular ion) producing a range of $[(CO)_xW{=}C(Ph)OHfCp_2Cl]^+$ ions (x=0-3, 5). Fragmentation of the $[W{=}C(Ph)OHfCp_2Cl]^+$ ion occurs *via* two different routes, 1 a) loss of the phenyl substituent or 1 b) the fragmentation of the $[C(Ph)OHfCp_2Cl]^+$ ion.

Route 2 is characterised by metallocene ligand fragmentation followed by stepwise loss of the carbonyl ligands, resulting in a range of $[(CO)_xW\text{-}C(Ph)O]^+$ ions (x=0, 2-5). $[W\text{-}C(Ph)O]^+$ and $[C(Ph)O]^+$ form according to routes 1 and 2. The molecular ion is present in both the FAB and EI mass spectra of complex **13**, [m/z 773 (53%)] and [m/z 773 (28%)] respectively.

Four fragmentation routes are identified for the EI mass spectrum of complex **13** (Scheme 2.31). Step 1 involves the stepwise loss of two carbonyl ligands, while the loss of the metallocene ligand occurs at the start of route 2. The $[(CO)_2W\text{-}C(OHf)]^+$ that forms in step 3 undergoes further fragmentation *via* stepwise carbonyl loss. The $[(CO)W\text{-}COHf]^+$ and $[W\text{-}COHf]^+$ ions form by either steps 3 or 4, as is shown in Scheme 2.31.

The $[C_3H_3]^+$ ion [m/z 39 (6%)] is also present in the spectra of compounds **13**, as was observed previously for complexes **7** and **11** (Scheme 2.27).

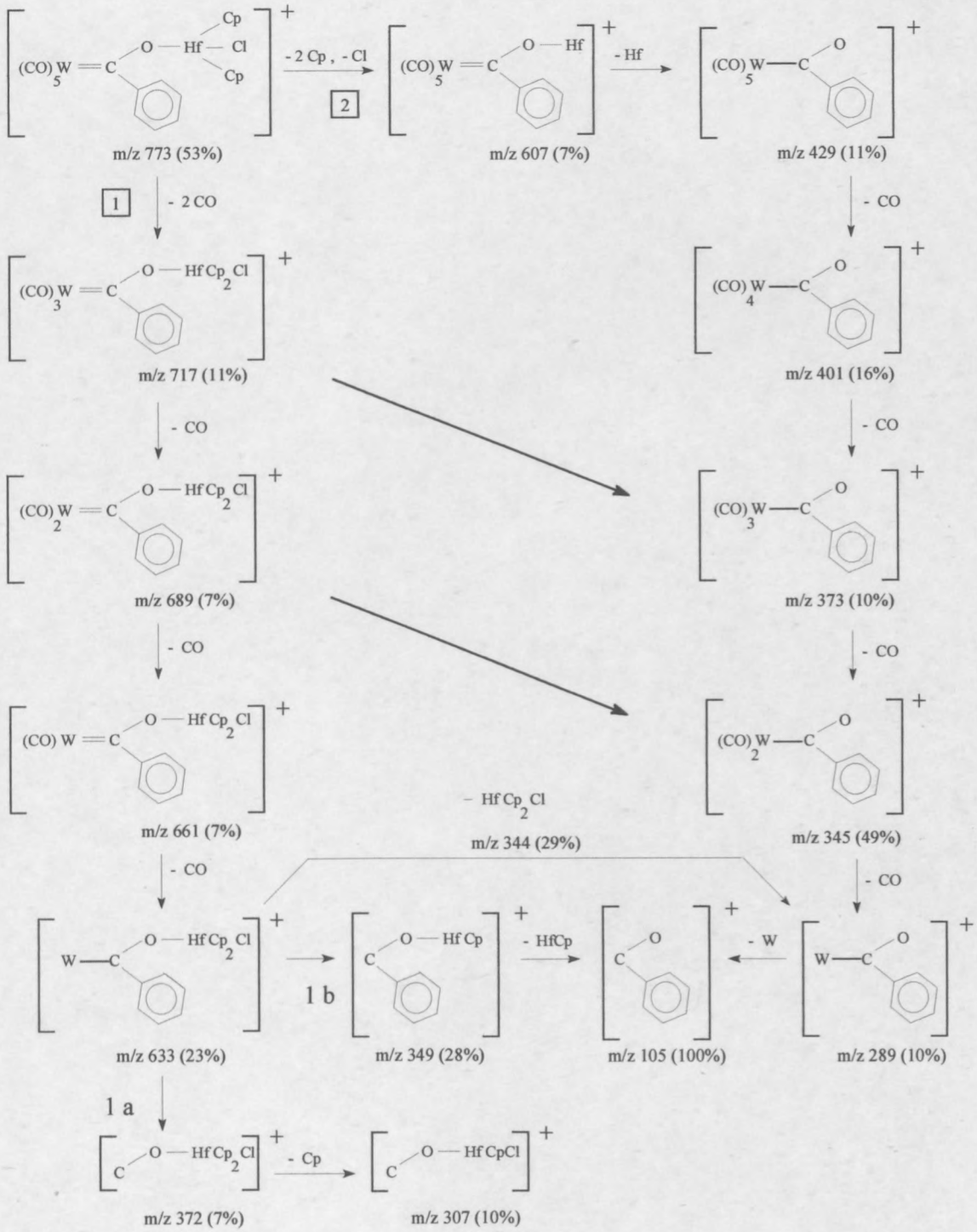

Scheme 2.30: FAB fragmentation diagram of $[(CO)_5W{=}C(Ph)OHf(Cl)Cp_2]$ **13**

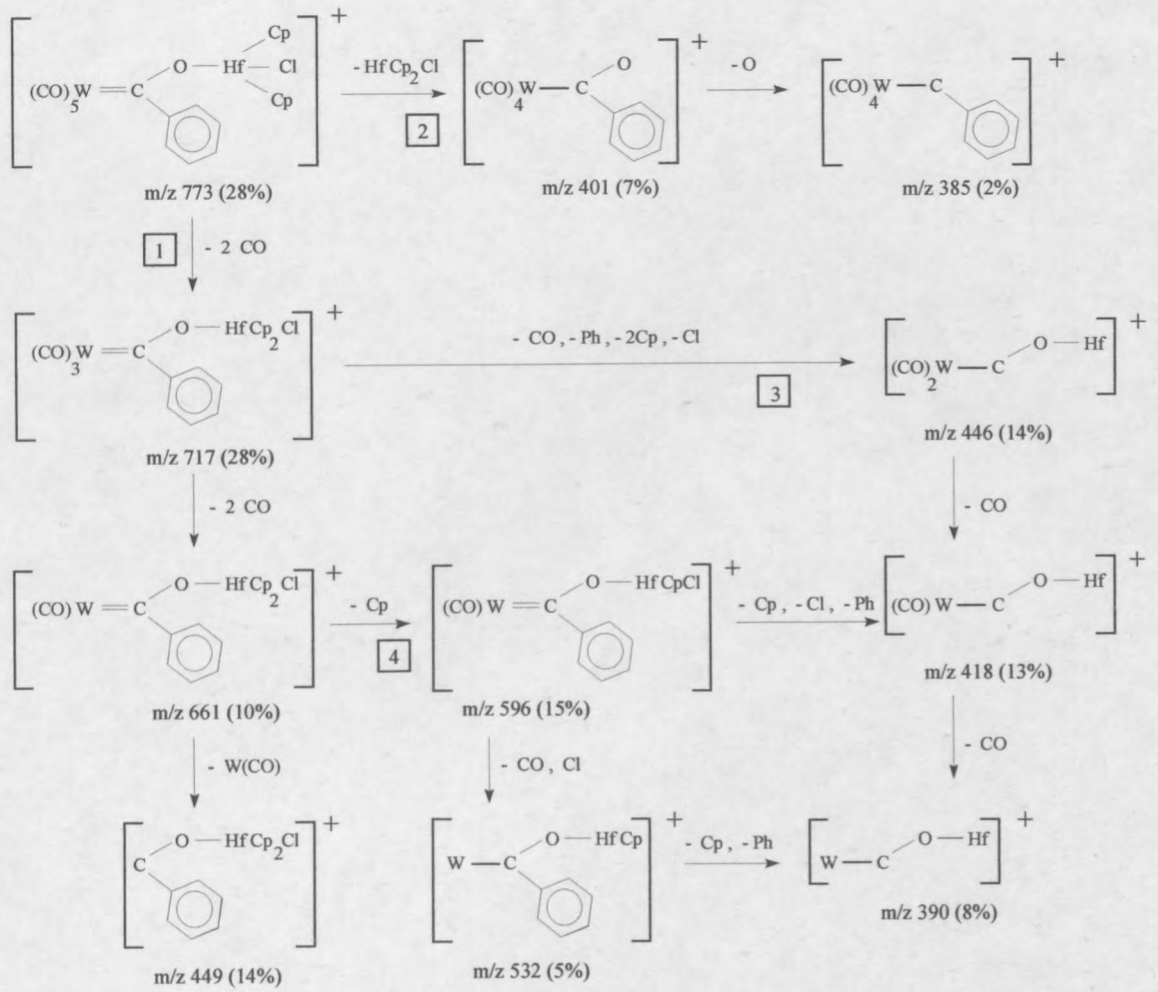

Scheme 2.31: EI fragmentation diagram of $[(CO)_5W{=}C(Ph)OHf(Cl)Cp_2]$ **13**

2.5.2.2.1.9 Mass spectrometry of $[(CO)_4Fe{=}C(Me)OTi(Cl)Cp_2]$, **14**

The molecular ion [m/z 424 (81%)] is present in the FAB mass spectrum of complex **14** (Scheme 2.32). Three main fragmentation pathways are identified; route 1 involves the stepwise loss of carbonyl groups followed by fragmentation of the metallocene ligand.

The loss of the methyl substituent followed by fragmentation of the metallocene ligand and stepwise carbonyl loss, represents route 2. A range of $[(CO)_xFe{=}COTiCp]^+$ ions form (x=1, 3, 4).

The methyl group stays intact according to pathway 3. The loss of two carbonyl ligands and the fragmentation of the metalollocene ligand occurs in the first step, this is followed

by the loss of the TiCp fragment leading to formation of the $[(CO)_2Fe\text{-}C(CH_3)O]^+$ ion, which undergoes further fragmentation according to route 3 (Scheme 2.32).

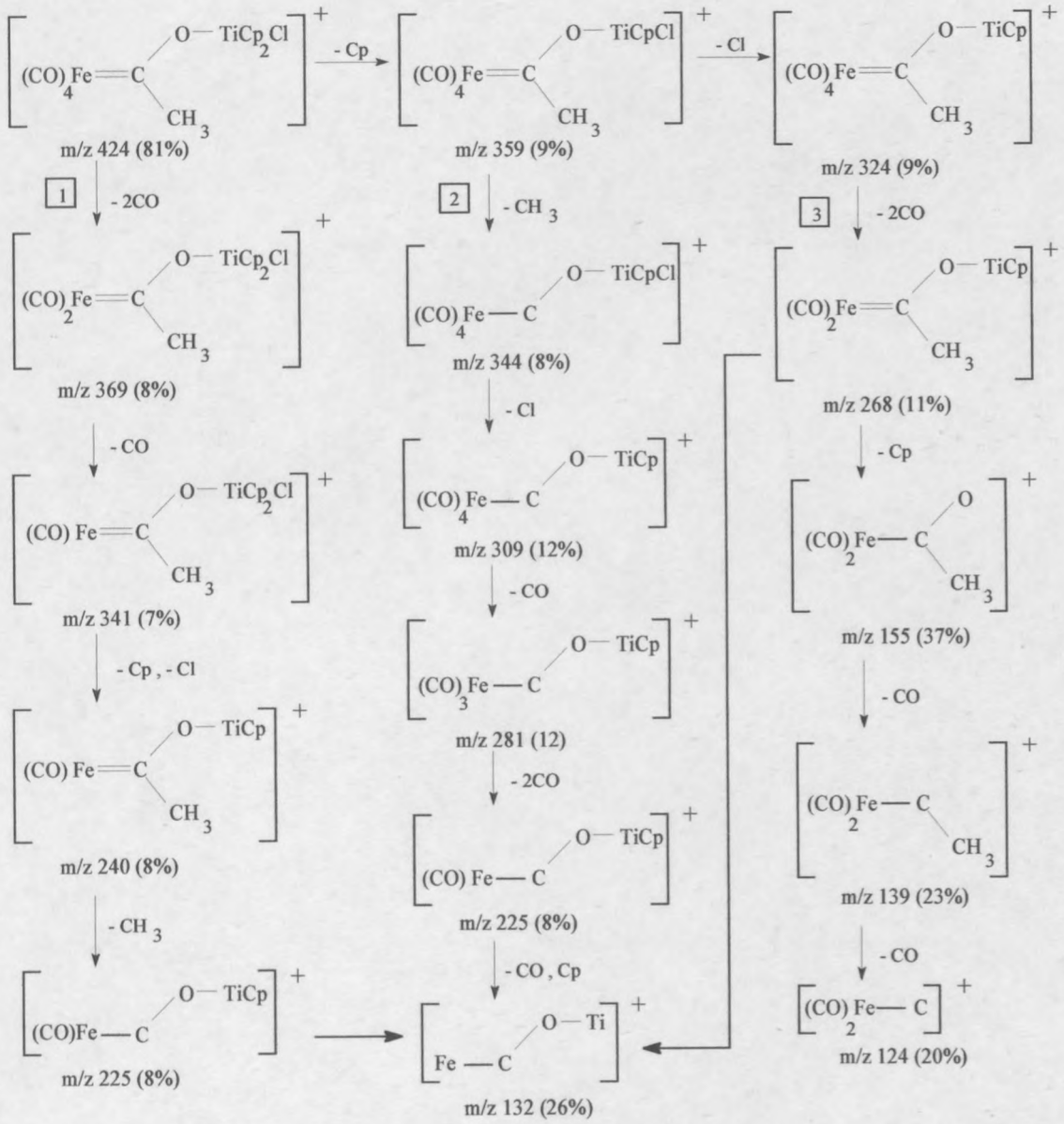

Scheme 2.32: FAB fragmentation diagram of $[(CO)_4Fe{=}C(Me)OTi(Cl)Cp_2]$ **14**

The EI mass spectrum of complex **14** reveals five possible pathways, Scheme 2.33 shows four of these possible pathways. Two of these pathways, a) the loss of two cyclopentadienyl rings followed by stepwise carbonyl loss, b) the loss of a cyclopentadienyl ring and a chloride atom, followed by stepwise carbonyl loss are represented jointly by route 1 (Scheme 2.33).

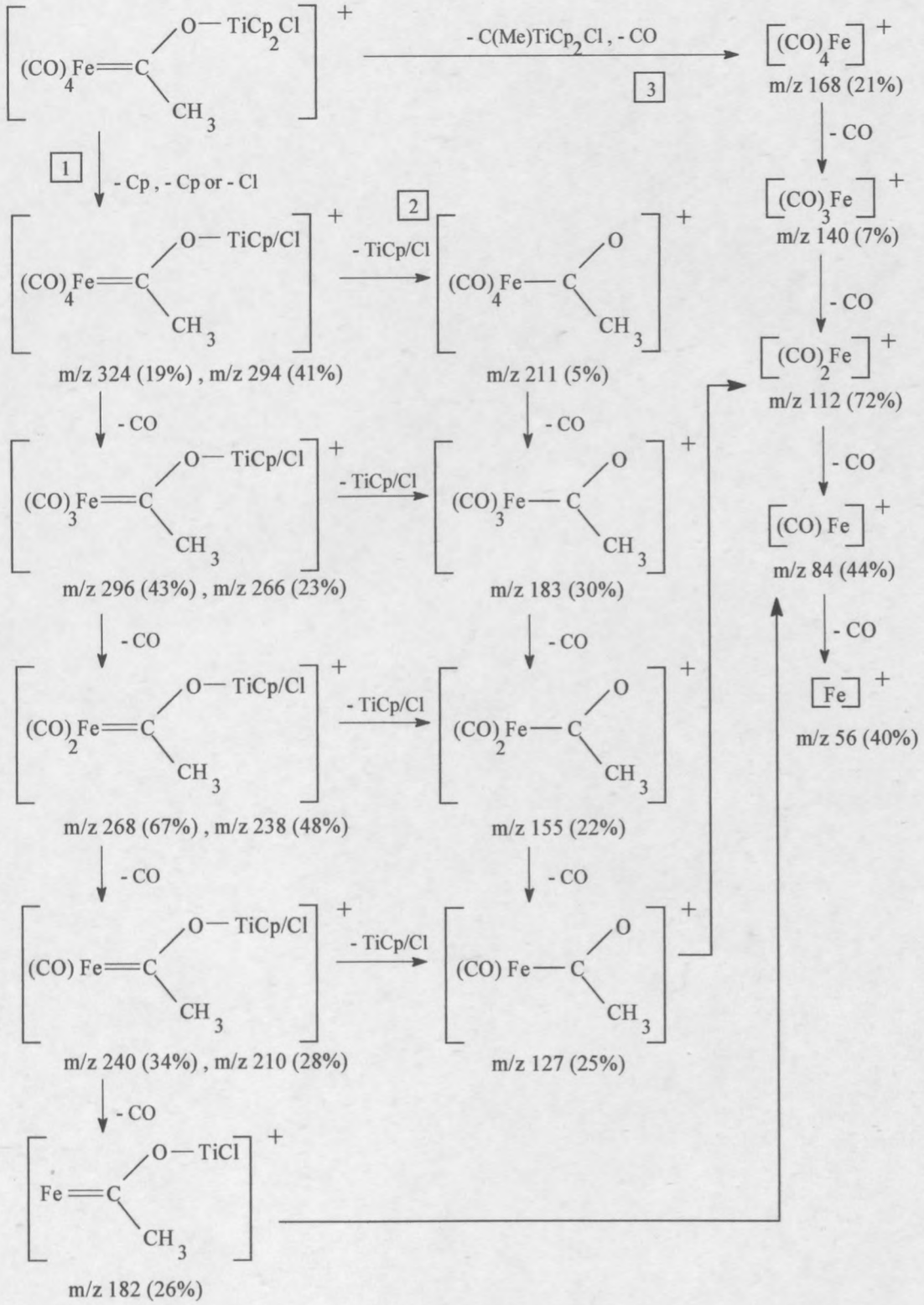

Scheme 2.33: EI fragmentation diagram of $[(CO)_4Fe{=}C(Me)OTi(Cl)Cp_2]$ **14**

According to step 2 the $[(CO)_4Fe\text{-}C(Me)O]^+$ ion undergoes stepwise carbonyl loss leading to the formation of a range of $[(CO)_xFe\text{-}C(Me)O]^+$ ions (x=1-4). Complex **14**

fragments to form $[Fe(CO)_4]^+$ ion as is shown in route 3. Stepwise carbonyl loss forms a range of $[(CO)_xFe]^+$ ions (x=0-4). The molecular ion is absent in the EI mass spectra of complex **14**.

2.5.2.2.10 Possible trends

The molecular ion is present in all the FAB mass spectra of complexes **6-14**, the harder EI technique resulted in the molecular ion observed ion in only four mass spectra; for complexes **6**, **7**, **10** and **13**. The isotopes present for group 4 and 6 transition metals complicated the allocation of peaks. Recombination of ions and the presence of p-nitrotoluene, used as reference during FAB data collection, resulted in additional peaks.

The fragmentation patterns derived for all the complexes **6-14** shows three dominant pathways: a) stepwise carbonyl loss followed by metallocene ligand and, or the methyl substituent fragmentation, b) metallocene fragmentation followed by stepwise carbonyl loss, and c) methyl substituent loss followed by stepwise loss of carbonyl ligands. The possible pathways and their relative importance depend on the MS technique used, the energy transferred through the molecule and the relative bond strengths between atoms in the molecule.

The $[Cp]^+$ ion present after fragmentation of the metallocene ligand, formed the $[C_3H_3]^+$ radical after the loss of a acetylene fragment. The $[C_3H_3]^+$ ion is present in the spectra of complexes **7**, **11** and **13.** This peak is most prominent in the mass spectrum of complex **11**.

2.5.2.3 IR Spectroscopy

Carbonyl stretching vibrations from IR- and Raman spectroscopy have been used extensively to determine the structure and bonding properties of metal carbonyl complexes. Given below are some contributing structures for the M-CO fragment in such complexes.

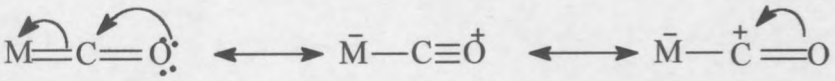

Scheme 2.34: M-CO resonance structures

An increase in metal-carbonyl bond order results in a decrease in carbon-oxygen bond order and a lower-energy IR-stretching vibration. The number of stretching vibrations and their intensities can be used to determine the molecular structure of carbonyl complexes. Metal carbonyl bond interactions can be explained using molecular orbital theory (Figure 2.4).[65]

The HOMO orbital has σ symmetry and points away from carbon. The σ orbital serves as weak donor to a metal atom (forming a σ bond). The LUMO orbitals can overlap with the metal d-orbitals that have local π symmetry (t_{2g} orbitals in an octahedral complex). This π-interaction leads to delocalisation of electrons from filled d-orbitals on the metal into empty π * orbitals on CO ligand.

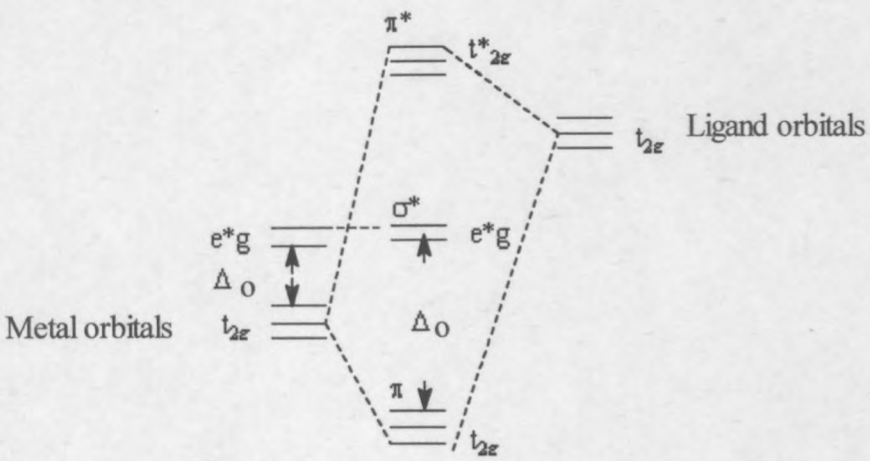

Figure 2.4: The effect of ligand π-acceptor orbitals on the outer molecular orbital energies of an octahedral complex

The CO group or ligands's ability to delocalise electron density away from the metal accounts for the prevalence of transition metal carbonyls in zero or negative oxidation states (Figure 2.5).

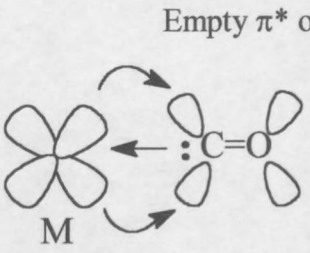

Figure 2.5: Electron back donation from filled metal d-orbitals

On the basis of local symmetry, octahedral molecules of the type $M(CO)_5L$ belong to the point group C_{4v} with four vibrations possible: $A_1^{(1)}+A_1^{(2)}+B_1+E$ (Figure 2.6).

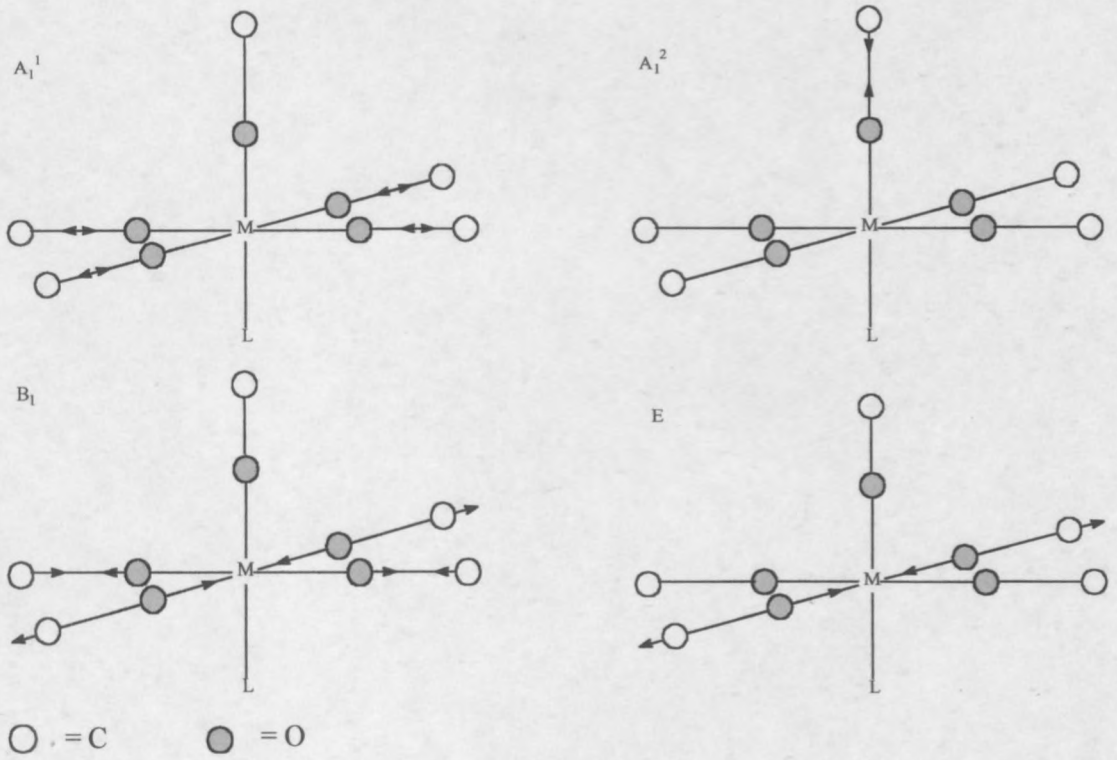

Figure 2.6: The fundamental vibrations from the character table of C_{4v}

Only $A_1^{(1)}$, $A_1^{(2)}$ and E will have significant intensities to be formally IR-active. The B^1-vibration is active when there is a distortion in the symmetry of the C_{4v} square planar carbonyls (the dipole moment then changes during the vibration).

The following factors can contribute in bringing this about:

1. If the ligand L is polyatomic and non-linear, then C_2 is the highest possible symmetry and the B_1-vibration mode is possible. (The E band is no longer doubly degenerated).
2. The absence of a non-linear ligand L distorts the equatorial CO-groups and the C_4 rotation symmetry and the molecule's symmetry changes to a D_{2d} point group. (D_{2d} point group has two C_2 axes perpendicular to the C_2 axis and two σd mirror planes through a C_2 rotation axis.)

The E-vibration has double degeneracy and also shows the most intense band in the IR-spectra. (Doubly degenerate vibrations occur when a molecule has an axis higher than two fold. For C_{4v} octahedral complexes the axis is four fold, rotation through 90°).

The $A_1^{(1)}$ is the symmetric vibration of the carbonyl ligands in the plane and $A_1^{(2)}$ is the vibration of the carbonyl ligand trans to the ligand L. The intensity of the $A_1^{(1)}$-vibration increases due to coupling with other A_1-vibrations and is observed at higher frequencies than the E-band.[66]

2.5.2.3.1 Results and Discussion

A characteristic of the pentacarbonyl Fischer-type carbene complexes is that $A_1^{(2)}$ is always shown as a shoulder on the lower frequency side of the E-band. The carbonyl stretching vibrations for complexes **1-14** are shown in Tables 2.9 and 2.10.

The infrared spectra in the CO-stretching region of most alkyl and acyl derivatives $RM(CO)_5$ are consistent with a lowering of symmetry, and a peak corresponding to the B_1 mode appears, with concurrent splitting of the E-band. The B_1-band is active for all the complexes tabulated, except complexes **5**, **9** and **12**, as a result of above-mentioned distortion of the C_{4v} symmetry.

Additional CO-stretching frequencies are observed for complexes **7**, **8**, **11** and **14** since the degeneracy of the E-mode, corresponding to C_{4v} symmetry has been lifted.

Table 2.9: Infrared results obtained for complexes **1-4**, **6-13**

	IR cm^{-1}				
Complex	A_1 (1)	B_1	E		A_1 (2)
1	2033 w	1936 w (sh)	1894 st		1863 st (sh)
2	2044 w	1953 m (sh)	1907 st		-
3	2044 w	1947 m (sh)	1900 st		-
4	2046 w	1949 w	1901 st		1865 m (sh)
6	2052 m	1975 m (sh)	1927 st (br)		1886 w (sh)
7	2048 m	1969 m (sh)	1929 st (br)	1918 st (sh)	1885 m
8	2056 m	1971 st (sh)	1928 st (br)	1917 st	1894 st
9	2060 w	-	1937 m		1886 w
10	2060 w	1977 st	1930 m (br)		1885 w (sh)
11	2060 w	1977 st	1933 st (br)	1916 st (sh)	1887 m (sh)
12	2054 w	-	1929 m		-
13	2067 m	1976 m (sh)	1938 st		1886 w (sh)

All IR spectra were recorded in $CHCl_3$

Table 2.10: Infrared results obtained for complexes **5**, **14**

	IR cm^{-1}					
Complex	A_1 (1)	B_1	E			A_1 (2)
5	2013 st	-	1917 m (sh)		1895 st (sh)	1875 st (sh)
14	2048 w	1977 st	1946 w (sh)	1911 m	1884 s	

All IR spectra were recorded in $CHCl_3$

The carbonyl stretching vibrations can also provide information about the σ/π relationship between the metal and ligands. For $M(CO)_5L$ complexes, ligand L in the neutral metaloxycarbene complex is a better π-acceptor than ligand L in the anionic ammonium salts of the acyl complex.

Better π-acceptor properties of ligand L result in less negative charge being localised on the metal atom. Thus less back donation from the metal atom occurs, resulting in higher C-O bond order. Thus more energy is needed to vibrate carbonyl bond. As is discussed above, Tables 2.9 and 2.10 shows lower $A_1^{(1)}$, B_1, $A_1^{(2)}$ and E stretching vibrations for the anionic ammonium salts of the acyl complexes **1-5** than for the corresponding neutral metaloxycarbene complexes **6-14**.

Red crystals (complex **67**) were isolated from a solution containing $Cp_2Zr(H)Cl$ and the ammonium salt of the acyl complex $[(CO)_5Cr{=}C(Me)OZr(H)Cp_2]$. The crystal structure obtained revealed (halo)*deca*carbonyldimetalate anion $[\{(CO)_5Cr\}_2Cl]^-$, with NEt_4^+ as counterion (see Chapter 4 for crystal structure and further discussions). Table 2.11 shows the Infrared results obtained for complex **67**.

Table 2.10: Infrared results obtained for complexes **67**

	IR cm^{-1}			
Complex	$A_1^{(1)}$	B_1	E	$A_1^{(2)}$
67	2064 w	1983 m	1927st	1865 m

All IR spectra were recorded in $CHCl_3$

2.6 SUMMARY AND FUTURE PROSPECTS

The aims and objectives set in section 1.5 can now be evaluated.

Nine metaloxycarbene complexes with monodentate oxycarbene groups were successfully prepared using a modified Fischer synthesis route. Five of these complexes were new compounds (**7**, **9**, **10**, **13** and **14**), thus expanding the collection of known metaloxycarbene complexes.

The X-ray crystal structures of two tungstenoxycarbene complexes (**11** and **13**) were determined. See Chapter 4 for discussion of the crystal structures of the new metaloxycarbene complexes **11** and **13**.

The use of $[Fe(CO)_5]$ as starting material, with titanocene dichloride and zirconocene dichloride for the preparation of metaloxycarbene complexes resulted in the successful

preparation (very low yield) and characterisation of only the titanium-containing derivative.

$Cp_2Zr(H)Cl$ as substrate for the preparation of metaloxycarbene complexes, $[(CO)_5M{=}C(Me)OZr(H)Cp_2]$ (M=Cr or W), proved too reactive, probably due to the Zr-H bond, leading to the formation of undesired products. The same synthesis route was employed as for the metaloxycarbene complexes **6-14**. Red crystals were isolated from a toluene solution containing the Cp2Zr(H)Cl and $[(CO)_5Cr{=}C(Me)ONEt_4]$.

The crystal structure obtained revealed (halo)*deca*carbonyldimetalate anion $[\{(CO)_5Cr\}_2Cl]^-$, with NEt_4^+ as counterion (complex **67**, see Chapter 4). The other products were unstable. Numerous group 6 (halo)*deca*carbonyldimetalate anions, prepared primarily from reactions involving photolysis are known. See Chapter 4 for the discussion of the crystal structure of complex **67**.

At the end of this part of this project some questions still remain unanswered: (i) Better separation techniques, especially for organozirconium complexes are still needed, how should they be applied? (ii) The role of ligands in the stability of metaloxycarbene complexes should be investigated. Could Cp-ligands be replaced and what would the effect of other ligands on the group 6 metals be? (iii) Other carbene precursors: which other metals can be used as starting materials?

Also which other metal substituents will afford metaloxycarbene complexes and will they be catalytically active? We have, as yet, not finally been able to prepare metallocene hydride derivatives and possibly Cp*-compounds (Cp*1,2,3,4,5-pentamethylcyclopentadienyl) are required. This formation of metallocene hydride derivatives could make the use of MAO unnecessary, as is dicussed in section 3.2.7.2 one role of MAO is the alkylation of the transition metal.

The $[Cp_2Zr(CH_3)]^+$ cation is converted to the $[Cp_2Zr(H)]^+$ ion (during the first cycle) believed to be the active species in the catalytic cycle. The Cp*-ligands stabilise the metallocene center and this will probably facilitate the formation of the hydride metallocene derivatives, thus forming the catalytic active species.

2.7 EXPERIMENTAL SECTION

2.7.1 General

All reactions were performed with standard vacuum line and Schlenk techniques under positive argon or nitrogen flow. All the solvents were distilled, dried and degassed before use. Diethyl ether, hexane, pentane and toluene were dried over sodium and freshly distilled under constant nitrogen pressure. Dichloromethane was distilled from calcium hydride.

The ^{1}H and ^{13}C NMR spectra were obtained at 25°C in deuterated acetone for all samples except where mentioned elsewhere. A Varian VXR spectrometer operating at 300 MHz was used to obtain the spectra of complexes **1-6** and complexes **8-14**. The spectra of complex **7** was recorded on a Varian VXR spectrometer operating at 600 MHz. Two-dimensional spectra (COSY) of complexes **6** and **7** were recorded using a 600 MHz VXR spectrometer to verify results obtained.

FAB Mass spectra of complexes **1-14** were recorded on a VGA70-70E mass spectrometer at 70 eV with xenon as bombardment gas and *m*-nitrobenzylalcohol as matrix. The EI mass spectra were recorded on a Finnigan Matt 8200 instrument at *ca.* 70 eV. IR spectra in the CO stretching region were measured on Perkin Elmer 1600 Series FTIR spectrophotometer in spectroscopically pure chloroform.

All the metal carbonyls, metallocenes, methyl lithium (1.6 M in diethyl ether), *t*-Butyl lithium (1.6 M in diethyl ether), magnesium sulphate, sodium sulphate, silver tetrafluoroborate and deuterated solvents were purchased from Aldrich. The phenyl lithium used to prepare complexes **11** and **13** were freshly prepared.

The melting points were measured using a standardised Büchi 535 apparatus.

2.8 SYNTHESES OF TRANSITION METAL CARBENE COMPLEXES

2.8.1 Synthesis of $[(CO)_5Cr=C(Me)O][NEt_4]$, 1

A white suspension of 11.10 g (50.44 mmole) of $Cr(CO)_6$ in 100 cm^3 of diethyl ether was prepared in a two neck, round-bottomed 500 ml flask, containing a magnetic stirring bar and equipped with a nitrogen inlet and a pressure equalizing dropping funnel. To the well-stirred suspension, 50.9 mmole of $LiCH_3$ (21 cm^3, 2.4 M) in 50 cm^3 of diethyl ether was added over a period of 45 min. During the addition of the base, the colour of the solution changed to yellow.

After the solution was stirred for 60 min the solvent was removed at room temperature *in vacuo*. The residue was dissolved in 150 cm^3 cold water saturated with N_2 and filtered over celite to remove any unreacted $Cr(CO)_6$. A solution of Et_4NCl (8.357 g, 50.43 mmole) in 50 cm^3 cold water saturated with N_2 was added to the filtrate. The solution was stirred for 30 min. The yellow precipitate was removed by filtration over celite and dissolved in warm CH_2Cl_2. This solution was dried by filtration over $MgSO_4$. The solvent was removed *in vacuo* at room temperature. Yellow microcrystalline material was stored in a refrigerator at –6°C.

Yield: 13.0 g (71%)
Melting point: 132.8 – 135.9°C

2.8.2 Synthesis of $[(CO)_5Mo=C(Me)O][NEt_4]$, 2

A white suspension of 3.961 g (15.030 mmole) of $Mo(CO)_6$ in 100 cm^3 of diethyl ether was prepared in a two neck, round-bottomed 500 ml flask, containing a magnetic stirring bar and equipped with nitrogen inlet and a pressure equalizing dropping funnel. To the well-stirred suspension at – 40°C, 15.0 mmole of $LiCH_3$ (9.4 cm^3, 1.6 M) in 50 cm^3 of diethyl ether was added over a period of 45 min. During the addition of the base, the colour of the solution changed to dark orange. The solution was stirred for 60 min and the temperature allowed to rise to –20°C, the solution was then removed *in vacuo*.

The residue was dissolved in 150 cm^3 cold water saturated with N_2 and filtered over celite to remove any unreacted $Mo(CO)_6$. A solution of Et_4NCl (4.974 g, 30.015 mmole) in 50 cm^3 cold water saturated with N_2 was added to the filtrate. The solution was stirred for 30 min. The orange precipitate was removed by filtration over celite and dissolved in warm CH_2Cl_2. This solution was dried by filtration over $MgSO_4$ after which the solvent was removed *in vacuo* at room temperature. Yellow microcrystalline material was stored in a refrigerator at –6°C.

Yield: 3.4 g (55%)
Melting point: 118.9 – 124.2°C

2.8.3 Synthesis of $[(CO)_5W{=}C(Me)O][NEt_4]$, 3

The methyl tungsten ammonium salt of the acyl complex **3** was synthesised using the same method as for the ammoniun salt of the acyl complex **1**, as described above. $W(CO)_6$ (17.652 g, 50.16 mmole), $LiCH_3$ (32 cm^3, 1.6 M, 50.5 mmole) and Et_4NCl (8.721 g, 52.62 mmole) were used. Orange-yellow microcrystalline material was stored in a refrigerator at –6°C.

Yield: 12.3 g (49%)

2.8.4 Synthesis of $[(CO)_5W{=}C(Ph)O][NEt_4]$, 4

The phenyl tungsten ammonium salt of the acyl complex **4** was synthesised using the same method as for the ammoniun salt of the acyl complex **1**, as described above. $W(CO)_6$ (17.802 g, 50.59 mmole), LiC_6H_5 (31 cm^3, 1.6 M, 50.2 mmole) and Et_4NCl (8.721 g, 52.62 mmole) were used. Orange-yellow microcrystalline material was stored in a refrigerator at –6°C.

Yield: 17.7 g (63%)
Melting point: 83.8 – 89.1°C

2.8.5 Synthesis of $[(CO)_4Fe=C(Me)O][NEt_4]$, 5

The methyl iron ammonium salt of the acyl complex complex **5** was synthesised using the same method as for the ammoniun salt of the acyl complex **4**, as described above. $Fe(CO)_5$ (6.512 g, 33.24 mmole), $LiCH_3$ (21 cm^3, 1.6 M, 33.28 mmole) and Et_4NCl (10.938 g, 66.0 mmole) were used. The purple microcrystalline material was stored in a refrigerator at –6°C.

Yield: 10.7 g (71%)
Decompose: 54.2 – 57.4°C

2.8.6 Preparation of $[(CO)_5Cr=C(Me)OTiCp_2Cl]$, 6

A red suspension of crystalline Cp_2TiCl_2 (0.506g, 2.032 mmol) in 40 cm^3 of dichloromethane was prepared in a two-neck, round-bottomed 250 ml flask, containing a magnetic stirring bar and equipped with nitrogen inlet and a pressure equalizing dropping funnel. This suspension was cooled to –40°C using a mixture of propanol and carbon dioxide. The ammoniun salt of the acyl complex **1**, {$[(CO)_5Cr=C(Me)O][NEt_4]$, 0.730g, 2.023 mmol} dissolved in 70 cm^3 of dichloromethane was added to the well-stirred suspension over 45 min. The reaction mixture was stirred for 30 min at -40°C, and $AgBF_4$ (0.397g, 2.039 mmol) was added. After the solution had been stirred for an additional 60 min, the solvent, was removed at room temperature *in vacuo*. The dark brown concentrate, stripped of solvent was purified by chromatography at –20°C on silica with dichloromethane-pentane (2:1) (column 15 x 2 cm). The eluent was reduced to dryness *in vacuo*. The dark brown microcrystalline product was dissolved in toluene and the saturated solution was layered with pentane and stored in the refrigerator at –6°C. The formed dark brown/black crystals were removed and washed with cold pentane. The concentrate was stored in a refrigerator at -6°C. The formed red-brown crystals were removed and washed with cold pentane.

Yield: 0.5 g (58%)
Melting point: 181.4 – 184.0°C

2.8.7 Preparation of $[(CO)_5Cr=C(t\text{-}Bu)OTiCp_2Cl]$, 7

The chromium titanium metaloxcarbene complex **7** was prepared using the same method as for the chromium zirconium metaloxycarbene complex **6**, as described above. ($[(CO)_5Cr=C(t\text{-}Bu)O][NEt_4]$, (1.699 g, 4.018 mmole), Cp_2TiCl_2 (1.001 g, 4.021 mmole) and $AgBF_4$ (0.784 g, 4.030 mmole) were used. Cp_2TiCl_2 was dissolved in dichloromethane before addition to the carbene salt solution.

The red-brown concentrate, stripped of solvent was purified by chromatography at –20°C on silica with dichloromethane-pentane (2:1) (column 15 x 2 cm). The eluent was dried at room temperature at high vacuum. The dark brown/black crystals were removed and washed with cold pentane and stored in a refrigerator at –6°C.

Yield: 0.5 g (24%)
Melting point: 128.2 – 132.5°C

2.8.8 Preparation of $[(CO)_5Cr=C(Me)OZrCp_2Cl]$, 8

The chromium zirconium metaloxcarbene complex **8** was prepared using the same method as for the chromium titanium metaloxycarbene complex **6**, as described above. $[(CO)_5Cr=C(Me)O][NEt_4]$ (0.741 g, 2.028 mmole), Cp_2ZrCl_2 (0.603 g, 2.063 mmole) and $AgBF_4$ (0.391 g, 2.008 mmole were used. Cp_2ZrCl_2 was dissolved in dichloromethane before addition to the carbene salt solution. The residue was extracted in 5 portions of 10 cm^3 of toluene. The extract was cooled to –40°C and filtered over celite to remove all solid byproducts. The filtrate was dried over anhydrous $MgSO_4$ and concentrated to saturation.
The yellow microcrystalline product was dissolved in toluene and the saturated solution was layered with pentane and stored in a refrigerator at –6°C. The formed yellow crystals were removed and washed with cold pentane.

Yield: 0.4 g (20%)
Melting point: 290.2 – 295.7°C

2.8.9 Preparation of $[(CO)_5Mo=C(Me)OTiCp_2Cl]$, 9

The molybdenum titanium metaloxycarbene complex **9** was prepared using the same method as for the chromium zirconium metaloxycarbene complex **8**, as described above. $[CO)_5Mo=C(Me)O][NEt_4]$ (0.827 g, 2.022 mmole), Cp_2TiCl_2 (0.504 g, 2.025 mmole) and $AgBF_4$ (0.394 g, 2.026 mmole) were used. Cp_2TiCl_2 was dissolved in dichloromethane before addition to the carbene salt solution.

The dark brown concentrate, stripped of solvent was purified by chromatography at –20°C on silica with dichloromethane-pentane (2:1) (column 15 x 2 cm). The eluent was reduced to dryness *in vacuo*. The red-brown microcrystalline product was washed with pentane and stored in a refrigerator at –6°C.

Yield: 0.1 g (9%)
Melting point: 127.2 – 131.0°C

2.8.10 Preparation of $[(CO)_5W=C(Me)OTiCp_2Cl]$, 10

The tungsten titanium metaloxycarbene complex **10** was prepared using the same method as for the chromium zirconium metaloxycarbene complex **8**, described above. $[(CO)_5W=C(Me)O][NEt_4]$ (0.0997 g, 2.006 mmole), $TiCp_2Cl_2$ (0.500 g, 2.012 mmole) and $AgBF_4$ (0.391 g, 2.014 mmole) were used. Cp_2TiCl_2 was dissolved in dichloromethane before addition to the carbene salt solution.

The red-brown concentrate, stripped of solvent was purified by chromatography at –20°C on silica with 500 ml of dichloromethane-pentane (1:2) followed by 100 ml of toluene (column 15 x 2 cm). The eluent was reduced to dryness *in vacuo*. The red-brown microcrystalline product was washed with pentane and stored in a refrigerator at –6°C.

Yield: 0.2 g (18%)
Melting point: 160.2 – 165.8°C

2.8.11 Preparation of $[(CO)_5W{=}C(Ph)OTiCp_2Cl]$, 11

The tungsten titanium metaloxycarbene complex **11** was prepared using the same method as for the chromium zirconium metaloxycarbene complex **8**, as described above. $[(CO)_5W{=}C(Ph)O][NEt_4]$ (1.132 g, 2.024 mmole), Cp_2TiCl_2 (0.505 g, 2.028 mmole) and $AgBF_4$ (0.393 g, 2.021 mmole) were used. Cp_2TiCl_2 was dissolved in dichloromethane before addition to the carbene salt solution. The red concentrate, stripped of solvent was purified by chromatography at –20°C on silica with 400 ml of dichloromethane-pentane (2:1) followed by 200 ml of diethyl ether-hexane (2:1) (column 15 x 2 cm). The eluent was reduced to dryness *in vacuo*. The red-brown powder was dissolved in toluene and the saturated solution was layered with pentane and stored in a refrigerator at –6°C. Dark brown crystals were removed and washed with cold pentane.

Yield: 0.5 g (38%)
Melting point: 134.2 – 134.7°C

2.8.12 Preparation of $[(CO)_5W{=}C(Me)OZrCp_2Cl]$, 12

A white suspension of crystalline $ZrCp_2Cl_2$ (0.354g, 1.212 mmol) in 30 cm^3 of toluene was prepared in a two-neck, round-bottomed 250 ml flask, containing a magnetic stirring bar and equipped with nitrogen inlet and a pressure equalizing dropping funnel. This suspension was cooled to –40°C using a mixture of propanol and carbon dioxide. The ammoniun salt of the acyl complex **3**, $[(CO)_5W{=}C(Me)O][NEt_4]$, (0.603g, 1.208 mmol)], dissolved in 30 cm^3 of toluene, was added to the well-stirred suspension over 20 min. The resulting reaction mixture was stirred for 30 min at -40°C, and $AgBF_4$ (0.239g, 1.225 mmol) was added. After the solution had been stirred for an additional 60 min the solution was allowed to rise to room temperature and evaporated to dryness *in vacuo*. The dark yellow microcrystalline product was washed with pentane and stored in a refrigerator at -6°C.

Yield: 0.1 g (15%)
Melting point: 136.6 – 140.7 ° C

2.8.13 Preparation of $[(CO)_5W{=}C(Ph)OHfCp_2Cl]$, 13

The tungsten hafnium metaloxycarbene complex **13** was prepared using the same method as for the chromium zirconium metaloxycarbene complex **8**, as described above. $[(CO)_5W{=}C(Ph)O][NEt_4]$ (0.740 g, 1.324 mmole), Cp_2HfCl_2 (0.505 g, 1.331 mmole) and $AgBF_4$ (0.261 g, 1.345 mmole) were used. Cp_2HfCl_2 was dissolved in dichloromethane before addition to the carbene salt solution.

After removal of the dichloromethane in vacuo the residue was extracted in 5 portions of 10 cm^3 toluene, the extract was cooled to –40°C to precipitate byproducts. The byproducts were removed by filtration through celite. The filtrate was dried over anhydrous $MgSO_4$ and concentrated to saturation. The solution was stored in a refrigerator at -6°C. The red crystals were removed and washed with cold pentane and stored in the refrigerator at –6°C.

Yield: 0.2 g (19%)
Melting point: 118.6 – 122.7°C

2.8.14 Preparation of $[(CO)_4Fe{=}C(Me)OTiCp_2Cl]$, 14

A white suspension of crystalline Cp_2TiCl_2 (0.996g, 4.002 mmol) in 40 cm^3 of toluene was prepared in a two-neck, round-bottomed 250 ml flask, containing a magnetic stirring bar and equipped with nitrogen inlet and a pressure equalizing dropping funnel. This suspension was cooled to –40°C using a mixture of propanol and carbon dioxide.

The ammoniun salt of the acyl complex {$[(CO)_4Fe{=}C(Me)O][NEt_4]$, 1.637 g, 4.088 mmol} dissolved in 40 cm^3 of toluene was added to the well-stirred suspension over 45 min.

The resulting brown solution solution was stirred for 30 min at - 40°C, and $AgBF_4$ (0.782 g, 4.016 mmol) was added. The mixture was stirred over night and the temperature was allowed to rise to 15°C. The solvent was evaporated *in vacuo* at – 20°C and the residue

was washed with cooled pentane. The red-brown microcrystalline product was stored in the refrigerator at –6°C.

Yield: 0.5 g (13%)
Melting point: 181.4 – 184.0°C

2.9 SYNTHESES OF METALLOCENES

2.9.1 Synthesis of Cp2Zr(OMe)Cl

A mixture of 0.8 ml (17 mmole) of ethanol, 1.2 ml (8 mmole) of triethylamine in 10 cm^3 benzene was added to a vigorously stirred mixture of white Cp_2ZrCl_2 (2.0 g, 8.0 mmole) and 90 ml benzene at 90°C. The mixture was prepared in a two neck, round-bottomed 250 ml flask containing a nitrogen inlet. The resulting solution was stirred for 3 hours at 60°C.

The colour of the solution changed from white to cream/yellow. After the solution was allowed to cool down to room temperature, the formed triethylammonium chloride was removed by filtration and the solvent then removed *in vacuo*. The cream microcrystalline material worked with pentane was stored in a refrigerator at –6°C.

Yield: 1.6 g (71%)

REFERENCES

1. R. Beckhaus in Metallocenes, E. Negishi and J.-L. Montchamp in *Metallocenes*, Ed. A. Togni and R.L. Halterman, Volume 1, Wiley-VCH, 1998, Chapters 4 and 5, 153-312.
2. A.H. Hoveyda and J.P. Morken, in *Metallocenes*, Ed. A. Togni and R.L. Halterman, Volume 2, Wiley-VCH, 1998, Chapter 10, 625-684.
3. B.A. Krentsel, Y. V. Kissin, V.J. Kleiner and L.L. Stotskaya in *Polymers and copolymers of higher α-olefins*, Hanser Publishers, Munich, 1997.
4. G. Erker, *Angew. Chem., Int. Ed. Engl.*, 1989, **28**, 397-412.
5. W.A. Herrmann and C. Köcher, *Angew. Chem., Int. Ed. Engl.*, 1997, **36**, 2162-2187.
6. J. Barluenga and F.J. Fañanás, *Tetrahedron*, 2000, **56**, 4597-4628.
7. D. Bourissou, O. Guerret, F.P. Gabbaï and G Bertrand, *Chem. Rev.* 2000, **100**, 39-91.
8. E.O. Fischer and S. Fontana, *J. Organomet. Chem.*, 1972, **40**, 159.
9. H.G. Raubenheimer and E.O. Fischer, *J. Organomet. Chem.*, 1975, **91**, C23.
10. R. W. Alder, C.P. Butts, A.G. Orpen, *J. Am. Chem. Soc.*, 1998, **120**, 11526.
11. W. Petz, *J. Organomet. Chem.*, 1974, **72**, 369.
12. G. Erker, *Angew. Chem., Int. Ed. Engl.*, 1989, **28**, 397.
13. A.W. Parkins, E.O. Fischer, G. Huttner and D. Regler, *Angew. Chem., Int. Ed. Engl.*, 1970, **9**, 633.
14. C.M. Jensen, C.B. Knobler and H.D. Kaesz, *J. Am. Chem. Soc.*, 1984, **106**, 5926.
15. E.O. Fischer, V. Kiener, D.S.P. Bunbury, E. Frank, P.F. Lindley and O.S. Mills, *J. Chem. Soc., Chem. Commun.*, 1968, 1378.
16. E.V. Anslyn, B.D. Santarsiero and R.H. Grubbs, *Organometallics*, 1988, **7**, 2137.
17. M. Sabat, M.F. Gross and M.G. Finn, *Organometallics*, 1992, **11**, 745.
18. M. Fritz, J. Breimair, B. Wagner and W. Beck, *J. Organomet. Chem.*, 1992, **426**, 343.
19. J.M. Manriquez, D.R. McAlister, R.D. Sanner and J. E. Bercaw, *J. Am. Chem. Soc.*, 1976, **98**, 6733.

20. J.M. Manriquez, D.R. McAlister, R.D. Sanner and J. E. Bercaw, *J. Am Chem. Soc.*, 1978, **100**, 2716.

21. G. Erker, U. Dorf, R. Lecht, M.T. Ashby, M. Aulbach, R. Schulnd, C. Krüger, R. Mynott, *Organometallics*, 1989, **8**, 2037.

22. G. Erker, U. Dorf, R. Benn, R.-D. Reinhardt and J.L. Petersen, *J. Am. Chem. Soc.*, 1984, **106**, 7649.

23. G. Erker, *Angew. Chem., Int. Ed. Engl.*, 1989, **28**, 397.

24. G. Erker, R. Lecht, C. Krüger, Y.-H. Tsay and H. Bönneman, *J. Organomet. Chem.*, 1987, **326**, C75.

25. G. Erker, R. Lecht, J.L. Petersen and H. Bönneman, *Organometallics*, 1987, **6**, 1962.

26. G. Erker, R. Lecht, Y.-H. Tsay and C. Krüger, *Chem. Ber.*, 1987, **120**, 1763.

27. G. Erker, R. Lecht, R. Shlund, K. Angermund and C. Krüger, *Angew. Chem., Int. Ed. Engl.*, 1987, **26**, 666.

28. G. Erker, F. Sosna, R. Pfaff, R. Noe, C. Sarter and A. Kraft, *J. Organomet. Chem.*, 1990, **394**, 99.

29. R. Beckhaus and K.-H. Thiele, *J. Organomet. Chem.*, 1989, **368**, 315.

30. R. Beckhaus, J. Oster, *J. Organomet. Chem.* 1998, **553**, 427

31. M.Brookhart, W.B. Studabaker, *Chem. Rev.* 1987, **87**, 411.

32. K.Öfele, *J.Organomet. Chem.* 1968, **12**, 42.

33. H.-W. Wanzlick, H.-J. Schönherr, *Angew. Chem., Int. Ed. Engl.* 1968, **7**, 141.

34. A.J. Arduengo III, R.L. Harlow, M. Kline, *J. Am. Chem. Soc.* 1991, **113**, 361.

35. M. Denk, R. Lennon, R. Hayashi, R. West, A.V. Belyakov, H.P. Verne, A. Haaland, M. Wagner,, N. Metzler, *J. Am. Chem. Soc.* 1994, **116**, 2691.

36. B. Gehrhus, M.F. Lappert, J. Heinicke, R.Boese, D. Bläser, *J. Chem. Soc., Chem. Commun.* 1995, 1931.

37. B. Gehrhus, P.B. Hitchcock, M.F. Lappert, J. Heinicke, R. Boese, D. Bläser, *J. Organomet. Chem.* 1996, **521**, 211.

38. K. Hirai, K.Komatsu, H. Tomioka, *Chem. Lett.* 1994, 503.

39. H. Tomioka, T. Watanabe, K. Hirai, K. Furukawa, T. Takui and K. Itoh, *J. Am. Chem. Soc.*, 1995, **117**, 6376.

40. N. Kuhn and T. Kratz, *Synthesis*,1993, 561.

41. A.J. Arduengo III, H.V.R. Dias, F. Davidson and R. L. Harlow, *J. Organomet. Chem.*, 1993, **462**, 13.

42. W.A. Herrmann and C. Köcher, *Angew. Chem. Int. Ed. Engl.*, 1997, **36**, 2162.

43. A. Berndt, *Angew. Chem., Int. Ed. Engl.*, 1993, **32**, 985.

44. M.A. St Clair, B.D. Santarsiero and J.E. Bercaw, *Organometallics,* 1989, **8**, 17.

45. Ch. Elschenbroich, A. Salzer in *Organometallics*, VCH Verlagsgesellschaft, Weinheim, 1989, p. 210, 212.

46. A.J. Hartshorn and M.F. Lappert, *J. Chem. Soc., Chem. Comm.*, 1976, 761.

47. E.O. Fischer, K. Richter, *Angew. Chem., Int. Ed. Engl.*, 1975, **14**, 345.

48. Ch. Elschenbroich, A. Salzer in *Organometallics*, VCH Verlagsgesellschaft, Weinheim, 1989, 211.

49. K.-W. Liangn and M. Chandrasekharam , *J. Org. Chem.*, 1998, **63**, 7289.

50. H.G. Raubenheimer and S.Cronje, *J. Organomet. Chem.*, 2001, **617-618**, 170-181.

51. E.J. O'Connor and P.Helquist et al., *J. Am. Chem. Soc.*, 1982, **104**, 1869.

52. K.H. Dötz and P. Tomuschat, *Chem. Soc. Rev.*, 1999, **28**, 187.

53. K.H. Dötz, *Angew. Chem., Int. Ed. Eng.*, 1975, **14**, 644.

54. M.L. Davies, E.G. Antoulinakis, *J. Organomet. Chem.*, 2001, **617-618**, 47.

55. E.O. Fischer, H. Fischer, *Chem. Ber.*, 1974, **107**, 657.

56. R.M. Dahlgren, J.I. Zink, *Inorg. Chem.*, 1977, **16**, 3154.

57. L.S. Hegedus, Acc. *Chem. Res.,* 1995, **28**, 299.

58. M. Landman, H. Görls, S. Lotz, *J. Organomet. Chem.*, 2001, **617-618**, 280.

59. N.N. Greenwood and A. Earnshaw in *Chemistry of the Elements* (2nd Edition), Reed Educational and Professsional Publishing Ltd. Boston, 1997, 929.

60. L. van Niekerk, *M.Sc.-thesis*, University of Stellenbosch, 2000.

61. A. Neveling, *M.Sc.- thesis*, University of Stellenbosch, 1999.

62. E.V. Abslyn, B.D. Santarsiero, R.H. Grubbs, *Organometallics,* 1988, **7**, 2137.

63. W.J. Chazin, L.D. Colebrock, *Magn. Reson. Chem.*, 1985, **23**, 597.

64. D. Neuhaus and M. Williamson in *The steady state NOE for spins*, Chapter 2, VCH Publischers, New York, 1989, 51-54.

65. L.M. Haines and M.H.B. Stiddard in *Adv. Inorg. Rad. Chem.*, Ed. H.J. Emeleus and A.G. Sharpe, Volume 12,1969, 53-132.

66. S. Lotz, *Ph.D.- thesis*, Rand Afrikaans University, 1972.

CHAPTER 3

OLIGOMERISATION OF α-OLEFINS USING METALOXYCARBENE COMPLEXES

3.1 ZIEGLER-NATTA CATALYSIS

3.1.1 INTRODUCTION

The discovery of transition metal catalysts for alkene polymerisation by Ziegler and Natta in the early 1950s formed the foundation for today's polyalkene industry.[1,2] Catalysis has made gigantic contributions to the chemical, petrochemical and oil-refining industry. It is estimated that 80% of all chemicals manufactured in 2001 will amount to 12.4 Billion $ (1995 the value was 10.3 Billion $). The products produced via catalysis are valued at 30% of the USA Growth National Product.[3,4]

Oil refining to gasoline, diesel and heating oils would be impossible without catalysis. Six processes dominate the field: cracking, reforming (paraffins to aromatics), hydrotreating (removal of impurities, by-products), isomerisation (linear to branched paraffins), conversion of synthesis gas to paraffins (Sasol) and alkylation.[3,4]

Numerous research groups have studied transition metals as catalysts for polymerisation and oligomerisation reactions, resulting in a wide range of active and selective known catalyst.[5]

3.1.2 HISTORICAL OVERVIEW

In the 1930's free radical ethene polymerisation, developed by ICI, was used to produce short and long-chain branched LDPE. This technique required pressures of more than 1000 atm and temperatures around 200°C. This process was costly and unsafe. The addition of catalysts e.g. alkyl-free SiO_2/CrO_3 (Phillips) and the molybdenum oxide (Standard Oil of Indiana) to this process was used to produce HDPE. These processes

were widely used in industry, and it was only after the discovery made by Karl Ziegler that the polymer revolution started.[6]

In the spring of 1953 Karl Ziegler tried to synthesise long chain aluminium alkyls from the reaction of aluminium triethyl with ethene under pressure. Contamination by nickel salts left over after cleaning the autoclave, led to the dimerisation of ethene to give a high melting linear polymer. This became known as the " Nickel effect" (Scheme 3.1).

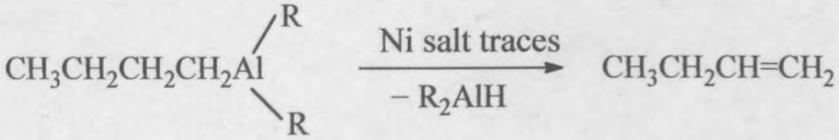

Scheme 3.1: The " Nickel effect "

Ziegler catalysts were later patented under German laws, directed to polymerisation of α-olefins at normal or low pressure and temperatures up to 150°C in a hydrocarbon medium into high-molecular weight polymers.[7]

In 1954 Guilio Natta and his research group applied this catalyst to the stereospecific polymerisation of propene. Industrial and commercial importance of their work was so significant that, Ziegler and Natta were both awarded the Noble Prize in 1963.

3.1.3. EARLY HETEROGENEOUS ZIEGLER CATALSYSIS

This study is primarily concerned with the polymerisation and oligomerization of α-olefins with homogeneous metallocene based catalysts. A short overview of presumed mechanisms involved in the heterogeneous systems is given. These mechanisms are well documented and serve as forerunners to help explain the mechanisms involved in homogeneous catalysis.

Work done by Natta, Cossee-Arlam and Rodriguez-van Looy on heterogeneous catalytic systems (Scheme 3.2) showed that: a) Ti has six-coordinated structure, b) it forms a

bridged structure with alkylaluminium and that Ti is coordinatively unsaturated c) the bridged structure of Ti and Al determines the activation of Ti and directs the olefin coordination.[8-10]

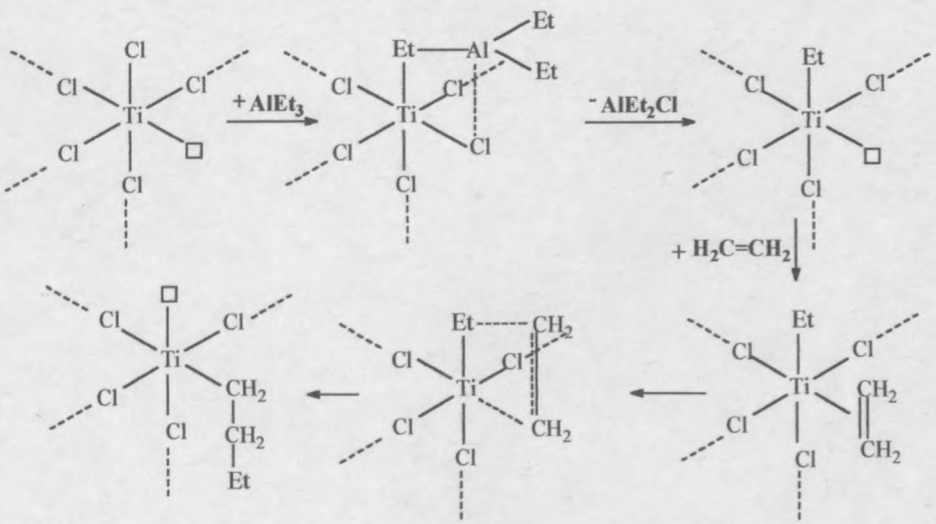

Scheme 3.2: Cossee-Arlam mechanism

3.2 HOMOGENEOUS ZIEGLER-NATTA CATALYSIS

3.2.1 INTRODUCTION

Over the last 15 years the interest in homogeneous metallocene based catalysts for olefin polymerisation has grown and it is expected that in future these catalysts will partially replace conventional Ziegler-Natta catalyst systems. Metallocene precursors have several desirable properties, such as high activity, high selectivity, and when used with MAO they produce high-molecular-weight polymers with narrow molecular-weight distribution.

Industrially the development of Ziegler-Natta catalysts are of extreme importance, as the total production of polyethylene and polypropylene, produced in 1995 exceeded 52 million tons worldwide. Ziegler-Natta catalysts produce over 60% of total polyolefins, a market, which is expected to grow by about 5% in the upcoming years (well exceeding

the 3% growth expected for other plastics).[11] This work, however, is mainly concerned with oligomerisation.

3.2.2 DEVELOPMENT OF CATALYSTS

In 1957, Breslow and Newburg, and Natta, independently discovered the first homogeneous Ziegler-Natta catalyst, Cp_2TiCl_2/R_2AlCl, which proved more agreeable to study than the earlier heterogeneous catalysts.[12,2,13] An important future of such catalyst systems is that tetravalent Ti centers are required for catalytic activity.[14,15] These soluble catalysts were inactive towards propene polymerisation, but active for ethene polymerisation and provided the opportunity to study the mechanism of Ziegler-Natta polymerisation reactions in more detail.[11,16] Their activities were low.

The discovery of stereospecific ansa-metallocene based catalysts, during the mid 1980s, together with Sinn and Kaminsky's discovery of the effective activation of group 4 transition metallocene complexes by means of partially hydrolysed Me_3Al, MAO for the polymerisation of ethylene, again revolutionized polymer synthesis and polyolefin technology.[13, 17,] Catalytic activities of homogeneous systems were now comparable to their heterogeneous counterparts.

3.2.3 GENERAL MECHANISM OF POLYMERISATION REACTIONS

Since the discovery of Ziegler-Natta catalysts in the 1950s different models were developed to try and explain the mechanisms involved in the polymerisation reactions, to enable scientist to understand and control selectivity more effectively.[18, 19]

Polymerisation can be divided into two broad classes, radical polymerisation and stepwise polymerisation. The mechanism believed to play a role in alkene polymerisation belongs to the latter (Scheme 3.3). The steps involved include alkene coordination to metal center followed by migratory insertion; this generates a coordinatively unsaturated species **22** that can repeat this propagation sequence and lastly

chain termination. Various chain transfer agents and termination product have been identified in homogeneous catalysis as shown in Scheme 3.3.

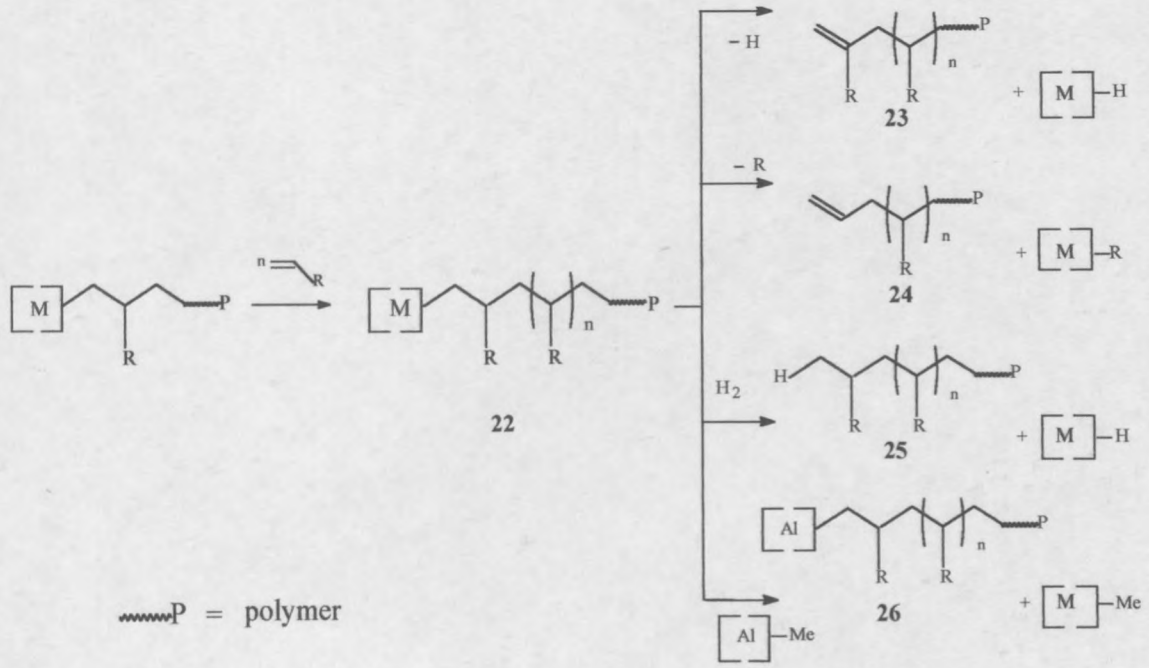

Scheme 3.3: Basic steps in the polymerisation of α-olefin with metallocene-based catalyst

Intramolecular β-H elimination produces a vinylidene-terminated polymer **23** and regenerates a catalytically active metal-hydride complex ([M]-H), while intramolecular β-alkyl elimination produces an active metal alkyl species ([M]-R) and an allyl-terminated polymer **24**.[20,21]

Hydrogen is an effective chain transfer agent in these systems, and produces polymers with saturated end groups **25** and regenerates an active [M]-H catalyst.[22-24] Alkyl aluminum compounds are also chain transfer agents, where trans-metallation produces an aluminum terminated polymer **26** and an active metal alkyl, ([M]-Me).[25]

3.2.4 COSSEE-ARLAM MECHANISM FOR METALLOCENE CATALYSTS

The Cossee-Arlman insertion mechanism, proposed in 1964, is also widely accepted as the correct pathway in polymerisation of α-olefin with metallocene-based catalysts under homogeneous conditions.[26-28] The essential features of this mechanism require a cationic coordinatively unsaturated metal-alkyl complex. The olefin complexes to the vacant coordination site, **27**, (Scheme 3.4), forming the π-complex, **28**, this is followed by 1,2-insertion of an olefin into the metal carbon bond via the four-membered cyclic transition state, **29**.[29-33] The product, **30**, resembles the starting structure, and a new vacant coordination site is formed where the next inserting olefin can coordinate to propagate the polymerisation further. Eventually chain termination occurs, most likely by β-elimination or chain transfer as mentioned before.

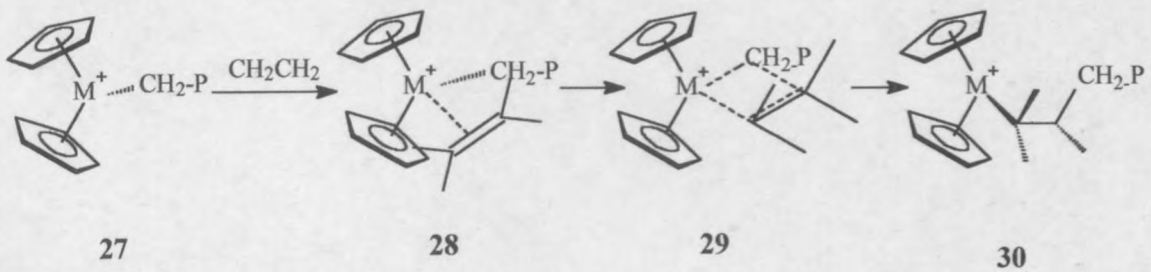

27 **28** **29** **30**

Scheme 3.4: The Cossee-Arlam mechanism

3.2.5 GREEN ROONEY / BROOKHART MECHANISMS

Green and Rooney suggested that the α-carbon transfers a hydride to the metal, forming a metal-carbon carbene bond.[34,35] This is then followed by the formation of a four-centered metalacycle as before in the Cossee-Arlam mechanism. This metathesis-like mechanism is impossible for high oxidation state d^0 metals, as they would be unable to form the required M-H bond and formally increase their oxidation state. Brookhart, suggested a modification to this route, with the hydrogen shared in a three-center two-electron bond, by the metal and carbon atom, known as an α-agostic bond **31** (Scheme 3.5).[36] In the transition state, such a bond would lower the insertion barrier, hence quick C migration to

the C=C takes place, while in insoluble 18 electron alkyl olefin complexes it tends to be slow. The reaction can be strongly accelerated by coordinative unsaturation. Recent work by Watson (f-block metals) and kinetic studies by Bercaw and Brintzinger confirmed that α-agostic assistance occurs in certain instances.[37-40]

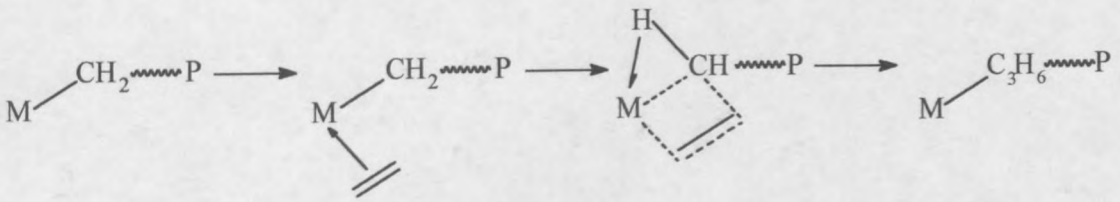

31

Scheme 3.5: α-Agostic assisted Ziegler-Natta insertion mechanism

3.2.6 NATURE OF THE ACTIVE SPECIES

In 1960, Shilov and coworkers proposed that the active species derived from homogeneous, metallocene-based catalysts was the co-ordinatively unsaturated cationic $[\eta\text{-}C_5H_5)_2MR]^+$ (14 VE) model system, which mimics the catalytic sites of surface-alkylated $TiCl_3$ of the classic Ziegler-Natta process.[41] This was later confirmed in the mid 1980's, when Eisch isolated the cationic insertion product **32** from the reaction of Cp_2TiCl_2 and $MeAlCl_2$ with [TMS-(CC)-Ph] (Scheme 3.6).[42]

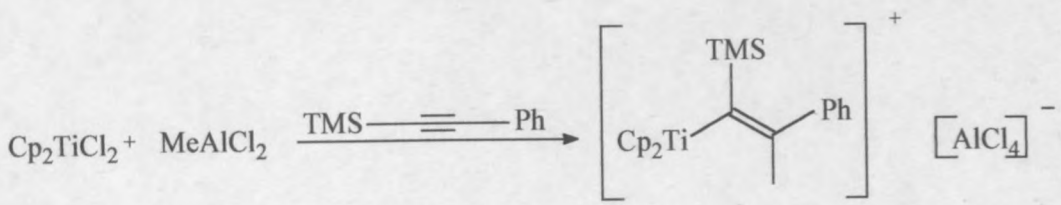

32

Scheme 3.6: Cationic metal alkyl

This result suggests that the metal alkyl cation $[Cp_2TiMe]^+$ is the initially formed catalytically active species.

3.2.7 MAO THE CO-CATALYST

In 1973 Riechert and Meyer discovered that traces of water, a catalyst poison, improved the $Cp_2TiEtCl/EtAlCl_2$ catalyst productivities in ethene polymerisation.[43] Breslow and Long believed this was due to the formation of aluminoxane.[44] This assumption was confirmed by Cam and co-workers by direct synthesis and characterization of $(MeAlO)_n$ ($5<n<20$).[45] In 1976 Sinn and Kaminsky activated zirconocene compounds using high molecular weight methylaluminoxanes (MAO) during ethylene polymerisation.[46]

3.2.7.1 Formation of MAO

Aluminoxanes are produced by partial hydrolysis of trialkylaluminum compounds. The reaction between organoaluminium compounds and water have been studied since the 1960's when aluminoxanes were found to be active catalysts for the polymerisation of propylene oxide, monosubstituted epoxides, acetaldehyde, butadiene, etc.[47] The proposed structures of aluminoxane are shown in Scheme 3.7, but it is not known whether alumoxanes are comprised of a single substance or whether they have a dynamic structure.[48] All that is known is that they consist of oligomeric [Al(Me)O] units, in a linear and/or cyclic form. Due to their reactivity towards oxygen and moisture and their incomplete solubility in hydrocarbons and aromatic solvents, characterisation of alumoxanes is very difficult.

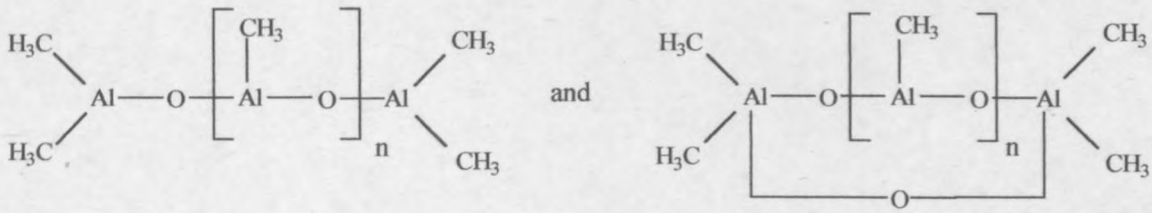

33 **34**

Scheme 3.7: Proposed structure of methylaluminoxane (MAO)

3.2.7.2 The role of MAO as co-catalyst

The co-catalyst performs at least three, and perhaps five, roles in the polymerisation or oligomerisation:

1) Alkylation of the transition metal;
2) Acting as a Lewis acid and creating a vacant coordination site by abstracting a halide or an alkyl ligand from the transition metal;
3) Most likely weakly associated with catalyst centers;
4) Could serve as a chain transfer agent;
5) Has a cleaning role by mopping up impurities such as water and oxygen (which are known to poison catalysts).[13, 49-52]

The MAO-activated precursors, Cp_2MCl_2 (M=Ti, Zr, Hf) first described by Sinn and Kaminsky, are completely non-selective towards prochiral propene, giving atactic polypropylene. Polymerisation again occurs by olefin coordination to Zr followed by C migration (Zr-C bond) to the alkene.

MAO appears to favour the formation of cationic Cp_2M (alkyl)(olefin)$^+$ by complexing the counterion X^-, thus producing more of the active cationic metallocenes at the expense of the dormant neutral metallocenes. In order to influence the equilibrium such as Cp_2MRX + MAO=$[Cp_2MR$ (olefin)$]^+[(MAO)X]^-$ and to increase the number of active cationic metallocenes, a large excess of MAO with respect to the transition metal is needed.[53] Conventionally soluble, MAO-activated metallocenes require Al/metallocene molar ratios in the range of 1000-5000: 1.

3.2.7.3 Activation with MAO

The $[Cp_2ZrR]^+$ cation has been identified as the active species and is most likely stabilised by coordinative contact with its $[(MAO)X]^-$ counterion. These contacts appear to give way, even in the presence of substituted olefins. If to strong ion pair formation takes place, before the olefin coordinates, addition to the cation can be inhibited (Figure

3.1). Formation the ion pairs $[Cp_2ZrR(olefin)]^+[(MAO)X]^-$ is a precondition for olefin insertion into the Zr-R bond. Unusually a low coordinating capability of the anion (A^-) in the ion pair $[Cp_2ZrMe]^+ A^-$ is crucial for the catalytic activity.[54]

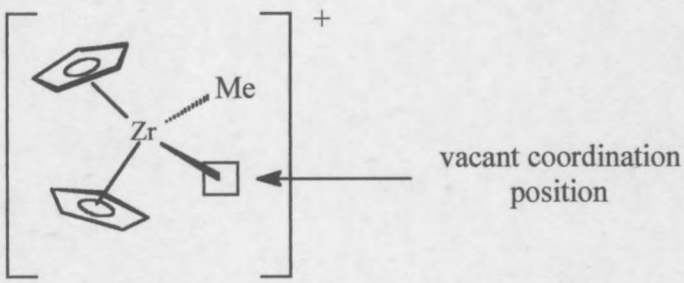

35

Figure 3.1: Cation involved in catalytic activity

3.2.8 OTHER WEAKLY-COORDINATED ANIONS

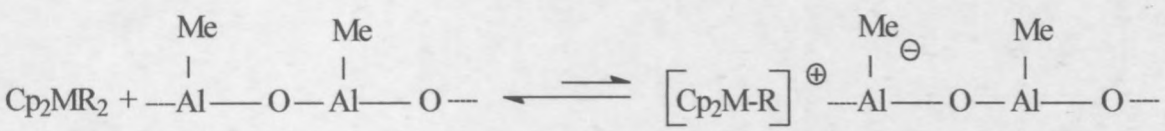

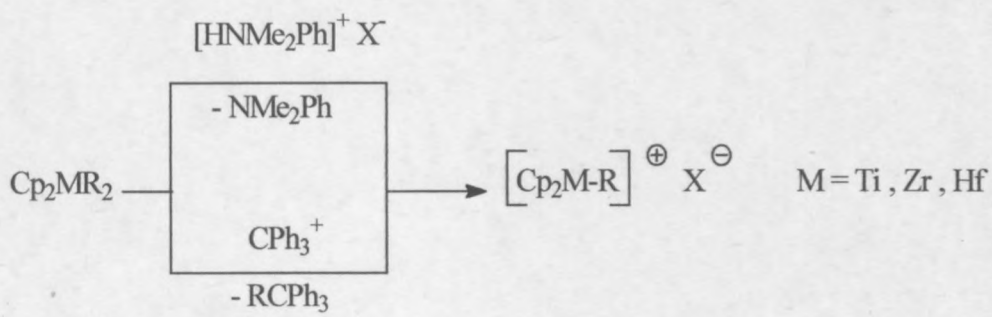

Figure 3.2: The cationic metallocene intermediate

In 1986, Jordan isolated and characterised the cationic species $[Cp_2ZrMe(THF)]^+[BPh_4]^-$ which polymerises ethene, confirming the involvement of cationic intermediates.[55,56] Jordan was able to show that in the case of group 4 metallocenes the active species is a

cationic alkyl complex with a vacant coordination site that is weakly bonded to a counterion.[57,58]

The same cationic complexes are obtained in the absence of aluminium alkyls from metallocene dialkyls by protolysis or R- abstraction with CPh_3^+. With non-coordinating counterions such as $B(C_6F_5)_4^-$ these cationic catalysts show very high activity.

3.3. OLIGOMERISATION AND POLYMERISATION OF α-OLEFINS

3.3.1 INTRODUCTION

"Alpha olefins" is a generic term referring to linear alkenes with the double bond in the terminal or alpha (α) position. Olefins, particularly ethene, propene, and butene, are the basic building blocks of the petrochemical industry. They are easily available, cheap, reactive and readily converted into a range of useful products.

α-Olefins are obtained through thermal and catalytical cracking of paraffins, oligomerisation of ethene, dehydrogenation of paraffins, dimerisation and methathesis of olefins, dehydration of alcohols, and electrolysis of C_{3-30} straight chain carboxylic acids.

Sasol's fuel production, based on coal conversion *via* the Fischer Tropsch process, generates odd-numbered α-olefins as primary products. Oligomerisation of these raw materials, using transition-metal complexes, organoaluminum compounds and inorganic salts and oxides as catalysts, produces polyolefins of high value. Of these catalysts the most important being transition-metal complexes.

3.3.2 APPLICATIONS OF POLYOLEFINS

During the last decade there has been a change in poly-olefin applications from commodity to more specialised products.[59,60] Poly-olefin uses include: packaging material, insulation wire, toys, fibers and yarn, fiber optics, dishwasher safe plasticware, non-stick and microwaveable cookware, shatter resistant glass, various car parts and specialised outdoor clothing. $C_{6\text{-}20}$ α-olefins are a source of biodegradable detergents, new kinds of polymers, lubricants, and many other industrially useful chemicals. Metallocenes[13, 61, 62] as catalysts for α-olefin polymerisation have offered new more economic routes to a whole range of products with new properties for new applications (Scheme 3.8).[13, 61-63]

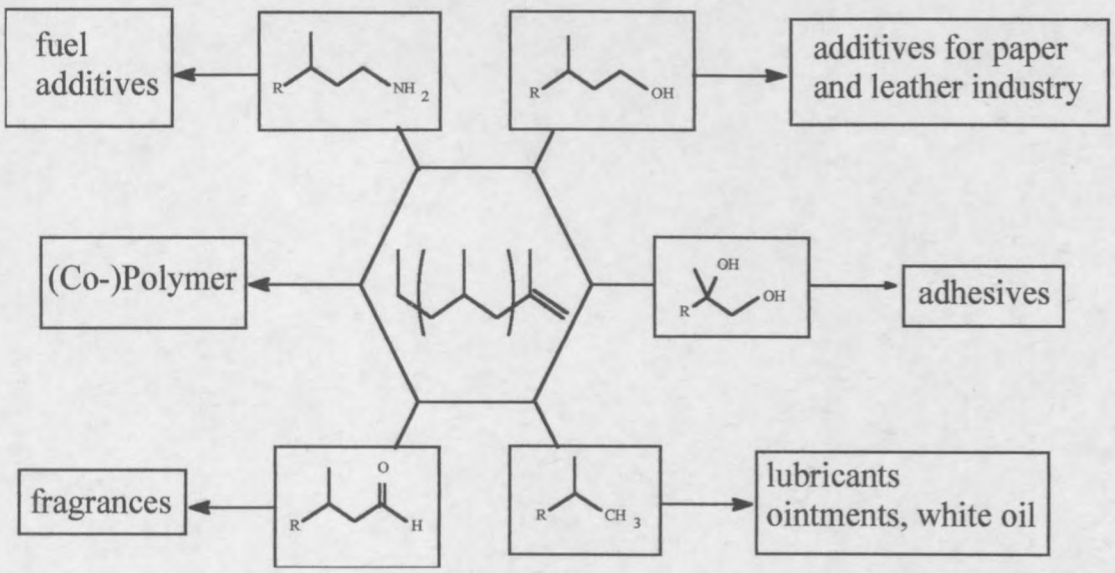

Scheme 3.8: Application of reactive α-olefin oligomers from metallocene catalysts

3.3.3 INDUSTRIAL ETHYLENE OLIGOMERIZATION PROCESSES

The Shell higher-olefins process (SHOP) is based on a homogeneous catalysts consisting of nickel chloride and potassium salts of o-(diphenylphosphino)benzoic acid in 1,4-butanediol, discovered by Keim.[64]

These catalysts oligomerise ethylene to give 1-alkenes of various chain lengths (C_6-C_{20}). Insertion is faster than β-elimination and hydroformylation of the C_{10}-C_{14} fraction gives C_{11}-C_{15} alcohols used in detergent manufacture.[65-68] Nickel complexes can also be used for the oligomerisation of butadiene.

Current work at Sasol is concerned with the synthesis of catalysts their utilization in the oligo- and polymerisation of higher α-olefins. Sasol's research on the oligo- and polymerisation of higher α-olefins focuses on two main areas: 1) catalysts based on late transition metals (Pd, Ni, Fe), Brookhard type catalysts, and 2) Zr and Hf based metallocene.[69, 70]

Brookhart and Gibson showed that late transition metal systems could also be efficient polymerisation catalysts, contrary to earlier beliefs that most late transition metals only dimerise and oligomerise alkenes rather than polymerise them.[71-73] The electrophilicity is important in these systems slowing down β-elimination by limiting the extent of back donation into the β-C-H σ^* orbital, required for the reaction to proceed. The unsaturated system, $[Cp^*Co\{P(OMe)_3\}Et]^+$, having an agostic ethyl group, was shown to slowly polymerise ethylene. These catalysts are usually activated with MAO and produce polymers of quite different microstructures than previously commercially possible. The exact properties of the resulting polymers are dependent on the steric environment of the catalysts used.[72-74]

3.4 AIMS AND OBJECTIVES

Previous work in our laboratory by Arno Neveling has shown the metaloxycarbene complex $[(CO)_5W{=}C(Me)OZrCp_2Cl]$ to be catalytically active for the oligomerisation of 1-pentene. MAO was used as co-catalyst and oligomerisation tests were performed using 1-pentene as substrate.

One aim of this project was to test similar, newly synthesised metaloxycarbene complexes, and to determine their catalytic activity for the oligomerisation of 1-hexene,

using MAO as co-actalyst. 1-Hexene was chosen as substrate for these experiments as it was less volatile than the previously used 1-pentene.

The oligomerisation reactions were performed at different temperatures using different MAO:catalyst ratios to determine the optimum conditions for the oligomerisation reactions, and to study the effect MAO:catalyst ratios and temperature have on the conversion of the monomer. The metaloxycarbene complexes were compared to various metallocene complexes; Cp_2ZrCl_2, $Cp_2Zr(H)Cl$, rac-$[C_2H_4(Ind)_2]ZrCl_2$, $Cp_2Zr(OMe)Cl$ and Cp_2TiCl_2. This would enable us to study the active center and help answer existing questions regarding the mechanism involved. The general mechanism for α-olefin polymerisation or oligomerisation catalysed by metallocenes is shown in Scheme 3.7.

3.5 OLIGOMERISATION OF 1-HEXENE

3.5.1 INTRODUCTION

Metallocene based catalyst precursors are successfully used in the oligomerisation and polymerisation of α-olefins. This project investigates the catalytic activity of group 6 metaloxycarbene complexes in the oligomerisation of α-olefins. Are the catalytic activities of these metaloxycarbene complexes comparable to their metallocene analogues, and what role does the group 6 metal carbonyl unit play in the convesion of the monomer?

During this project oligomerisation was performed in Schlenk tubes. The catalyst precursors dissolved in toluene, and activated with excess MAO (co-catalyst), were stirred for 2 minutes after which the internal reference standard, nonane, was added.

The substrate 1-hexene (**37**) was added to this mixture and stirred for 24 hours after which the reaction was quenched using MeOH. The filtered reaction products were resolved on a GC column using a set temperature program.

3.5.2 METHOD

The investigation of the oligomerisation of 1-hexene was done into two plans: 1) Variation of the oligomerisation temperature (10°, 60° and 100° C). 2) Variation of the MAO:catalyst precursor ratio's (500:1, 1000:1, 2000:1 and 4000:1).

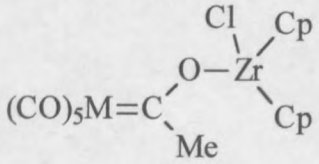

8 M = Cr
12 M = W

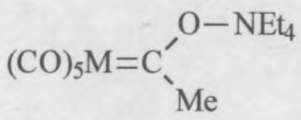

1 M = Cr
3 M = W

Scheme 3.9: Metaloxycarbene complexes **8** and **12**, and ammonium salts of the acyl complexes **1** and **3**, used as catalyst precursors

The ammonium salts of the acyl complexes $[(CO)_5Cr{=}C(Me)ONEt_4]$, **1** and $[(CO)_5W{=}C(Me)ONEt_4]$, **3,** metaloxycarbene complexes $[(CO)_5Cr{=}C(Me)OZrCp_2Cl]$, **8** and $[(CO)_5W{=}C(Me)OZrCp_2Cl]$, **12** and metallocenes, **36-40**, were used as catalyst precursors (Schemes 3.9 and 3.10). Cp_2ZrCl_2 (**36**) was used as a control during these experiments.

The catalyst precursors, dissolved in toluene, were activated by MAO and stirred for 2 minutes. Nonane (1 cm^3) used as internal reference was added followed by 1-hexene, **41**, (18.6 cm^3). The solution was stirred for 24 hours after which it was quenched by adding 5 cm^3 MeOH. The resulting solution was filtered and gas chromatography was used to identify the products (dimers **42**, trimers **43** and tetramers **44**) of the oligomerisation reaction (Scheme 3.11).

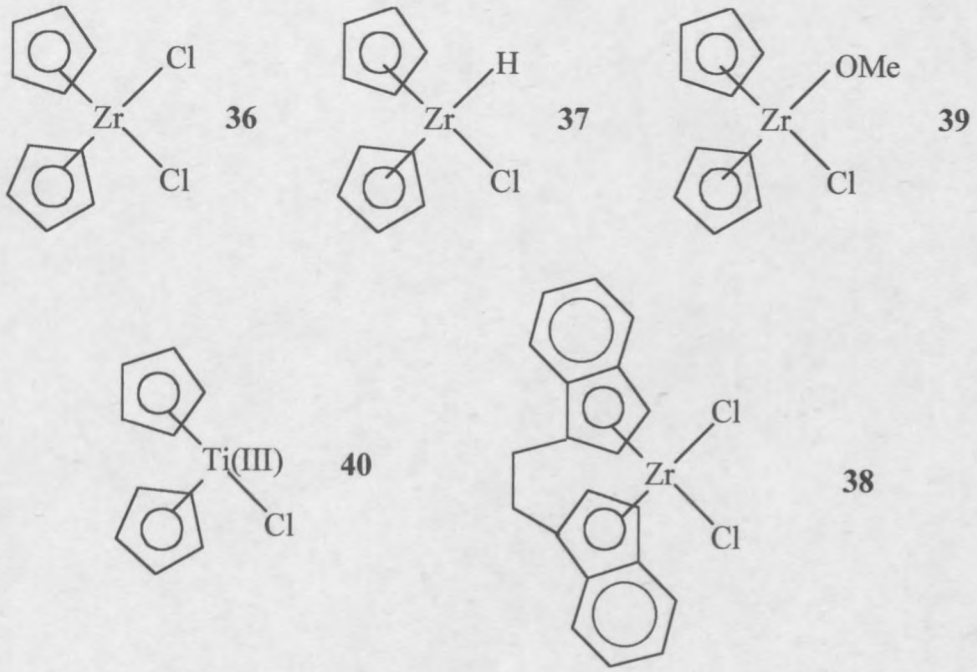

Scheme 3.10: Metallocene precursors

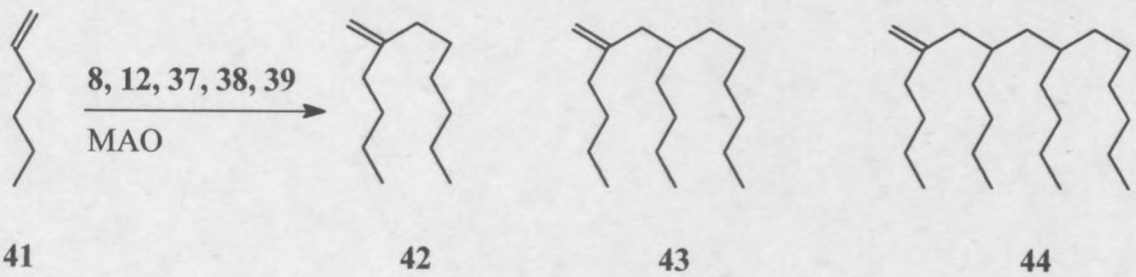

Scheme 3.11: Oligomerisation products of 1-hexene

The retention times of known compounds and a set temperature program were used to identify the products obtained. Quantitative analysis (monomer conversion and catalytic activity) was possible using known amounts of nonane, used as reference, added to the reaction mixture. It is assumed that the detector interprets the internal reference and the oligomer products in the same manner. All reactions were performed in duplicate, and reproducible results are reported. 1-Hexene was chosen as subtrate because it was readily available (SASOL). All solvents were dried and distilled prior to use.

3.5.3 RESULTS AND DISCUSSION

The results obtained for different MAO:catalyst ratio's are inconsistent and are ommitted from this thesis. There is an increase in the total % conversion of the monomer (dimer, trimer and tetramer) for MAO:catalyst ratio's of 500:1 to 1000:1 and to 2000:1, then an unexpected decrease in the total % conversion for MAO:catalyst ratio of 4000:1. These results are contrary to oligomerisation results obtained previously in our group.[75] Further investigation is required to prove or disprove MAO:catalyst ratio results obtained during this projects. Cp_2ZrCl_2 (**36**) is used as a control during these experiments.

Percentage conversion of the monomer to dimer, trimer and tetramer products are calculated as follows: In the experiment 0.148 mol 1-hexene is used. 100% Conversion of the sustrate to the dimer forms 0.0741 mol dimer, and for a 100% coversion to trimer, 0.0494 mol trimer forms, while 100% conversion to the tetramer results in 0.0371 mol tetramers. The conversion yields of 1-hexene to dimers, trimers and tetramers using metallocene catalysts are shown in Table 3.1.

The coversion of 1-hexene with Cp_2ZrCl_2, **36**, is strongly temperature dependent and the highest catalytic activity is observed at 60°C. The decrease in activity at higher temperatures is most likely due to the degradation of the catalyst. The conversion of the monomer with $Cp_2Zr(H)Cl$, **37**, is most effective at 15°C.

The total conversion of the substrate is practically unaffected by changes in oligomerisation temperatures using *rac*-$[C_2H_4(Ind)_2]ZrCl$, **38**, as catalyst precursor. $Cp_2Zr(OMe)Cl$, **39**, and $Cp_2Ti(III)Cl$, **40**, prove to be poor catalyst precursors for the oligomerisation of 1-hexene. The overall conversion using **39** as catalyst precursor is only 2.93% (at 60°C). The conversion yields of 1-hexene to dimers, trimers and tetramers using ammonium salts of the acyl complexes **1** and **3**, and metaloxycarbene complexes **8** and **12** are shown in Table 3.2.

Table 3.1: Persentage convertion of monomer using metallocenes as catalyst precursors (temperature study)

Complex	Temperature	% Conversion Dimer	Trimer	Tetramer	Total
36	15 °C	1.20%	2.20%	7.10%	10.50%
	60 °C	5.90%	9.10%	22.00%	37.10%
	100 °C	4.30%	5.30%	10.90%	20.40%
37	15 °C	13.29%	23.83%	19.67%	56.79%
	60 °C	0.31%	0.32%	1.11%	1.73%
	100 °C	0.18%	0.12%	1.37%	1.67%
38	15 °C	31.91%	10.90%	44.71%	87.51%
	60 °C	24.81%	11.48%	53.82%	90.10%
	100 °C	22.00%	26.76%	39.92%	88.01%
39	15 °C	0.35%	0.40%	0.34%	1.08%
	60 °C	1.73%	0.99%	0.22%	2.93%
	100 °C	0.38%	0.54%	0.34%	1.26%
40	15 °C	0.14%	0.15%	0.42%	0.71%
	60 °C	0.32%	0.47%	0.66%	1.44%
	100 °C	0.13%	0.28%	0.22%	0.63%

The ammonium salts of the acyl complexes **1** and **3** are poor catalyst precursors for the oligomerisation of 1-hexene, showing overall yields of 1.57% and 1.33% respectively (at 60°C). The metaloxycarbene complexes are better catalyst precursors with overall monomer conversions of 38.1% and 43.4% respectively (at 15°C).

Neveling obtained similar results for the oligomerisation of 1-pentene. He reported a value of 48.2% for the total % conversion of 1-pentene to di-,tri- and tetramers for complex **12**, slightly higher than the results obtained during this project.[76]

Table 3.2: Persentage convertion of the substrate using ammonium salts of the acyl complexes **1** and **3**, and metaloxycarbene complexes **8** and **12** as catalyst precursors (temperature study)

		% Conversion			
Complex	Temperature	Dimer	Trimer	Tetramer	Total
1	15 °C	0.00%	0.00%	0.75%	0.75%
	60 °C	0.07%	1.50%	0.00%	1.57%
	100 °C	0.00%	0.67%	0.00%	0.67%
3	15 °C	0.00%	0.18%	0.54%	0.72%
	60 °C	0.02%	1.13%	0.18%	1.33%
	100 °C	0.00%	0.53%	0.36%	0.89%
8	15 °C	2.03%	28.22%	7.81%	38.07%
	60 °C	0.43%	7.05%	1.95%	9.44%
	100 °C	1.54%	0.89%	0.74%	3.17%
12	15 °C	0.24%	36.55%	6.65%	43.44%
	60 °C	0.71%	5.65%	2.43%	8.78%
	100 °C	1.82%	0.96%	0.56%	3.35%

The present oligomerisation test reveal a decrease in the total % conversion of 1-hexene to dimers, trimers and tetramers at moderate to high temperatures (60-100°C). This is contrary to the results reported by Raubenheimer and co-workers, their results showed the highest total % conversion of 1-pentene with complexes **36** and **12** at temperatures between 50 and 100°C. They proposed that a decrease of catalyst activity at higher temperatures was due to catalyst degradation at temperatures above 100°C.[75]

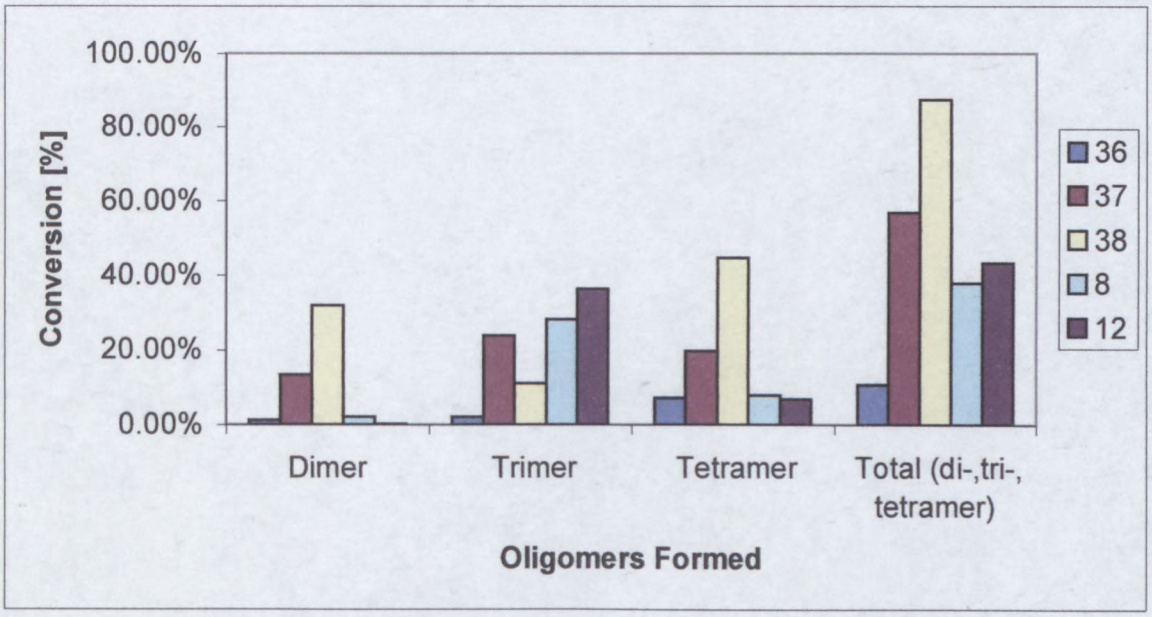

Figure 3.3: % Conversion of 1-hexene to dimers, trimers and tetramers with catalyst precursor at 15° C and a MAO:catalyst ratio of 1000:1

The oligomerisation of 1-hexene using metaloxycarbene complexes **8** and **12** as catalyst precursors, at 15° C favour the formation of trimers. An increase in the oligomerisation temperatures favour the formation of dimers due to β-elimination occurring more readily. This confirmed the results obtained by Raubenheimer and co-workers for the oligomerisation of 1-pentene.[75]

3.5.4 PROPOSED MECHANISM

As was shown earlier (section 2.4, Chapter 2) the acyl form (II) is an important contributing resonance form of metaloxycarbene complexes (Figure 3.4). This could imply that the methylated ion pair (III) (Figure 3.5), formed after activation with MAO, acts as the catalyst precursor.

I II

M = Cr , W

Figure 3.4: Acyl resonance form of metaloxycarbene complexes, showing the weak Zr-O interaction

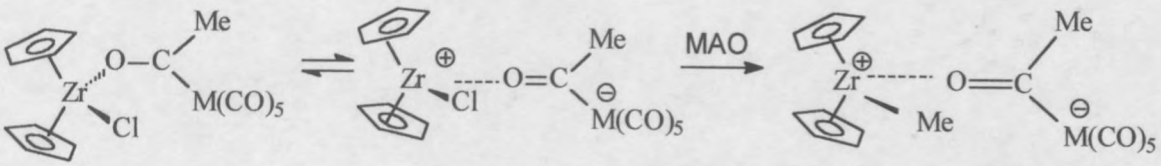

III

M = Cr , W

Figure 3.5: Activation of the metaloxycarbene complex with MAO affords the methylated ion pair (III)

If the methylated ion pair is the active species in the proposed catalytic cycle, repeated alkene coordination, to the methylated ion pair, and insertion followed by β-H elimination would afford the methylated oligomerisation products. Since this was not observed, the real catalyst in the oligomerisation sequence is probably the hydride species formed after the first catalytic cycle.

The proposed mechanism involving the real catalyst is shown in Scheme 3.12 and the oligomerisation products (dimers, trimers and tetramers) formed from the hydride species are shown in Scheme 3.13.

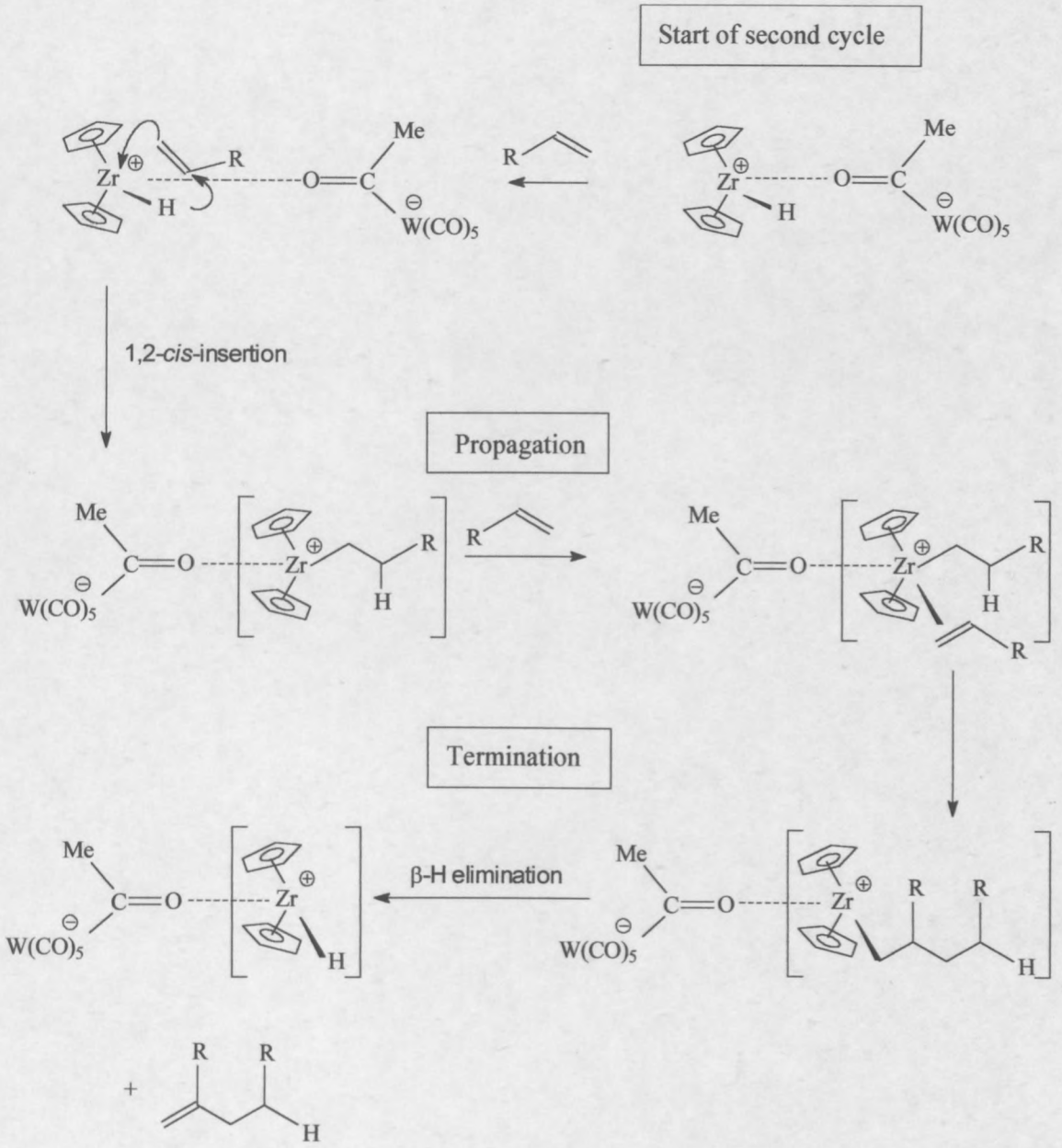

Scheme 3.12: The 'real' catalysts $[(CO)_5M{=}C(Me)O]^-Cp_2Zr(H)^+$

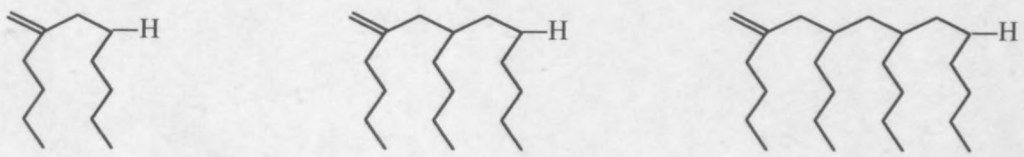

Scheme 3.13: Oligomerisation products formed from hydride species (dimer, trimer and tetramer)

3.6 EXPERIMENTAL

3.6.1 General

All reactions were conducted using a standard vacuum line and Schlenk tubes under positive nitrogen flow.

Toluene and 1-hexene with a low sulphur content were dried with sodium turnings, and distilled at low temperatures. The solvents were distilled fresh daily before use. Spectroscopic pure nonane was distilled at low temperatures and stored over 3 Å sieves. The oligomerisation products of 1-hexene were analysed using a Perkin Elmer Autosystem XL gas chromatograph. The peaks were identified using the retention times of known samples and a set temperature program.

1-Hexene, nonane, Cp_2ZrCl_2, **36**, $Cp_2Zr(H)Cl$, **37**, rac-$[C_2H_4(Ind)_2]ZrCl_2$, **38**, and Cp_2TiCl, **40**, were purchased from Aldrich. The aminocarbene complexes **1** and **3**, and the metaloxycarbene complexes **8** and **12**, and $Cp_2Zr(OMe)Cl$, **39**, were synthesised as discussed in Chapter 2.

3.6.2 Oligomerisation of 1-Hexene

3.6.2.1 Oligomerisation with $[Cp_2ZrCl_2]$, **36**

Cp_2ZrCl_2 (1.61 mg, 5.5 x 10^{-3} mmol) dissolved in toluene (5.5 cm^3) was transferred to a Schlenk tube by means of a syringe. The catalyst solution activated by MAO (2.5 cm^3 MAO:Catalyst ratio of 1000:1) was stirred for 3 minutes. 1 cm^3 nonane (internal reference standard) and toluene (10 cm^3) was added followed by 1-hexene (18.6 cm^3, MAO:Catalyst ratio of 1000:1). The reaction mixture was stirred for 24 hours at the required temperature. Unreacted MAO was quenched with 5 cm^3 MeOH and the solution filtered.

Temperature study: The reaction was carried out at 15°C, 60°C and 100°C. MAO (2.5 cm^3) was used to activate the catalyst.

MAO study: The temperature was kept constant at 15°C. Different amounts of MAO were used to activated the catalysts: 1.25 mmol (MAO : Catalyst, 500 : 1), 2.5 mmol (1000 : 1) 5 mmol (2000:1), 10 mmol (4000:1).

3.6.2.2 Oligomerisation with $[Cp_2Zr(H)Cl]$, **37**

The same reaction method was used as described in section 3.4.2.1. (1.42 mg, 5.5 x 10^{-3} mmol) metallocene was used as catalyst precursor.

3.6.2.3 Oligomerisation with $\{rac\text{-}[C_2H_4(Ind)_2]ZrCl_2\}$, **38**

The same reaction method was used as described in section 3.4.2.1. (2.30 mg, 5.5 x 10^{-3} mmol) metallocene was used as catalyst precursor.

3.6.2.4 Oligomerisation with $[Cp_2Zr(OMe)Cl]$, **39**

The same reaction method was used as described in section 3.4.2.1. (1.60 mg, 5.5 x 10^{-3} mmol) metallocene was used as catalyst precursor.

3.6.2.5 Oligomerisation with $[Cp_2TiCl]$, **40**

The same reaction method was used as described in section 3.4.2.1. (1.17 mg, 5.5 x 10^{-3} mmol) metallocene was used as catalyst precursor.

3.6.2.6 Oligomerisation with complex **1**

The same reaction method was used as described in section 3.4.2.1. (2.73 mg, 5.5 x 10^{-3} mmol) ammonium salt of the acyl complex was used as catalyst precursor.

3.6.2.7 Oligomerisation with complex **3**

The same reaction method was used as described in section 3.4.2.1. (2.01 mg, 5.5 x 10^{-3} mmol) ammonium salt of the acyl complex was used catalyst precursor.

3.6.2.8 Oligomerisation with complex **8**

The same reaction method was used as described in section 3.4.2.1. (2.71 mg, 5.5 x 10^{-3} mmol) metaloxycarbene complex **8** was used as catalyst precursor.

3.6.2.9 Oligomerisation with complex **12**

The same reaction method was used as described in section 3.4.2.1. (3.43 mg, 5.5 x 10^{-3} mmol) metaloxycarbene complex **12** was used as catalyst precursor.

3.6.3 Oligomerisation data collection and calculations

Filtered oligomerisation reaction mixtures were injected onto a GC column. Dimers, trimers, tetramers and higher oligomers were resolved using a set gradient program. The starting temperature of the GC oven was kept at 80°C for 10 minutes, followed by stepwise temperature increase of 7°C/min. The column temperature was kept at 250°C for 15.71 minutes (end temperature). The total run time amounted to 50.00 min per run.

Resolution peaks were observed at 2.67 min., 3.98 min., 6.95 min., 12.87 min., 21.10-26.58 min., 29.10-33.88 min. and 38.21-43.44 min. These peaks were identified as belonging to MeOH, Hexene, Nonane, Toluene, dimer, trimer and tetramer, from retention times of known control samples, generated using the same temperature program described above.

1. K. Ziegler, E. Holzkamp, H. Breil and H. Martin, *Angew. Chem.* 1955, **67**, 541.
2. G. Natta, P. Pino, G. Mazzanti and U. Giannini, *J. Am. Chem. Soc.* 1957, **79**, 2975.
3. Prof. Dr. Dr.h.c. W Keim in *Homogeneous Catalysis for Industry, Lectures for Honours Students*, University of Stellenbosch, 2001, 1-8.
4. I. Omea in *Applications of Organometallic Compounds*, John Wiley & Sons, New York, 1998, 107-108.
5. P. Pino and R. Mülhaupt, *Angew. Chem., Int. Ed. Engl.* 1980, **19**, 857.
6. R. Mülhaupt in *Ziegler Catalysts*, Eds. G. Fink, R. Mülhaupt, H. H. Brintzinger, Springer-Verlag, Berlin, Heidelberg, 1995,1-37.
7. R. Mülhaupt in *Ziegler Catalysts*, Eds. G. Fink, R. Mülhaupt, H.H. Brintzinger, Springer-Verlag, Berlin, Heidelberg, 1995, 35.
8. G. Natta and G. Mazzanti, *Tetrahedron*, 1960, **8**, 86.
9. P. Cossee, *Tetrahedron Lett.*, 1960, **17**, 12; E.J. Arlam and P. Cossee, *J. Catal.*, 1964, **80**, 89-99.
10. L.A.M. Rodriguez and H.M. van Looy, *J. Polymer. Sci. (A-I)*, 1966, **4**, 1951 and 1971.
11. R.H. Crabtree in *The Organometallic Chemistry of the Transition Metals*, 3rd Ed., John Wiley & Sons, New York, 1996, 69-71.
12. D. S. Breslow and N. R. Newburg, *J. Am. Chem. Soc.*, 1957, **79**, 5072.
13. H. Sinn, W. Kaminsky, H.J. Vollmer and R. Woldt, *Angew. Chem., Int. Ed. Engl.*, 1980, **19**, 390.
14. J.C.W. Chien and P. Bres, *J. Polym. Sci. A. Polym. Chem..*, 1986, **24**, 1967.
15. J. C. W. Chien, *J. Am. Chem. Soc.*,1981, **103**, 86.
16. P. Pino, P. Cionoi, and J. Wei, *J. Am. Chem. Soc.*, 1987, **109**, 6189-6191.
17. H. Sinn and W. Kaminsky, *Adv. Organomet. Chem.*, 1980, **18**, 99.
18. P. Burger, K. Hartmann and H.H. Brintzinger, *Makromol. Chem., Makromol. Symp.*, 1993, **66**, 127.
19. J. Boor in *Ziegler-Natta Catalyst and Polymerization*, Academic Press, New York, 1991, 1.

20. B.J. Burger, M.E. Thompson, W.D. Lotter and J.E. Bercaw, *J. Am. Chem. Soc.*, 1990,**112**, 1566.
21. W.E. Piers and J.E. Bercaw, *J. Am. Chem. Soc.*, 1990,**112**, 9406.
22. R.F. Jordan, R.E. LaPointe, N. Baenziger and G.D. Hinch, *Organometallics*, 1990, **9**, 1539.
23. R.F. Jordan, *Adv. Organomet. Chem.*, 1991, **32**, 325.
24. D.J. Crowther, S.L. Barkowsky, D. Swenson, T.Y. Meyer and R.F. Jordan, *Organometallics*, 1993, **12**, 2897.
25. A.L. Mogstadt and R.M. Waymouth, *Macromolecules*, 1992, **25**, 2282.
26. L. Clawson, J. Soto, S. Buchwald, M. Steigerwald and R. J. Grubbs, *J Am. Chem. Soc.*, 1985, **107**, 7219-7220.
27. E. Arlman and P. Cossee, *Catal.*, 1964, **3**, 99.
28. J.C.W. Lohrenz, T.K. Woo, L. Fan and T. Ziegler, *J. Organomet. Chem.*, 1995, **497**, 91-104.
29. J.A. Ewen, L. Haspeslagh, J. Atwood and H. Zhang, *J. Am. Chem. Soc.*, 1987, **109**, 6544-6545.
30. G.G. Hlatky, H.W. Turner and R.R. Echman, *J. Am. Chem. Soc.*, 1989, **111**, 2728.
31. J.C.W. Chien, W.M. Tsai and M.D. Rausch, *J. Am. Chem. Soc.*, 1991, **113**, 3623.
32. R.F. Jordan, *J. Chem. Educ.*, 1988, **65**, 285.
33. M.L.H. Green and J.J. Rooney, *J. Chem. Soc., Chem. Comm.*, 1978, 604.
34. H.H. Turner and R.R. Schrock, *J. Am. Chem. Soc.*, 1982, **104**, 2331.
35. M Brookhart, M.L.H. Green and L. Wong, *Prog. Inorg. Chem.*, 1988, **36**, 1.
36. P. Watson and D.C. Roe, *J. Am. Chem. Soc.*, 1982, **104**, 1982.
37. W.E. Piers and J.E. Bercaw, *J. Am. Chem. Soc.*, 1990, **112**, 9406.
38. H. Krauledat and H.H. Brintzinger, *Angew. Chem., Int. Ed. Engl.*, 1990, **29**, 1412.
39. M.K. Leclerc and H.H. Brintzinger, *J. Am. Chem. Soc.*, 1995, **117**, 1651.
40. G.W. Coates and R.M. Waymouth in *Comprehensive Organometallic Chemistry Part II*, Vol. 12, Elsevier Science Ltd., Oxford, UK, 1995, 1195.

41. J.J. Eisch, A.M. Piotrowski, S.K. Brownstein, E.J. Grabe, and F.L. Lee, *J. Am. Chem. Soc.*, 1985, **107**, 7219.

42. K.H. Riechert and K.R. Meyer, *Makromol. Chem.*, 1973, **169**, 163.

43. W.P. Long, D.S. Breslow, *Liebigs, Ann. Chem.* 1973, **169**, 163.

44. D. Cam, E. Albizzati and P. Cinquina, *Marcromol. Chem.*, 1990, **191**, 1641.

45. W. Kaminsky, H. Sinn, H.J. Vollmer and R.Woldt, *Angew. Chem.*, 1976, **88**, 689.

46. S. Pasynkiewicz, *Polyhedron* 1990, **9**, 429.

47. A.R. Siedle, R.A. Newmark, W.M. Lamanna and J.N. Schroepfer, *Polyhedron*, 1990, **9**, 301.

48. J.C.W. Chien and R. Sugimoto, *J. Polym. Sci. A. Polym. Chem.*, 1991, **29**, 459.

49. J.C.W. Chien and B.P. Wang, *J. Polym. Sci. A. Polym. Chem.*, 1988, **26**, 3089.

50. J.C.W. Chien and B.P. Wang, *J. Polym. Sci. A. Polym. Chem.*, 1990, **28**, 15.

51. A.D. Horton in Trends in Polymer Science, Cambridge, UK., 1994, **2**, 158.

52. N.J. Long in *Metallocenes*, Blackwell Science, Oxford, 1998, 231.

53. A.R. Siedle, R. A. Newmark, D. E. Richardson, M. Ryan, C. R. Landis, J. Wright, D. Root, M. G. Hill and K. P. Mann, *Proc. Met. Con. Houston*, 1993, 351.

54. R.F. Jordan, C.S. Bajhur, R. Willett and B. Scott, *J. Am. Chem. Soc.*, 1986, **108**, 7410.

55. R.F. Jordan, W.E. Dasher and S.F. Echols, *J. Am. Chem. Soc.*, 1986, **108**, 1718.

56. Y.W. Aleynuas, R.F. Jordan, S.F. Echols, S.L. Borkowsky and P.K. Bradley, *Organometallics*, 1991, **10**, 1406.

57. R.F. Jordan, C.S. Bajgur, R. Willett and B. Scott, *J. Am. Chem. Soc.*, 1986, **108**, 7410.

58. W. Kaminsky, *Angew. Makromol. Chem.*, 1994, **223**, 101.

59. B. Rieger, C. Janiak, *Angew. Makromol. Chem.*, 1994, **215**, 35.

60. J. A. Ewan, *J. Am. Chem. Soc.*, 1984, **106**, 6355.

61. W. Kaminsky, K. Külpert, H. H. Brintzinger, F. R. W. P. Wild, *Angew. Chem., Int. Ed. Engl.*, 1985, **24**, 507.

62. J. Skupenska, *Chem. Rev.*, 1991, **283**, 173.

63. W. Keim., *Organometallics* 1983, **2**, 594.

64. A. H. Turner, *J. Am. Oil Chem. Soc.*, 1983, **60**, 623.

65. E. F. Lutz, *J. Chem. Educ.*, 1986, **63**, 203.

66. B. Reuben and H. Wittcoff, *J. Chem. Educ.*, 1988, **65**, 605.

67. *Chem. Abstr.* 1980, **93**, 7580t.

68. B. L. Small, M.Brookhart, *J. Am. Chem. Soc.*, 1998, **120**, 7143.

69. C. M. Killian, D. J. Temple, L.K. Johnson, M. Brookhart, *J. Am. Chem. Soc.*, 1996, **118**, 11664.

70. G.F. Schmidt and M. Brookhart, *J. Am. Chem. Soc.*, 1985, **107**, 1443. M. Brookhart and E. Hauptman, *J. Am. Chem. Soc.*, 1992, **114**, 4437.

71. B.L. Small, M. Brookhart and A.M.A. Bennett, *J. Am. Chem. Soc.*, 1998, **120**, 4050.

72. G.J.P. Britovsek, M. Bruce, V.C. Gibson, B.S. Kimberley, P.J. Maddox, S. Mastroianni, S.J. McTavish, C. Redshaw, G.A. Solan, S. Strömberg, A.J.P. White and D.J. Williams, *J. Am. Chem. Soc.*, 1999, **121**, 8729.

73. A.C.L. Su, *Adv. Organometal. Chem.*, 1979, **17**, 269.

74. U.M. Wahner, R. Brüll, H. Pasch, H.G. Raubenheimer and R. Sanderson, *Angew. Makromolekul. Chem.*, 1999, **270**, 49.

75. A. Neveling, *M.Sc.-thesis*, University of Stellenbosch, 1999.

CHAPTER 4

CRYSTALLOGRAPHIC STRUCTURE DETERMINATION

4.1 INTRODUCTION

Single crystal X-ray diffraction structure determination provides valuable information regarding the molecular structure of the complexes e.g. bond lengths and angles and structural orientation.

The syntheses of metaloxycarbene complexes are of interest in our group and many group 6 carbene group 4 metallocene complexes have successfully been characterised crystallographically.

Recent contributions from our group include: $[(CO)_5W{=}C(CH_3)OZrCp_2Cl]$, **12**, $[(CO)_5Cr{=}C(CH_3)OZrCp_2Cl]$, **8**, and $[CO)_5Cr{=}C(Ph)OTiCp_2Cl]$, **44**.[1-3]

This chapter focuses on the crystal- and molecular structures of the newly prepared metaloxycarbene complexes $[(CO)_5W{=}C(Ph)OTiCp_2]$, **11**, and $[(CO)_5W{=}C(Ph)OHfCp_2]$, **13**. These complexes are discussed with reference to known complexes.

Attempts to prepare the metaloxycarbene complex $[(CO)_5Cr{=}C(Me)OZr(H)Cp_2]$ from reaction of $Cp_2Zr(H)Cl$ and $[(CO)_5Cr{=}C(Me)ONEt_4]$ resulted in red crystals of $[(CO)_5Cr\text{-}Cl\text{-}Cr(CO)_5]^-$. This structure is discussed in the second part of this Chapter with reference to comparable complexes.

4.2. RESULTS AND DISCUSSION

Metaloxycarbene complexes are readily synthesised by metallation of pentacarbonyl chromium acylate intermediates (Scheme 4.1). The syntheses of these complexes are discussed in detail in Chapter 2. Single crystals of these complexes were obtained from a saturated toluene solution at -6°C. Complexes **11** and **13** are monoclinic with $P2_1/c$ space

group symmetry. The tungsten atom, in both complexes, is octahedrally surrounded by five carbonyl ligands and a carbene ligand that also contain Ti or Hf (Figures 4.1 and 4.2).

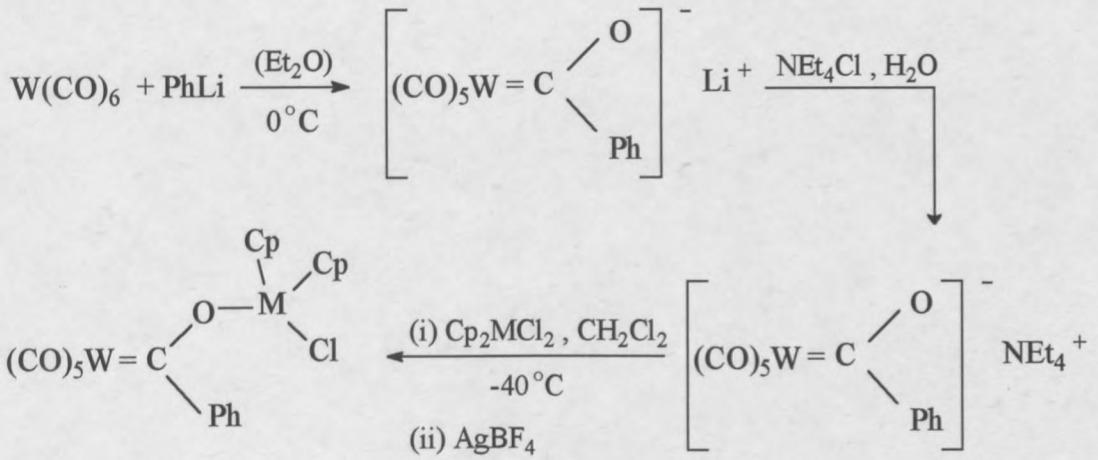

11 M = Ti

13 M = Hf

Scheme 4.1: Preparation of metaloxycarbene complexes **11** and **13**

Selected bond angles and bond lengths for complex **11** are tabulated in Tables 4.1 and 4.3. The corresponding bond angles and lengths for complex **13** are shown in Tables 4.5 and 4.6 respectively. Comparative values of other metaloxycarbene complexes are tabulated in Tables 4.2 and 4.4. A summary of the selected geometrical parameters is given in Tables 4.7 and 4.8.

4.2.1 STRUCTURE OF [(CO)$_5$W=C(Ph)OTiCp$_2$Cl], 11.

Numerous titanium metaloxycarbene– and alkoxycarbene complexes are known and will be used in the discussion of [(CO)$_5$W=C(Ph)OTiCp$_2$Cl] **11**.

Deviations from the idealised 90 and 180° angles around the W atom [C(2)-W-C(4) 173.28(16), C(5)-W-C(6) 175.79(16), C(3)-W-C(2) 86.93 (16), C(5)-W-C(4) 93.55(16),

C(3)-W-C(6) 93.62(16), C(6)-W-C(1) 86.31(15)°] of complex **11**, accommodate the bulky oxotitanocene ligand (Figure 4.1 and Table 4.1). Similar deviations have been observed in the structures of $[(CO)_5W{=}C(Me)OZrCp_2Cl]$, **12**, $[(CO)_5Cr{=}C(Me)OZrCp_2Cl]$, **8**, and $[(CO)_5Cr{=}C(Ph)OTiCp_2Cl]$, **44**, recently prepared in our group.[1-3]

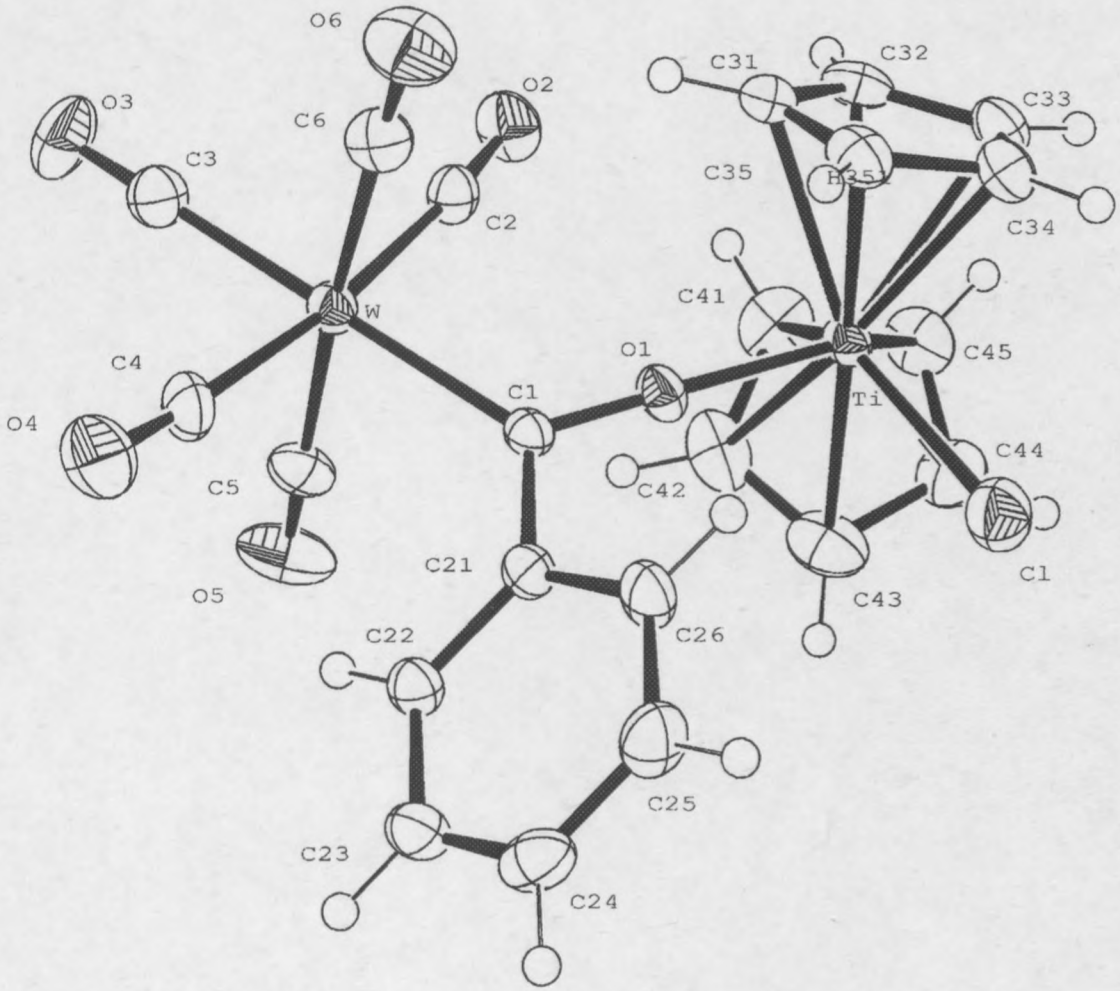

Figure 4.1: Thermal ellipsoid plot of $[(CO)_5W{=}C(Ph)OTiCp_2Cl]$, **11**, showing the atomic numbering scheme (50% probability ellipsiods with the hydrogens as spheres of arbitrary diameter)

Deviations from the theoretical 120° angles (trigonal planar) around the carbene carbon atom [W-C(1)-O(1) 123.0(2), W-C(1)-C(21) 125.6(2), O(1)-C(1)-C(21) 111.3(3)] help

accomadate the oxotitanocene ligand. The angle between the pentacarbonyl tungsten fragment and the phenyl ring increases to 125.6(2)°, while the angle between the phenyl ring and the coordinated oxygen, decreases to 111.3(3)°.

Table 4.1 Selected bond angles (°) of complex **11**

C(1)-W-C(2)	92.82(14)	C(1)-W-C(3)	179.74(1)
C(1)-W-C(4)	91.82(15)	C(2)-W-C(4)	173.28(2)
C(1)-W-C(5)	89.48(15)	C(5)-W-C(6)	175.79(2)
C(2)-W-C(3)	86.93(16)	O(2)-C(2)-W	174.1(4)
C(2)-W-C(5)	91.34(15)	O(3)-C(3)-W	177.3(4)
C(2)-W-C(6)	88.96(15)	O(4)-C(4)-W	176.3(4)
C(3)-W-C(4)	88.42(16)	O(5)-C(5)-W	178.7(3)
C(3)-W-C(5)	90.59(16)	O(6)-C(6)-W	177.2(4)
C(3)-W-C(6)	93.62(16)	W-C(1)-O(1)	123.0(2)
C(4)-W-C(5)	93.55(16)	W-C(1)-C(21)	125.6(2)
C(4)-W-C(6)	86.50(15)	C(21)-C(1)-O(1)	111.3(3)
C(1)-W-O(6)	86.31(15)	C(1)-O(1)-Ti	171.7(2)
Cp_{cent}-Ti-Cp_{cent}	132.56	O(1)-Ti-Cl	96.16(8)

Similar deviations have been observed in the structures of $[(CO)_5W{=}C(Me)OZrCp_2Cl]$, **12**, $[(CO)_5Cr{=}C(Me)OZrCp_2Cl]$, **8**, and $[(CO)_5Cr{=}C(Ph)OTiCp_2Cl]$, **44**, recently prepared in our group.[1-3] The deviations from the theoretical 120° angles are very similar for both methyl and phenyl substituents, $[(CO)_5W{=}C(Me)OZrCp_2Cl]$, **12**, showed angles around the carbene carbon atom of 111.8(7), 123.7(5) and 124.5(6)°, compared to 111.3(3), 123.0(2) and 125.6(2)° of complex **11.**[1]

Finn's complex $[(CO)_5Cr{=}C\{C(CH_3){=}CH_2\}OTiCp_2Cl]$, **45**, show the same deviation as for complex **11**, with angles of 111.6(2), 122.0(2) and 126.1(2)°.[5] Heydenrych reported a Cr-$C_{carbene}$-O bond angle of 123.49(1)° for complex **44**.[3] It appears as if these angles are insensitive to the metal used or of the substituent on the $C_{carbene}$ atom (Table 4.2).

Table 4.2: Comparable bond angles (°) of metaloxycarbene complexes

Complex	M-$C_{carbene}$-O	M-$C_{carbene}$-R	O-$C_{carbene}$-R	$C_{carbene}$-O-M^1	O-M^1-Cl
11	123.0(2)	125.6(2)	111.3(3)	171.7(2)	96.1(8)
13	123.2(4)	126.1(4)	110.5(5)	171.4(3)	97.5(1)
12	123.7(5)	124.5(6)	111.8(7)	178.0(5)	95.6(2)
8	123.2(4)	124.3(4)	112.5(3)	170.5(3)	97.3(1)
44	123.5(2)	125.6(0)	110.7(8)	171.8(9)	96.14(5)
45	122.0(2)	126.1(2)	111.6(2)	173.2(2)	95.3(7)
46	123.2(6)	125.8(9)	-	173.2(9)	95.2(4)
47	123.0(9)	118.8(2)	-	173.8(1)	95.7(8)

M=Cr and W, M^1=Ti, Zr and Hf, R=Me, Ph, C=CH_2 and C(CH_2)CH_3

Complex **11** showed a C1-O1-Ti bond angle of 171.7(2)°, almost the same as the $C_{carbene}$-O-Ti bond angle reported for the chromium derivative 172.0(1)°. The almost linear C1-O1-Ti bond angle of **11** can be explained on steric grounds laid by Finn et al.[5] They explain that the complex assumes a large bond angle because the oxygen atom has almost sp hybridization in order to make both p orbitals available for π delocalisation to the M-$C_{carbene}$ and O-Ti units.

Finn suggests that π delocalisation in the M-$C_{carbene}$-O-M' unit is increased for titanoxycarbene complexes, compared to that of alkoxycarbene complexes, by virtue of the π acidity of the d^0 metal center.[5, 6]

Results from our group showed zirconium metalloxycarbene complexes with remarkably different $C_{carbene}$-O-Zr bond angles, ie. 178.0(5)° and 170.5(3)° for [$(CO)_5$W=C(Me)OZrCp_2Cl], **12,** and [$(CO)_5$Cr=C(Me)OZrCp_2Cl], **8,** respectively.[1,2] The $C_{carbene}$-O-Zr is essentially linear for **12**, this suggests a marked delocalization for W than for Cr carbene complexes.

Complex **11** shows a Cl-Ti-O bond angle of 96.16(8)°, similar to those obtained for Finn's complexes, $[(CO)_5M=C\{C(CH_3)CH_2\}OTiCp_2Cl]$ M=Cr 95.30(7)° **45**, M=W 95.24(4)° **46**] and 95.78(1)° for $[(CO)_5Cr=C(CHCH_2)OTiCp_2Cl]$ **47**.[5, 6] The chromium derivative of complex **11**, $[(CO)_5Cr=C(Ph)OTiCp_2Cl]$ **44,** prepared in our laboratory showed a Cl-Ti-O bond angle of 96.14(5)°.[3]

The metallocene alkoxide complex prepared by Huffman $[Cp_2Ti(OR)Cl]$, R= C_2H_5 **48**, has a comparable bond angle of 93.1(1)°.[7] Metallocene alkoxide complexes with bulkier R groups showed similar angles. Chloro-bis(η^5-cyclopentadienyl)-(1,1-dimesilyl-3,3-dimethyl-1-buten-2-oxy)-titanium(IV) **49** has a Cl-Ti-O bond angle of 98.33(3)°, compared to 92.00(5)° of μ^3-[chlorobis(η-cyclopentadienyl)titaniummethylidynecyclo-tris(tricarbonylcobalt(I)] **50**.[8,9]

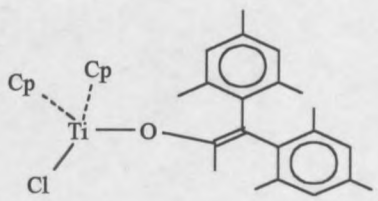

49

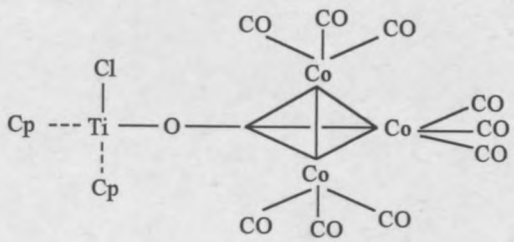

50

Figure 4.2: Metallocene alkoxide complexes with bulky R groups

The centroids of the two partially eclipsed cyclopentadienyl rings (Figure 4.3) of complex **11** are at similar distances away from the Ti atom (2.056 Å and 2.061 Å) and forms a Cp-Ti-Cp angle of 132.56°, with the Cp rings arranged symmetrically about the Ti atom. The cone angle for titanocene is between 129-131°.[10] The cone angle is possibly on the large side because the Cp rings in complex **11** is partially eclipsed. This observation is confirmed by the large Cp-Hf-Cp bond angle of 132.56° for complex **13**, compared to 121.19° for hafnocene.

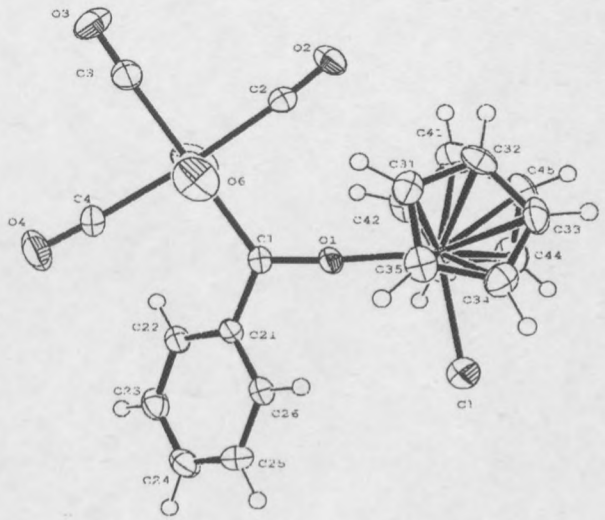

Figure 4.3: Thermal ellipsoid plot of $[(CO)_5W{=}C(Ph)OTiCp_2Cl]$, **11**, with atomic numbering scheme (50% probability ellipsiods with the hydrogens as spheres of arbitrary diameter). This angle shows the partial eclipsed cyclopentadienyl rings

Bonding in Fischer carbene systems is often evaluated in terms of competitive π donation by the metal and the heteroatom substituent(s) to the carbene p orbital; for monoalkoxycarbene complexes these are described as carbene and acyl resonance forms (Figure 4.4).

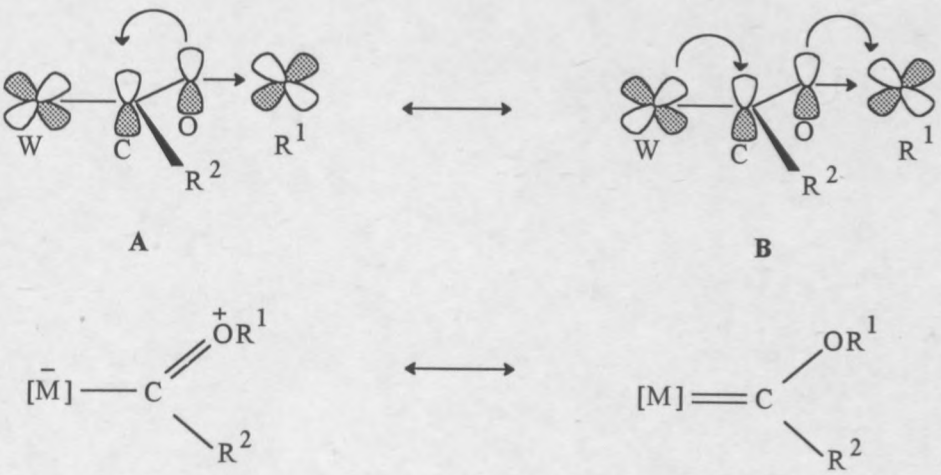

Figure 4.4: Orbital interactions in acyl (A) and carbene (B) resonance forms of metaloxycarbene complexes

The alkoxycarbene complexes $[(CO)_5W=C(Me)OEt]$, **51**, $[(CO)_5W=C(C_5H_7)OEt]$, **52**, $[(CO)_5W=C(Ph)OEt]$, **53**, and **54** (Figure 4.5), are used to show the relative importance of the acyl and carbene resonance forms for the metaloxycarbene complexes.[11,12,4]

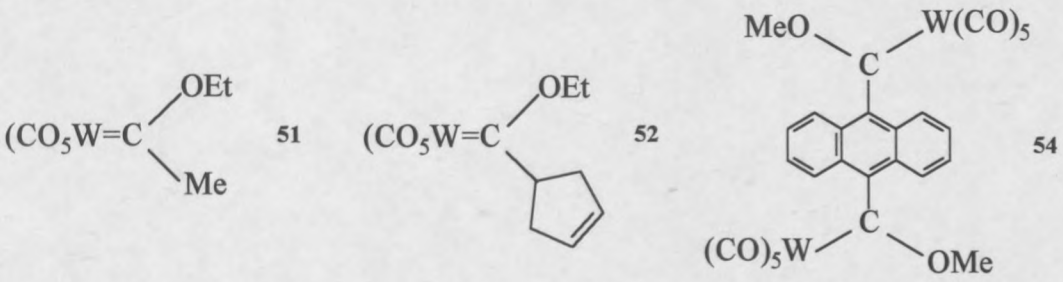

Figure 4.5: Alkoxycarbene complexes

Table 4.3 Selected bond lengths (Å) for complex **11**

W-C(1)	2.204(4)	C(1)-O(1)	1.279(4)
W-C(2)	2.039(4)	C(2)-O(2)	1.134(5)
W-C(3)	2.029(4)	C(3)-O(3)	1.143(5)
W-C(4)	2.047(4)	C(4)-O(4)	1.132(5)
W-C(5)	2.042(4)	C(5)-O(5)	1.138(5)
W-C(6)	2.051(4)	C(6)-O(6)	1.135(5)
C(1)-C(21)	1.499(5)	Ti-Cl	2.345(1)
Ti-O(1)	1.928(2)	Ti-C(41)	2.359(4)
Ti-C(31)	2.381(4)	Ti-C(42)	2.378(4)
Ti-C(32)	2.359(4)	Ti-C(43)	2.376(4)
Ti-C(33)	2.375(4)	Ti-C(44)	2.385(4)
Ti-C(34)	2.408(4)	Ti-C(45)	2.377(4)
Ti-C(35)	2.384(4)		

The W-$C_{carbene}$ bond distance of the titanoxycarbene complex $[(CO)_5W=C(Ph)OTiCp_2Cl]$, **11**, [2.204(4) Å] is much longer than that in the alkoxycarbene complex $[(CO)_5W=C(Me)OEt]$ [2.086(2) Å], **52**.[11] Thus the acyl resonance form is much more important in **11** than in the corresponding alkoxycarbene complex.

The prevalent importance of the acyl resonance form, however, is less prenounced when compared to the alkoxycarbene complexes **51** (2.185 Å), **53** (2.195 Å) and **54** [2.164(6) Å].[12,4] Known bond distances are reported for metaloxycarbene complexes in Table 4.4.

Table 4.4: Comparable bond lengths (Å) of metaloxycarbene complexes

Complex	M-$C_{carbene}$	$C_{carbene}$-O	M^1-Cl	M^1-O
11	2.204	1.279	2.345	1.928
13	2.180	1.291	2.414	2.007
12	2.187	1.275	2.441	2.020
8	2.053	1.269	2.421	2.039
44	2.061	1.278	2.357	1.929
45	2.062	1.279	2.356	1.929
46	2.045	1.268	2.368	1.926
47	2.187	1.265	2.353	1.916

M=Cr and W, M^1=Ti, Zr and Hf, R=Me, Ph, C=CH_2 and C$(CH_2)CH_3$

The $C_{carbene}$-O bond distance of the titanoxycarbene complex $[(CO)_5W{=}C(Ph)OTiCp_2Cl]$, **11**, [1.279(4)Å], is shorter than that in the three alkoxycarbene complexes, **51** (1.321 Å), **52** [1.323(2) Å], **53** (1.299 Å) and **54** [1.311(8) Å].[11, 12, 4] This strengthened C-O interaction suggests that the acyl resonance structure (Figure 4.4 A) is an important contributor to the bonding in these species, as has been noted by Erker for a series of zirconoxycarbene complexes.[20]

The Ti-O bond length of **11**, [1.928(2) Å] is significantly longer than the corresponding bond length of the following titanium alkoxide complexes and titanoxy metallacycle: $[Cp_2Ti(OMe)Cl]$ (1.840 Å), **55**, $[Cp_2Ti(OEt)Cl]$ [1.855(2) Å], **56**, $[\{Ti(C_5Me_4Et)Cl_2\}_2$ $(\mu$-$OC_6H_4O)]$ [1.865 (2) Å], **57**, chloro-bis(η5-cyclopentadienyl)-(2-methoxyacetophenone)-titanium (1.861 Å), **58**, and $[CpTi(OC_6H_3$-2,6-*i*-$Pr_2)$ μ-$Cl]_2$ [1.808(8) Å], **59**, (Figure 4.6).[13,7,14-16] Again this confirms the importance of the acyl resonance form for metaloxycarbene complexes.

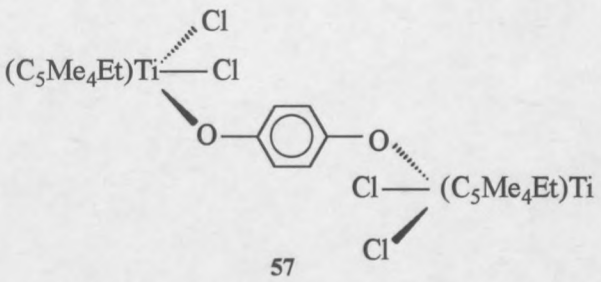

57

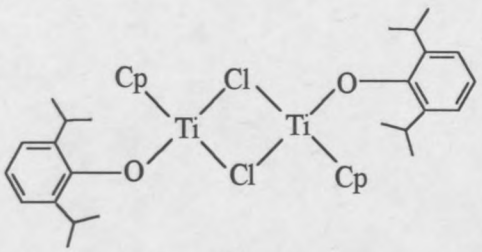

59

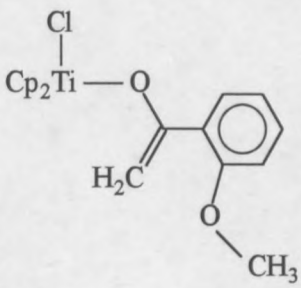

58

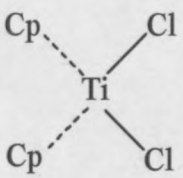

60

Figure 4.6: Cyclopentadienyl-titanium alkoxide complexes **57**, **58**, titanoxy metalacycle **59** and titanocene **60** used in discussion of comparable bond lengths and bond angles of complex **11**

Increased π electron overlap between the O atom and the carbene carbon atom and resulting increased $C_{carbene}$-O bond order, reduces the electrondensity available for pπ and dπ overlap between the O and Ti atoms. Thus the bond order between the O and Ti atoms decreases and bond length increases.

The Ti-Cl bond length of complex **11** [2.345(1) Å] is significantly shorter than the corresponding bond of [2.405(1) Å] **57**, [2.401(4) Å] **57**, (2.403 Å) **58** and [2.393(7) Å] **59,** but closer to the Ti-Cl bond length of titanocene [2.364(2) Å] **60**.[7,14-16,17] From the comparative values it can be deduced that metaloxycarbene complexes have an opposite affect on the electron density of the titanium atom than other alkoxide complexes. The Ti-Cl bond lengths of metaloxycarbene complexes are similar to that obtained for complex **11** (Table 4.4), $[(CO)_5M{=}C\{C(CH_2)CH_3\}OTiCp_2Cl]$ [M=Cr 2.368(1) Å **45** and M=W 2.353(2) Å **46**] and $[(CO)_5Cr{=}C(CH_3)OTiCp^*_2Cl]$ [2.347(2) Å] **61**.[5,6,18]

The metal carbonyl bond *trans* to the carbene ligand [W-C3 = 2.029(3) Å] is 0.016 Å shorter than the average length of the four *cis*-metal carbonyl bonds 2.045(3) Å. These differences in *cis*- and *trans* metal carbonyl bonds with respect to the carbene ligand are usually attributed to the trans influence, which refer to the thermodynamic stabilization destabilization of the ground state of the complex.[19] It is the ability of a ligand to weaken the bond towards ligand trans thereto. The *trans* carbonyl receives more electron density in its antibonding π^* orbitals and the W-C(O) bond order increases, resulting in shorter bond lengths.

The molecular packing of complex **11** in the unit cell as viewed along the a-axis (bc plane) is shown in Figure 4.8. Four molecules are present per unit cell. It appears as if the molecules are paired together (groups of two) with one cyclopentadienyl ring of each molecule pointed towards each other. Figure 4.8 shows layers along the a-axis of molecules of similar orientation.

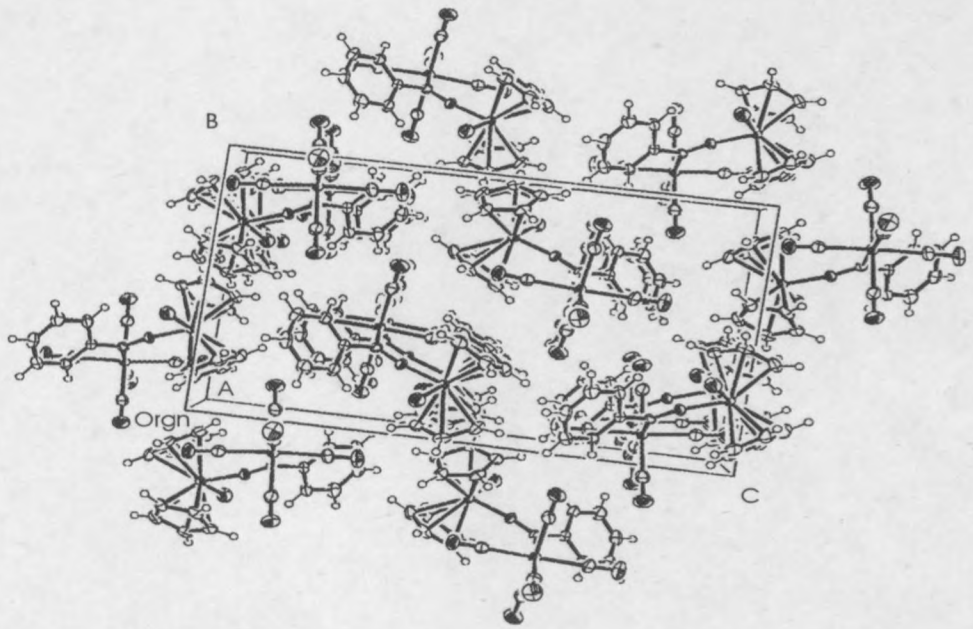

Figure 4.8: Molecular packing of complex **11** in the unit cell

4.2.2 STRUCTURE OF $[(CO)_5W{=}C(Ph)OHfCp_2Cl]$, 13.

This is the first example of a hafnium metaloxycarbene complex. Attempts to find other hafnium metaloxycarbene complexes proved fruitless. The Cambridge Crystallographic database search revealed numerous hafnium metallacycles, prepared mainly by Erker and co-workers and a few hafnium alkoxycarbene complexes. These known complexes are used to discuss the crystallographic data obtained for complex **13**.

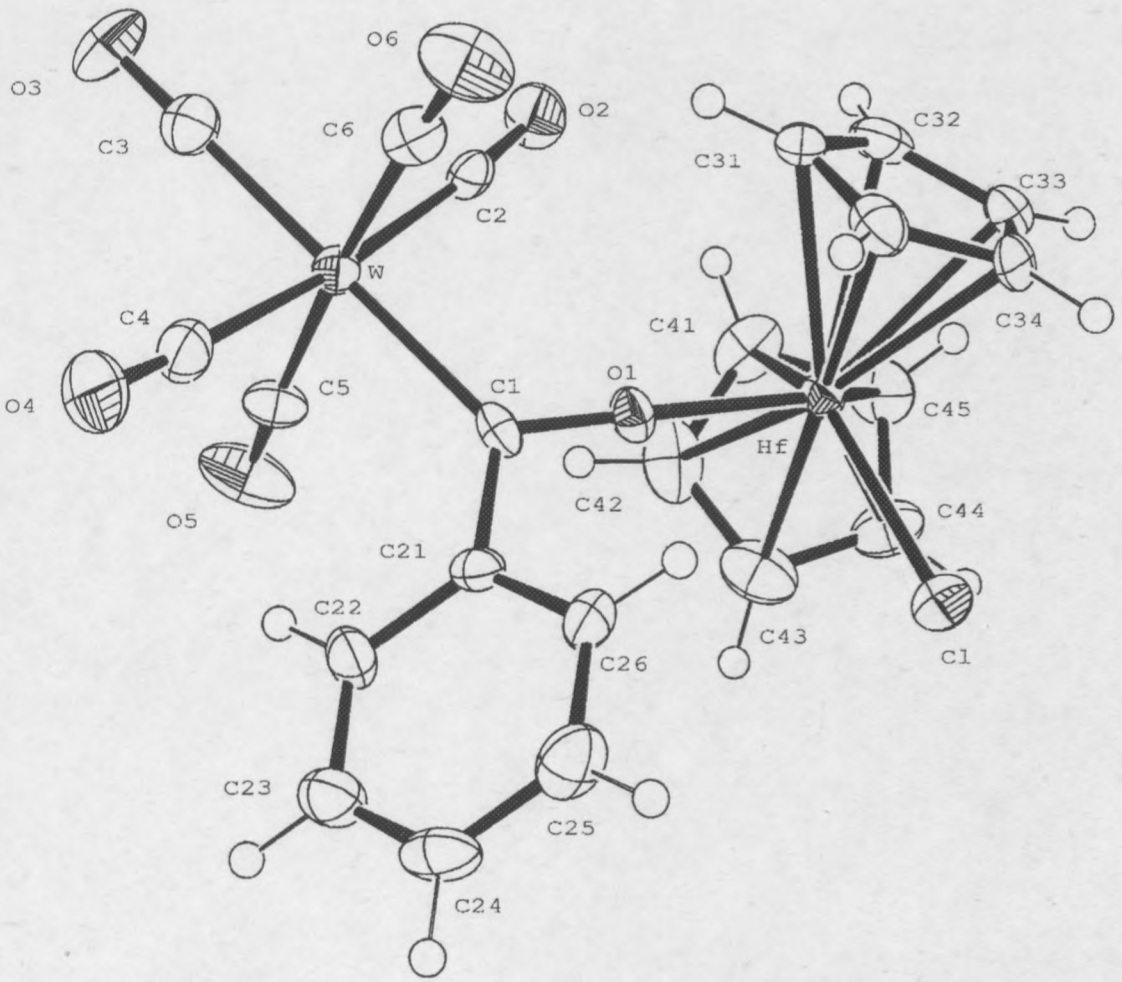

Figure 4.9: Thermal ellipsoid plot of $[(CO)_5W{=}C(Ph)OHfCp_2Cl]$, **13**, showing atomic numbering scheme (50% probability ellipsiods with the hydrogens as spheres of arbitrary diameter)

As was discussed earlier for complex **11**, the crystal structure of complex **13** shows the same deviations from the idealised 90 and 180° angles around the W atom [C(3)-W-C(1) 179.3(2), C(4)-W-C(2) 173.9(2), C(6)-W-C(5) 176.0(2), C(3)-W-C(6) 93.7(2), C(6)-W-C(1) 85.8(2), C(4)-W-C(5) 93.7(2)°]. Again this is probably to accommodate the bulky oxohafnocene ligand (Figure 4.7 and Table 4.5).

Deviations from the expected 120° angles (trigonal planar) around the carbene carbon atom [W-C(1)-O(1) 123.2(4), W-C(1)-C(21) 126.1(4), O(1)-C(1)-C(21) 110.5(5)] are similar to those obtained previously for complex **11**. Again the angle between the pentacarbonyl tungsten fragment and the phenyl ring increases 126.1(4)°, while the angle between the phenyl ring and the coordinated oxygen, decreases 110.5(5)°. The above-mentioned deviations are present in the crystal structures of Zr, Ti and Hf metaloxycarbene complexes, containing either methyl or phenyl substituents on the $C_{carbene}$

Table 4.5: Selected bond angles (°) of complex **13**

C(2)-W-C(3)	87.3(2)	C(2)-W-C(4)	173.9(2)
C(2)-W-C(6)	88.9(2)	C(3)-W-C(1)	179.3(2)
C(2)-W-C(5)	90.8(2)	C(6)-W-C(5)	176.0(2)
C(2)-W-C(1)	92.1(2)	O(2)-C(2)-W	174.9(5)
C(3)-W-C(4)	88.5(2)	O(3)-C(3)-W	177.5(5)
C(3)-W-C(6)	93.7(2)	O(4)-C(4)-W	176.2(6)
C(3)-W-C(5)	90.3(2)	O(6)-C(6)-W	176.0(6)
C(4)-W-C(6)	86.9(2)	O(5)-C(5)-W	177.9(6)
C(4)-W-C(5)	93.7(2)	W-C(1)-O(1)	123.2(4)
C(4)-W-C(1)	92.1(2)	W-C(1)-C(21)	126.1(4)
C(6)-W-C(1)	85.8(2)	C(21)-C(1)-O(1)	110.5(5)
C(5)-W-C(1)	90.2(2)	C(1)-O(1)-Hf	171.4(3)
Cp_{cent}-Hf-Cp_{cent}	130.769	O(1)-Hf-Cl	97.51(1)

The C6-O6-Hf bond angle of complex **13** [171.4(3)°] is virtually the same as the O_1-Ti-C_1 bond angle of complex **11** [171.7(2)°]. As was discussed previously for complex **11** metaloxycarbene complexes assume larger bond angles because the oxygen atom has almost sp hybridization in order to make both p orbitals available for π delocalization to the M-$C_{carbene}$ and O-Ti systems. There appears to be no difference in the pπ orbital availability of Ti and Hf atoms, in complexes **11** and **13** respectively, to the O atom. The hafnium metallacycles prepared by Erker and co-workers, showed similar C-O-Hf bond angles, [173.95(5)] **62,** [172.25(0)]° **63**.[20,21]

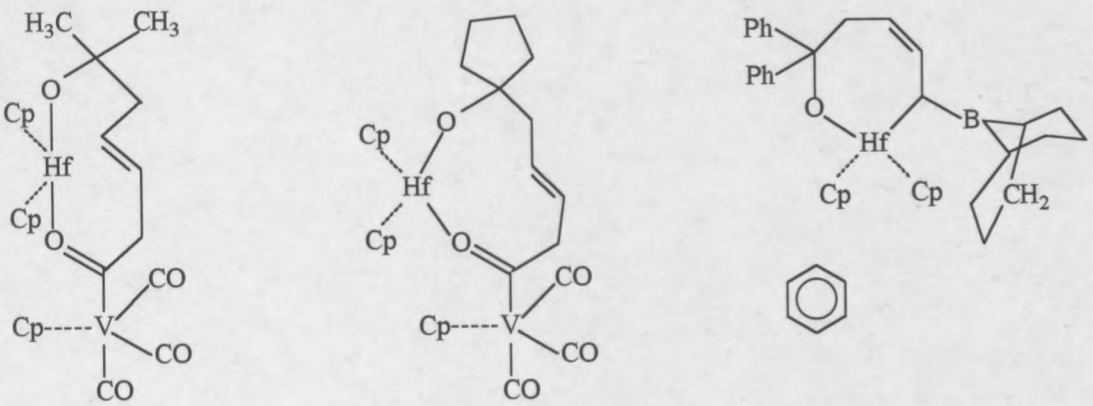

62 63 64

Figure 4.10: Hafnium metallacycles

Complex **13** shows a Cl-Hf-O bond angle of 97.51(1)° which compares well with the Cl-Ti-O angle obtained for complex **11** [96.16(8)°]. The Cl-Hf-O bond angle of the hafnium alkoxide complex, prepared by Stutte, **65**, is more than 3° smaller at 94.47(2)°.[22]

In complex **13** the $C_{carbene}$-O6 and W-$C_{carbene}$ bond lengths are 1.290(6)Å and 2.179(6)Å respectively (Table 4.4). The $C_{carbene}$-O bond distance of **13** is the same as that of **11** [1.279(6)Å], but shorter than the $C_{carbene}$-O bond lengths of the alkoxycarbene complexes (see discussion of complex **11**). This once again shows the importance of the acyl resonance structure (Figure 4.6 A) in metalloxycarbene complexes. The W-$C_{carbene}$ bond distance of **13** is the same as for the alkoxycarbene complexes **51** (2.185 Å), **53** (2.195 Å)

and **54** [2.164(6) Å] and longer than that in the alkoxycarbene complex **52** [2.086(2) Å] (Figure 4.6).[4,11,12] Similar W-$C_{carbene}$ and $C_{carbene}$-O bond distances are reported for metaloxycarbene complexes (Table 4.4).

Table 4.6: Selected bond lengths (Å) for complex **13**

W-C(6)	2.179(6)	C(6)-O(6)	1.290(6)
W-C(1)	2.037(6)	C(1)-O(1)	1.138(7)
W-C(2)	2.021(7)	C(2)-O(2)	1.155(8)
W-C(3)	2.037(6)	C(3)-O(3)	1.135(7)
W-C(4)	2.041(6)	C(4)-O(4)	1.148(7)
W-C(5)	2.045(7)	C(5)-O(5)	1.138(7)
C(6)-C(7)	1.506(7)	Hf-Cl	2.414(1)
Hf-O(6)	2.007(3)	Hf-C(13)	2.513(5)
Hf-C(18)	2.470(6)	Hf-C(14)	2.495(6)
Hf-C(19)	2.483(6)	Hf-C(15)	2.497(6)
Hf-C(20)	2.485(6)	Hf-C(16)	2.463(5)
Hf-C(21)	2.480(6)	Hf-C(17)	2.465(5)
Hf-C(22)	2.480(6)		

Again as was discussed for complex **11**, the contribution of both the acyl and carbene resonance forms suggests that π-electron density may be delocalised over the hafnoxycarbene moiety (**13**) to greater extend than in alkoxycarbene systems.

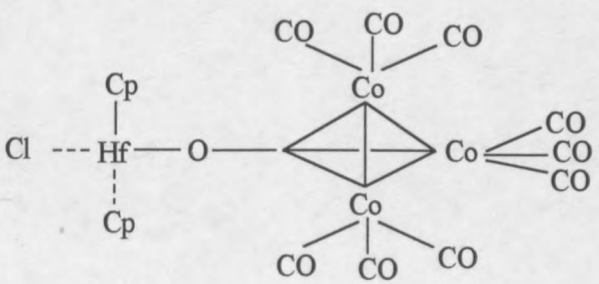

65

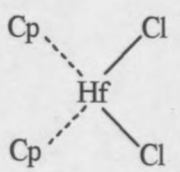

66

Figure 4.11: Stutte's hafnium alkoxide complex and hafnocene dichloride

The Hf-O bond distance of complex **13** [2.007(3) Å] is significantly longer than the Hf-O bond lengths for the metallacycle prepared by Erker, (1.904 Å) **62,** (1.900 Å) **63** and

(1.926 Å) **64**.[20,21,23] Stutte's hafnium alkoxide complex **65** has a Hf-O bond length of (1.968 Å), almost 39 Å shorter than the comparative bond of complex **13** (Table 4.4 and Figures 4.10 and 4.11).[22]

The Hf-Cl bond length of complex **13** [2.414(1) Å] is the same as Stutte's hafnium alkoxide complex **65**, [2.413(5) Å], (Figures 4.9 and 4.11) and that of hafnocene dichloride (2.419 and 2.427 Å) **66**.[24]

The centroids of the partially eclipsed cyclopentadienyl rings (Figure 4.12) of complex **13** are at similar distances away from the Hf atom (2.056 Å and 2.061 Å) and forms a Cp-Hf-Cp angle of 132.56°, with the Cp rings arranged symmetrically about the Hf atom. The cone angle for hafnocene is 121.190°.[24] Again the cone angle is possibly on the large side due to the partially eclipsed cyclopentadienyl rings

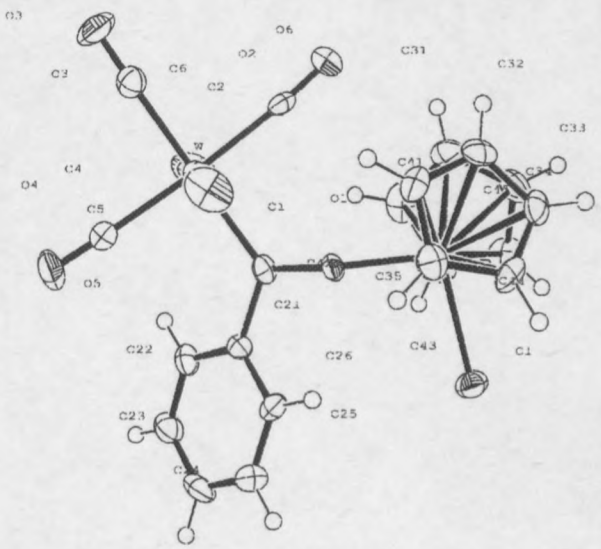

Figure 4.12: Thermal ellipsoid plot of $[(CO)_5W{=}C(Ph)OHfCp_2Cl]$ **13** with atomic numbering scheme (50% probability ellipsiods with the hydrogens as spheres of arbitrary diameter). This angle shows the partial eclipsed cyclopentadienyl rings

The metal carbonyl bond *trans* to the carbene ligand (W-C2 = 2.021 Å) is 0.019 Å shorter than the average length of the four *cis*-metal carbonyl bonds (2.040 Å), similar to the results obtained for complex **11**. Once again this is attributed to trans influence.

Carbene complexes are generally represented as in structure I, although this is not necessarily the most important resonance form. Structure II explains the electrophilic nature of the carbene carbon atom and its low resonance in ^{13}C NMR spectra. Contributing structure III accentuates the acyl contribution and I, III and V the delocalised π system between M-$C_{carbene}$-O-M^1. Finally IV shows the possibility of a ion pair formation that could be responsible for catalyst properties of the Zr-complex. The M-$C_{carbene}$-O-M^1 delocalised π-system results in a short $C_{carbene}$-O bond length. The importance of π-bonding in structure V explains the almost linear $C_{carbene}$-O-M^1 bond angle.

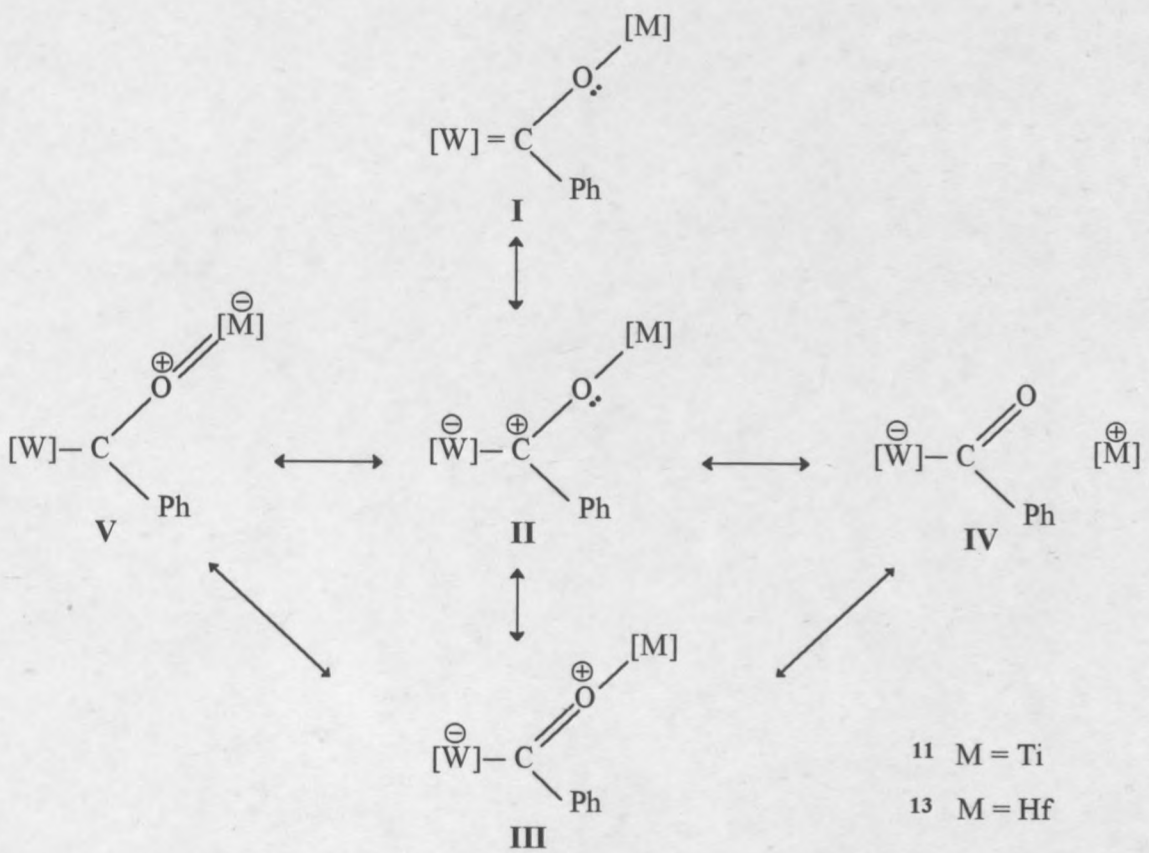

Figure 4.13: Possible resonance structures for complexes **11** and **13**

The molecular packing of complex **13** in the unit cell as viewed along the a-axis (bc plane) is shown in Figure 4.14. Four molecules are present per unit cell. It appears as if the molecules are paired together (groups of two) with one cyclopentadienyl ring of each molecule points towards each other. Figure 4.14 shows layers along the a-axis of molecules of similar orientation.

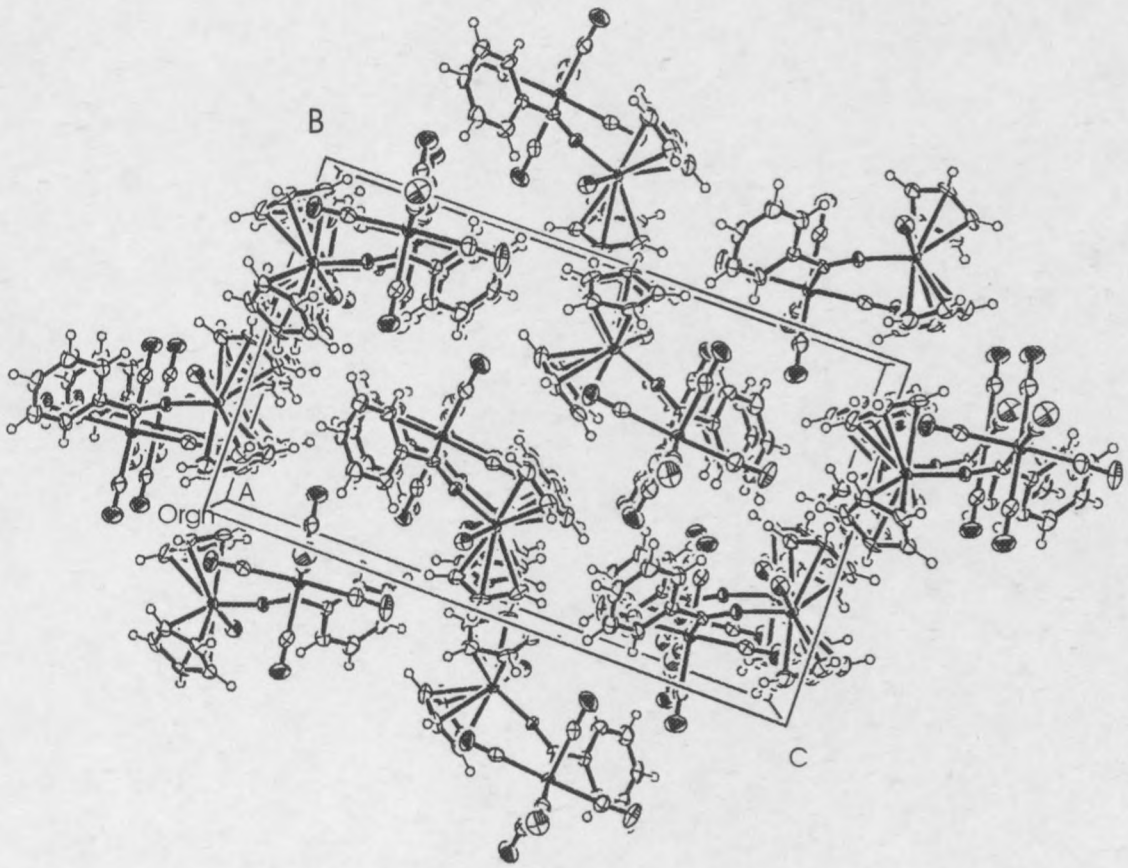

Figure 4.14: Molecular packing of complex **13** in the unit cell

4.2.3 CRYSTAL DATA AND EXPERIMENTAL PARAMETERS

The crystal data and refinement particulars for the X-ray crystallographic determination of the structures of complexes **11** and **13** are summarized in Table 4.7 and 4.8. The crystal structure data were collected by Dr. John Bacsa, University of Cape Town and solved by Dr. Catherine Esterhuysen and Matthias Esterhuysen using full matrix least squares on F^2 as refinement method.

Table 4.7: Crystal data and structure refinement parameters for complex **11**

Crystal size	0.17 x 0.14 x 0.12
Crystal colour	Brown
Crystal form	Monoclinic
Formula	$C_{22}H_{15}ClO_6TiW$
Formula weight (g/mol)	642.54
Space group	$P2_1/c$
a/Å	8.5530(10)
b/Å	12.26678(10)
c/Å	20.7890(3)
α (°)	90.0000(10)
β (°)	95.9030(10)
γ (°)	90
Cell volume ($Å^3$)	2169.8(3)
Z	4
Dc/g.cm^{-3}	1.967
Radiation	MoK/α (0.71073Å)
T (K)	173(2)
F(000)	1232
Scanning limit, θ	$1.93 \leq \theta \leq 27.51$
hkl limits	-11 to 11, -12 to 15, -26 to 27
Reflextions measured	14265
Unique reflextions used for refinement	4980
Parameters refined	295
Absorption coefficient (mm^{-1})	5.825
Absorption corrections	0.4376 - 0.5416
Final R Index	R1 = 0.0276, *w*R = 0.0637
R Index (all data)	R1= 0.0397, *w*R2= 0.0674
Goof (Goodness of fit)	1.034
Refinement Method	Full matrix least squares on F^2

Table 4.8: Crystal data and structure refinement parameters for complex **13**

Crystal size	0.17 x 0.14 x 0.12
Crystal colour	Red
Crystal form	Monoclinic
Formula	$C_{22}H_{15}ClO_6HfW$
Formula weight (g/mol)	773.13
Space group	$P2_1/c$
a/Å	8.5422(2)
b/Å	12.5546(3)
c/Å	21.0237(7)
α (°)	90
β (°)	96.1520(10)
γ (°)	90.00
Cell volume (Å^3)	2241.68(11)
Z	4
Dc/g.cm^{-3}	2.291
Radiation	MoK/α (0.71073Å)
T (K)	173(2)
F(000)	1432
Scanning limit, θ	$1.89 \leq \theta \leq 27.49$
hkl limits	-11 to 8, -16 to 15, -26 to 27
Reflextions measured	12410
Unique reflextions used for refinement	5106
Parameters refined	280
Absorption coefficient (mm^{-1})	9.91
Absorption corrections	none
Final R Index	R1 = 0.0321, *w*R = 0.0774
R Index (all data)	R1= 0.0443, *w*R2= 0.0831
Goof (Goodness of fit)	0.925
Refinement Method	Full matrix least squares on F^2

4.2.4 STRUCTURE OF $[(CO)_5Cr\text{-}Cl\text{-}Cr(CO)_5]^- NEt_4^+$

The halodecacarbonyldimetalate anion $[\{(CO)_5Cr\}_2Cl]^-$, with NEt_4^+ as counterion, was isolated (Figure 4.15) from the reaction mixture containing $Cp_2Zr(H)Cl$ and $[(CO)_5Cr{=}C(Me)O]^-NEt_4^+$ in dichloromethane at -40°C. Red crystals were isolated from a saturated toluene solution at -6°C.

The X-Ray crystal structure revealed $[\{(CO)_5Cr\}_2Cl]^- NEt_4^+$, **67**, instead of the expected $[(CO)_5Cr{=}C(Me)OZr(H)Cp_2]$. The Cambridge crystallographic data base contains numerous group 6 (halo)*deca*carbonyldimetalate anions, prepared primarily from reactions involving photolysis.[25-29] Similar, known, chromium (halo)*deca*carbonyldimetalate anions are used to discuss results obtained for complex **67**.

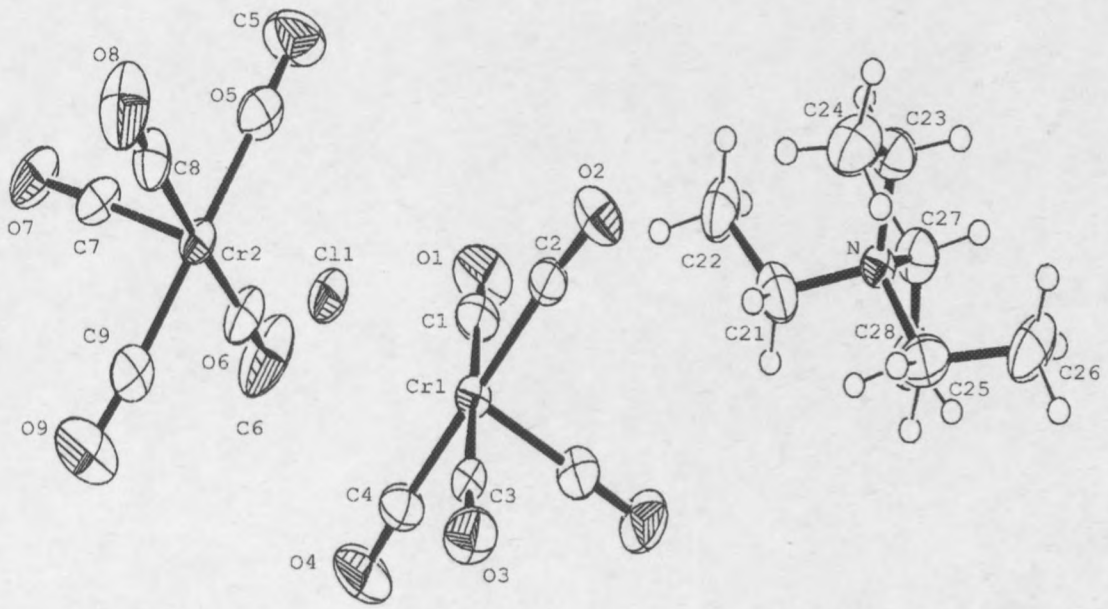

Figure 4.15: Thermal ellipsoid plot of $[\{(CO)5Cr\}_2Cl]^- NEt_4^+$ **67** showing atomic numbering scheme (50% probability ellipsiods with the hydrogens as spheres of arbitrary diameter)

The crystal structure of complex **67** shows Cr-Cl bond lengths of 2.486(1) Å and 2.467Å (Table 4.10), slightly larger than that observed for complex **68** 2.394 Å (Figure 4.17).[25] The negative charge localized on the chloride atom increases the electron density about

the chloride atom, resulting in a larger electron cloud. It is a known fact that anions have bigger radii than their neutral analogues. This is probably the reason for the large bond distance of Cr-Cl for complex **67**,

Table 4.10: Selected bond lengths (Å) for complex **67**

Cr(1)-Cl	2.467(1)	Cr(2)-Cl	2.486(1)
Cr(1)-C(1)	1.913(5)	C(1)-O(1)	1.134(6)
Cr(1)-C(2)	1.913(5)	C(2)-O(2)	1.138(6)
Cr(1)-C(3)	1.903(5)	C(3)-O(3)	1.132(6)
Cr(1)-C(4)	1.894(5)	C(4)-O(4)	1.146(6)
Cr(1)-C(10)	1.834(5)	C(10)-O(10)	1.158(6)
Cr(2)-C(5)	1.908(6)	C(5)-O(5)	1.139(7)
Cr(2)-C(6)	1.897(6)	C(6)-O(6)	1.137(7)
Cr(2)-C(7)	1.824(5)	C(7)-O(7)	1.170(6)
Cr(2)-C(8)	1.905(6)	C(8)-O(8)	1.144(7)
Cr(2)-C(9)	1.887(6)	C(9)-O(9)	1.143(7)

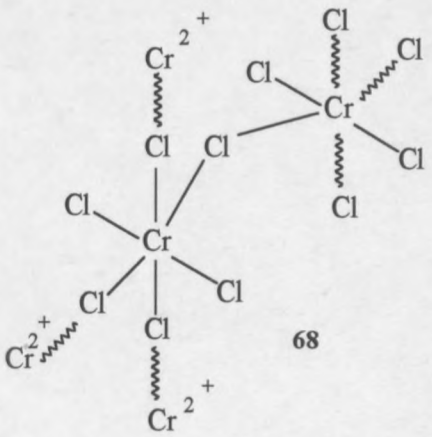

68

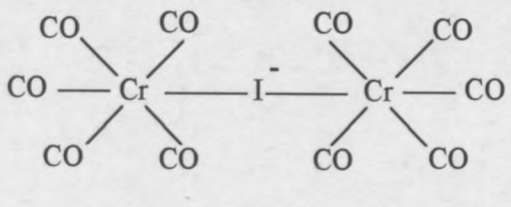

69

Figure 4.16: (Halo)*deca*carbonyldimetalate complexes **68**, and **69**

The average Cr-C_{co} bond length in complex **67** [1.88(7) Å] is slightly longer than that reported for complex **69** [1.82(2) Å], this is probably due to the electronegativities of the

bridged halogens [Cl (2.8), I (2.2)].[26] Less electron density is available to the Cr atom of complex **67** for π electron back donation to the carbonyl ligands compared to that of complex **69**, resulting in an increase in Cr-C_{co} bond distances. These in turn affect the C-O bond distances. The average C-O bond length in complex **70** [1.14(4) Å] is 0.02Å shorter than the average C-O bond length in complex **67**.[27]

Table 4.9: Selected bond angles (°) of complex **67**

O(1)-C(1)-Cr(1)	176.9(5)	C(5)-Cr(2)-C(6)	88.6(2)
O(2)-C(2)-Cr(1)	175.8(4)	C(5)-Cr(2)-C(7)	90.2(2)
O(3)-C(3)-Cr(1)	176.6(4)	C(5)-Cr(2)-C(8)	89.5(3)
O(4)-C(4)-Cr(1)	177.5(5)	C(5)-Cr(2)-C(9)	176.7(2)
O(10)-C(10)-Cr(1)	178.7(5)	C(6)-Cr(2)-C(7)	90.4(2)
O(5)-C(5)-Cr(2)	177.1(5)	C(6)-Cr(2)-C(8)	177.9(2)
O(6)-C(6)-Cr(2)	178.2(5)	C(6)-Cr(2)-C(9)	93.8(2)
O(7)-C(7)-Cr(2)	178.1(5)	C(7)-Cr(2)-C(8)	90.6(2)
O(8)-C(8)-Cr(2)	176.0(5)	C(7)-Cr(2)-C(9)	87.6(2)
O(9)-C(9)-Cr(2)	175.5(5)	C(8)-Cr(2)-C(9)	88.1(3)
C(1)-Cr(1)-C(2)	90.2(2)	C(1)-Cr(1)-Cl	90.67(2)
C(1)-Cr(1)-C(3)	179.4(2)	C(2)-Cr(1)-Cl	90.06(2)
C(1)-Cr(1)-C(4)	89.5(2)	C(3)-Cr(1)-Cl	89.11(1)
C(1)-Cr(1)-C(10)	91.2(2)	C(4)-Cr(1)-Cl	90.05(2)
C(2)-Cr(1)-C(3)	89.2(2)	C(10)-Cr(1)-Cl	178.09(2)
C(2)-Cr(1)-C(4)	179.7(2)	C(5)-Cr(2)-Cl	92.19(2)
C(2)-Cr(1)-C(10)	89.9(2)	C(6)-Cr(2)-Cl	83.59(2)
C(3)-Cr(1)-C(4)	91.1(2)	C(7)-Cr(2)-Cl	173.43(2)
C(3)-Cr(1)-C(10)	89.0(2)	C(8)-Cr(2)-Cl	95.53(2)
C(4)-Cr(1)-C(10)	90.0(2)	C(9)-Cr(2)-Cl	90.24(2)
Cr(1)-Cl-Cr(2)	130.28(6)		

Recently Handy and co-workers synthesised a iodo-bridged complex (**69**) by the photolytic reaction of a mixture of $Cr(CO)_6$ and $[(C_6H_5)_3P]_2I$ in THF, showing a Cr-I-Cr bond angle of 117.9(1)° (Figure 4.16). The Cr-Cl-Cr bond angle of complex **67** (130.3°) is much larger than the Cr-I-Cr bond angle of complex **69.** Complex **70** shows a Cr-Cl-Cr bond angle similar to that of complex **67** of [124.8(3)°] (Figure 4.17).[27] Complex **68** shows a Cr-Cl-Cr bond angle of 162.3 °, much larger than that obtained for complex **67**, probably due to the bulkier $Cl\text{-}Cr^{2+}$ ligands.

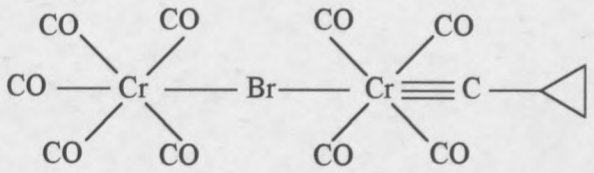

70

Figure 4.17: Halodecacarbonyldimetalate complex **70**

Other group 6 halodecacarbonyldimetalate complexes show similar M-Cl-M bond angles of 128.4(3)°, **72**, and 134.0(3)°, **73** (Figure 4.18).[28,29]

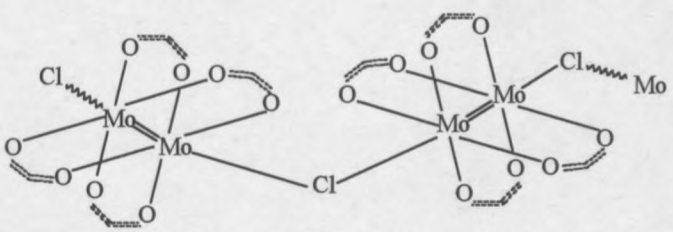

71

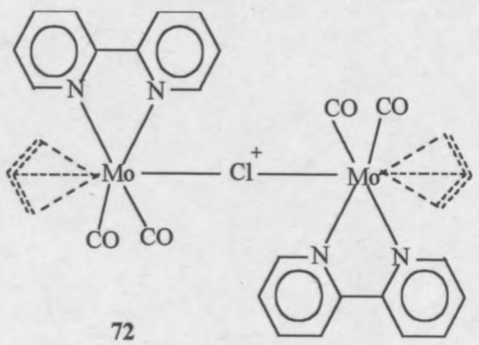

72

Figure 4.18: Halodecacarbonyldimetalate complexes **71** and **72**

The average O-C-Cr bond angle of complex **67** [176.9(6)°] is closer to the idealised 180.0° compared to that of complex **69** [174.9(5)° (average)].

The molecular packing of complex **67** in the unit cell as viewed along the a-axis (bc plane) is shown in Figure 4.19. There are two molecules per unit cell.

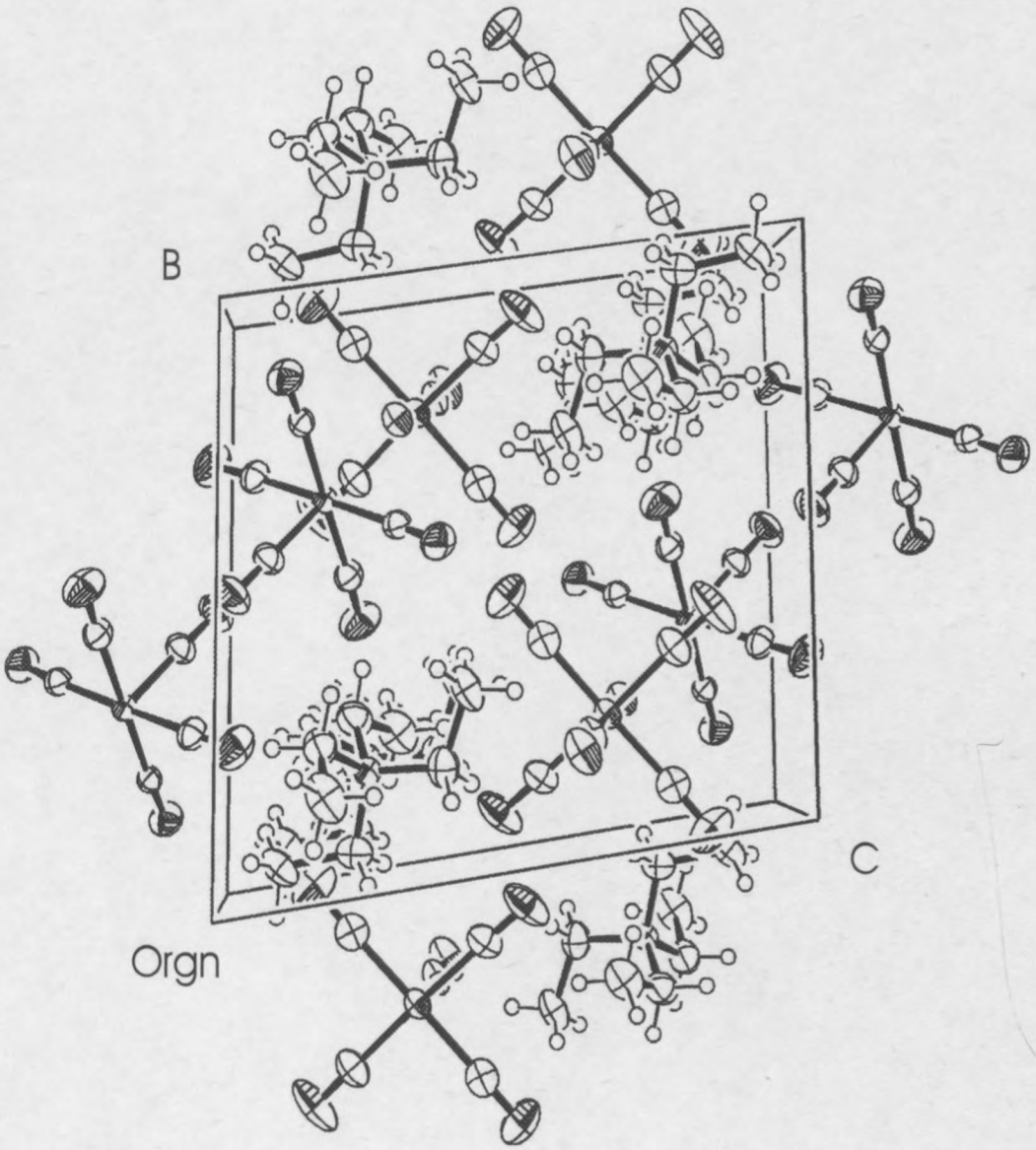

Figure 4.19: Molecular packing of complex **67** in the unit cell

The crystal structure data were collected by Dr. John Bacsa, University of Cape Town and solved by Dr. Catherine Esterhuysen and Matthias Esterhuysen using full matrix least squares on F^2 as refinement method. The crystal data and structure refinement parameters for complex **67** are shown in Table 4.10.

Table 4.11: Crystal data and structure refinement parameters for complex **67**

Crystal size	0.9 x 0.11x 0.12
Crystal colour	Red
Crystal form	Triclinic
Formula	$C_{17}H_{14}Cl_{0.5}CrN_0O_6PSi_{0.5}Zr$
Formula weight (g/mol)	520.24
Space group	H-M P-1
a/Å	8.9688(2)
b/Å	11.773(2)
c/Å	12.262(3)
α (°)	78.242(0)
β (°)	76.783(0)
γ (°)	72.752(0)
Cell volume ($Å^3$)	1190.8(4)
Z	2
Dc ($g.cm^{-3}$)	1.451
Radiation	MoK/□ (0.71073Å)
T (K)	293(2)
F(000)	517
Scanning limit, □	$1.72 \leq \theta \leq 27.43$
hkl limits	-11 to 11, -15 to 15, -15 to 14
Reflextions measured	7700
Unique reflextions used for refinement	5362
Parameters refined	293
Absorption coefficient (mm^{-1})	1.067
Absorption corrections	None
Final R Index	R1 = 0.0764, *w*R = 0.2019
R Index (all data)	R1= 0.1009, *w*R2= 0.2201
Goof (Goodness of fit)	1.065
Refinement Method	Full matrix least squares on F^2

REFERENCES

1. A. Neveling, M.Sc.-*thesis*, University of Stellenbosch, 1999.
2. L. van Niekerk, M.Sc.-*thesis*, University of Stellenbosch, 2000.
3. G. Heydenrych, M.Sc.-*thesis*, University of Stellenbosch, 2001.
4. T. Albrecht and J. Sauer, *Tetrahedron Letters*, 1994, **35**, 561-564.
5. M. Sabat, M.F. Gross and M.G. Finn, *Organometallics*, 1992,**11**, 745-751.
6. M. Sabat, K.M Reynolds and M.G. Finn, *Organometallics*, 1994,**13**, 2064.
7. J.C. Huffman, K.G. Moloy and K.G. Caulton, *Inorg. Chem.*, 1988, **27**, 2190-2192.
8. H.Werner, M. Laubender, M. Schmittel and R. Sollner, *Z. Kristallogr.- New Crystal Structures*, 1999, **214**, 47.
9. G. Schmid, V. Batzel and B. Stutte, *J. Organomet. Chem.*, 1976, **113**, 67.
10. A. Clearfield, D.K. Warner, C.H. Saldarriaga-Molina and R. Ropal, *Can J. Chem.*, 1975, **53**, 1622.
11. C.A. Toledano, A. Paelier, H. Rudler, J.-C. Daran and Y. Jeannin, *J. Chem. Soc. Chem. Comm.*, 1984, 576-578.
12. R.J. Staples, D.M. Potts and J.C. Yoder, *Z. Kristallogr.*, 1995, **210**, 381.
13. D.H. Gibson, Y. Ding, M.S. Mashula and J.F. Richardson, *Acta Crystallogr. Sec. C(Cr. Str. Comm.)*, 1996, **52**, 559.
14. A. Künzel, M. Sokdow, F.-Q. Liu, H.W. Roesky, M. Noltemeyer, H.-G. Schmidt and I. Uson, *J. Chem. Soc. Dalton Trans.*, 1996, 913-919.
15. P. Vaya, C. Floriani, A. Chiesl-Villa and C. Rozzoli, *Organometallics*, 1993,**12**, 4892.
16. A.V. Frith, D.W. Stephan, *Inorg. Chem.*, 1998, **37**, 4726-4731.
17. K. Hortmann, J. Diebold and H.-H. Brintzinger, *J. Organomet. Chem.*,1993, **445**, 107.
18. E.V. Anslyn, B.D. Santarsiero and R.H. Grubbs, *Organometallics*, 1988,**7**, 2137-2145.
19. U. Schubert, *Coord. Chem. Rev.*, 1984, **55**, 261.
20. G. Erker, R. Pfaff, C. Krüger and S. Werner, *Organometallics*, 1991,**10**, 3559.
21. M. Berlekamp, G. Erker and J.L. Petersen, *J. Organomet. Chem.*, 1993, 456, 97.
22. B. Stutte, V. Batzel, R. Boese and G. Schmid, *Chem. Ber.*,1978, **111**, 1603.

23. R. Noe, D. Wingbermuhle, G.Erker, C. Krüger and J. Bruckmann, *Organometallics*, 1993,**12**, 4993.

24. G.L. Soloveichik, T.M. Arkhireeva, V.K.Bel'skii and B.M. Bulychev, *Metalloorg. Khim.* (Organometallic Chem. In USSR), 1988, **1**, 226.

25. M.A. Babar, M.F.C. Ladd, L.F. Larkworthy, g.P. Newell and D.C. Povey, *J. Cryst. Mol. Struct.*, 1978, **8**, 43.

26. L.B. Handy, J.K. Ruff and L.F. Dahl, *J. Am. Chem. Soc.*, 1970, **92**, 7327.

27. E.O. Fischer, N.H. Tran-Huy and D. Neugebauer, *J. Organomet. Chem.*, 1982, **229**, 169.

28. G.A. Robbins and D.S. Martin, *Inorg. Chem.*, 1984, **23**, 2086.

29. M.D. Curtis and N.A. Fortinos, *J. Organomet. Chem.*, 1984, **272**, 43.